AD_____

Award Number: W81XWH-12-1-0390

TITLE: Connexins and Cadherin Crosstalk in the Pathogenesis of Prostate Cancer

PRINCIPAL INVESTIGATOR: Keith Johnson

CONTRACTING ORGANIZATION: University of Nebraska
                                              Omaha, NE 68198

REPORT DATE: September 2014

TYPE OF REPORT: Annual

PREPARED FOR: U.S. Army Medical Research and Materiel Command
                        Fort Detrick, Maryland 21702-5012

The views, opinions and/or findings contained in this report are those of the author(s) and should not be construed as an official Department of the Army position, policy or decision unless so designated by other documentation.

REPORT DOCUMENTATION PAGE		*Form Approved* OMB No. 0704-0188

Public reporting burden for this collection of information is estimated to average 1 hour per response, including the time for reviewing instructions, searching existing data sources, gathering and maintaining the data needed, and completing and reviewing this collection of information. Send comments regarding this burden estimate or any other aspect of this collection of information, including suggestions for reducing this burden to Department of Defense, Washington Headquarters Services, Directorate for Information Operations and Reports (0704-0188), 1215 Jefferson Davis Highway, Suite 1204, Arlington, VA 22202-4302. Respondents should be aware that notwithstanding any other provision of law, no person shall be subject to any penalty for failing to comply with a collection of information if it does not display a currently valid OMB control number. **PLEASE DO NOT RETURN YOUR FORM TO THE ABOVE ADDRESS.**

1. REPORT DATE	2. REPORT TYPE	3. DATES COVERED
September 2014	Annual	1 Sep 2013-31Aug 2014

4. TITLE AND SUBTITLE	5a. CONTRACT NUMBER
Connexins and Cadherin Crosstalk in the Pathogenesis of Prostate Cancer	
	5b. GRANT NUMBER
	W81XWH-12-1-0390
	5c. PROGRAM ELEMENT NUMBER
6. AUTHOR(S)	5d. PROJECT NUMBER
Keith R. Johnson	
	5e. TASK NUMBER
	5f. WORK UNIT NUMBER
E-Mail: kjohnsonr@unmc.edu	

7. PERFORMING ORGANIZATION NAME(S) AND ADDRESS(ES)	8. PERFORMING ORGANIZATION REPORT NUMBER
University of Nebraska Omaha, NE 68198-7835	

9. SPONSORING / MONITORING AGENCY NAME(S) AND ADDRESS(ES)	10. SPONSOR/MONITOR'S ACRONYM(S)
U.S. Army Medical Research and Materiel Command Fort Detrick, Maryland 21702-5012	
	11. SPONSOR/MONITOR'S REPORT NUMBER(S)

12. DISTRIBUTION / AVAILABILITY STATEMENT

Approved for Public Release; Distribution Unlimited

13. SUPPLEMENTARY NOTES

14. ABSTRACT

Gap junctions are conglomerations of cell-cell channels that are formed by a family of distinct proteins, called connexins. Cell-cell adhesion is mediated by cadherins, which assemble into adherens junctions. Our central hypothesis is that bidirectional signaling between cadherins and connexins is required for the assembly of gap junctions. We have postulated that connexins are the downstream targets of the signaling initiated by the classical cadherins, with epithelial-cadherin facilitating assembly and neuronal cadherin inhibiting the assembly. We have found that expression of a cell-cell adhesion deficient mutant of E-cadherin, in which tryptophan at position 156 in the first extracellular domain is replaced with alanine, acts in a dominant-negative manner when expressed in E-cadherin-expressing human prostate cancer cell line, LNCaP, and abolishes cell-cell adhesion as well as alters their morphology. Expression of α-catenin in metastatic prostate cancer cell line, PC3M, in which this gene is deleted and in which connexins are not assembled into gap junctions, induces mesenchymal to epithelial transformation and partially restores gap junction assembly. These findings highlight the importance of connexins and cadherins in the pathogenesis of prostate cancer.

15. SUBJECT TERMS
Gap junctions, E-cadherin, N-cadherin; Prostate cancer; cell motility; connexins

16. SECURITY CLASSIFICATION OF:			17. LIMITATION OF ABSTRACT	18. NUMBER OF PAGES	19a. NAME OF RESPONSIBLE PERSON USAMRMC
a. REPORT	b. ABSTRACT	c. THIS PAGE	UU	60	19b. TELEPHONE NUMBER *(include area code)*
U	U	U			

Standard Form 298 (Rev. 8-98)
Prescribed by ANSI Std. Z39.18

Keith R. Johnson, Ph.D.

Table of Contents

Keith R. Johnson, Ph.D.

1. Introduction:

Gap junctions (**GJ**) are conglomerations of cell-cell channels that are formed by a family of 21 distinct proteins, called connexin **(Cx)**s. The Cxs are transmembrane proteins, which are designated according to molecular mass. They are assembled into GJs through many steps (**Figure 1**). Communication through GJs is crucial for maintaining homeostasis [1;2]. Impaired, or loss of, Cx expression has been documented in the pathogenesis of various carcinomas [1;3-5]. Moreover, many studies have shown that over-
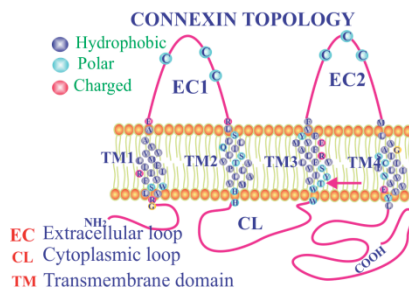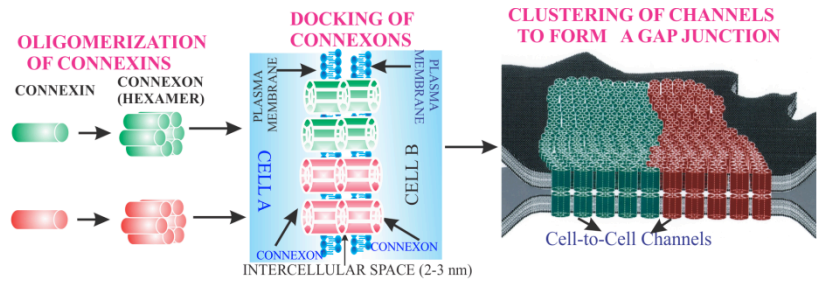

Figure 1. A cell-cell channel is formed by Cxs, which first oligomerize as hexamers(called connexons or hemichannels), and then are transported to the cell surface and dock with connexons in the adjacent cells to form cell-cell channels. A GJ is formed when several channels cluster at one particular spot. A GJ may be formed of channels formed of more than one Cx. Connexins have 4 transmembrane domains (TM1-TM4 or MI-M4), 2 extracellular loops, and one cytoplasmic domain. The amino and the carboxyl termini face the cytoplasm.
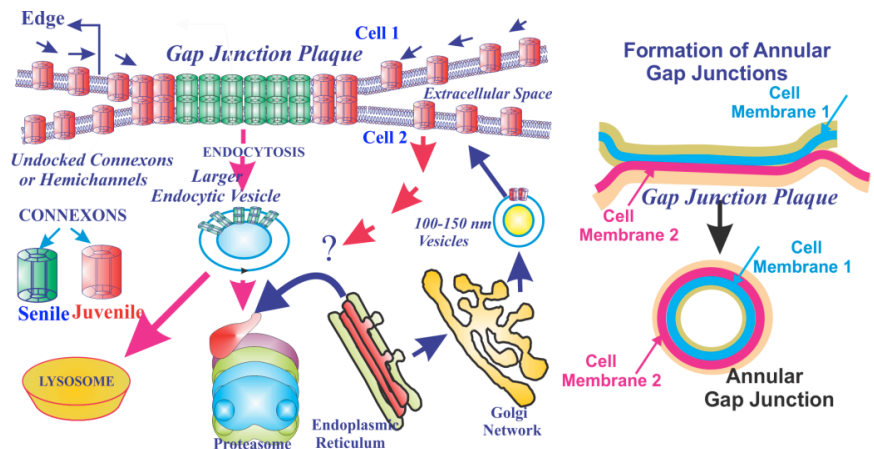
expression of Cxs in tumor cells attenuates the malignant phenotype *in vivo* and *in vitro*, reverses the changes associated with epithelial to mesenchymal transformation (**EMT**), and induces differentiation [3;4;6]. For example, Cx32 is expressed in the liver, lung, and exocrine glands, and knock out studies have shown that the incidence of carcinogen-induced tumors in these mice is higher [7-9]. Moreover, mutations in several Cx genes have been characterized in inherited diseases associated with aberrant proliferation and differentiation [1;10]. These studies support the notion that Cxs act as tumor suppressors. Despite this the molecular mechanisms by which Cxs are assembled into GJs and how GJs are disassembled are poorly understood.

2. Body

Our central hypothesis is that bidirectional signaling between cadherin(Cad)s and Cxs is required to maintain the polarized and differentiated state of epithelial cells and that GJ assembly is the downstream target of the signaling initiated by the classical Cads, with epithelial (E)-cad facilitating assembly and neuronal (N)-cad disrupting the assembly. We had proposed 2 specific aims to test this hypothesis:

1. **Determine how E-cad mediated cell-cell adhesion controls the assembly of Cxs into gap junctions in human prostate cancer (PC) cell lines.**

Figure 2. Assembly and Disassembly of GJs. Cxs are short lived proteins with a half life of 2-5 h. Connexons (see Figure 1) traffic to the plasma membrane (PM) in 100-150 nm particles, diffuse laterally and dock with their counterpart connexons in the PM of apposed cells. Juvenile connexons (red) are recruited to the periphery of the GJ plaque while senile connexons (green) are pinched off from the middle as double membrane vesicles into either one or the other cell. Alternatively, an entire GJ plaque is also endocytosed in its entirety into one or the other cell called annular GJs(left).

2. **Determine the molecular mechanisms by which E-cad and N-cad modulate gap junction assembly differentially in human prostate cancer cell lines.**

It is as yet unknown how a bi-cellular structure, such as a GJ, also called a GJ plaque, is endocytosed [1;10-12]. Connexins are short-lived proteins and both the assembly of Cxs into GJs and their disassembly are multi-step processes, which are poorly understood (**Figures 1 & 2**). A GJ can be endocytosed into one or the other cell, either in its entirety, also called an annular GJ, or as fragments pinched off from the center of the plaque as double membrane vesicles, by endocytosis and targeted to the lysosome for degradation. Alternatively, undocked connexons may be endocytosed by clathrin mediated or non-clathrin mediated endocytosis (**Figure 2**) [13-16].

Tasks of Aim 1:

1. Prepare recombinant retroviruses that contain various E-cad constructs that alter its ability to mediate cell-cell adhesion.
   a. Prepare recombinant retrovirus containing E-cad (W156A) (**Johnson**).
   b. Prepare recombinant retrovirus containing E-cad with deleted β-catenin binding site (**Johnson**).
   c. Prepare recombinant retrovirus containing E-cad with mutated p120 catenin binding site (**Johnson**).

2. Generate stable polyclonal cultures of several human PC cell lines (LNCaP - **ATCC**; PC3 - **ATCC**; RWPE1 - **ATCC**; PZ-HPV-7 -**ATCC**) expressing the constructs shown in 1 (**Mehta**).

3. In the cells described in 2, determine if connexins are assembled into gap junctions using Triton X-100 solubility assays (**Mehta and Johnson**).

4. In the cells described in 2, determine if cadherins are assembled into adherens junctions using Triton X-100 solubility assays (**Mehta and Johnson**).

5. In the cells described in 2, observe the trafficking of connexins and their assembly into gap junctions (**Mehta and Johnson**).
   a. Perform cell surface biotinylation to detect connexins at the plasma membrane (**Mehta**).
   b. Determine if connexins co-localize with EEA1, clathrin or caveolin-1 (**Mehta and Johnson**).

6. Knock down endogenous E-cadherin in LNCaP prostate cancer cells (**ATCC**) with or without connexin expression (**Mehta**).

   a. Determine if motility is altered in cells expressing E-cadherin or connexins (**Johnson**).

7. Determine if the trafficking of connexins is altered in knock down cells described in 6 (**Mehta**).

Statement of Work

Aim 1: Determine how E-cadherin mediated cell-cell adhesion controls the assembly of connexins into gap junctions in human prostate cancer cell lines.

Tasks:

1)   Prepare recombinant retroviruses that contain various E-cadherin constructs that alter its ability to mediate cell-cell adhesion. (Months 1-9)
        a)   Prepare recombinant retrovirus containing E-cadherinW156A (E-cad-W156A)(Johnson).
        b)   Prepare recombinant retrovirus containing E-cadherin$\Delta\beta$-catenin (E-cad$\Delta\beta$-cat)(Johnson).

        c)   Prepare recombinant retrovirus containing E-cadherinΔp120 (E-cadΔp120-cat)(Johnson).

The preparation of the constructs E-cad-W156A, E-cadherin$\Delta\beta$-cat (E-cad$\Delta\beta$-cat) and E-cadherinΔp120 (E-cadΔp120-cat) in retroviral vectors as well as production of recombinant viruses was described in the previous report.

2)   Generate stable polyclonal cultures of several human prostate cancer cell lines (LNCaP - ATCC; PC3 - ATCC; RWPE1 - ATCC; PZ-HPV-7 -ATCC) expressing the constructs shown in 1) (Mehta). (Months 3-12).

We used a well-characterized *in vitro* LNCaP cell culture model of PC that progresses from androgen-dependent state to androgen-independent state (developed in Dr. Lin's laboratory) as described elsewhere [17-20]. The salient features of LNCaP cell culture model are:

(**1**) Early passage LNCaP cells (between passage number 33-51), called C-33 cells, are androgen-responsive, grow slowly in normal medium, stop proliferating in androgen-depleted medium, are stimulated to grow in response to androgen, and fail to form tumors in the absence of androgens.

(**2**) Late passage LNCaP cells (between passage numbers 81-150), called C-81 cells, are non-responsive to androgens, grow rapidly in normal serum, do not stop proliferating in androgen-depleted medium, are not stimulated to grow faster in the presence of androgens (i.e., are androgen-independent), and form large tumors in vivo.

(**3**). Compared to C-33 cells, C-81 cells appear round, adhere less firmly to plastic, and appear to have lost cell-cell adhesion (**Figure 3**).

In our earlier studies, we had characterized LNCaP cells with regard to expression of E-cad and N-cad and had found that they expressed E-cad but not N-cad [21-23]. Moreover, as assessed by Western blot analysis and immunocytochemically, expression of E-cad was not discernibly different between C-33 and C-81
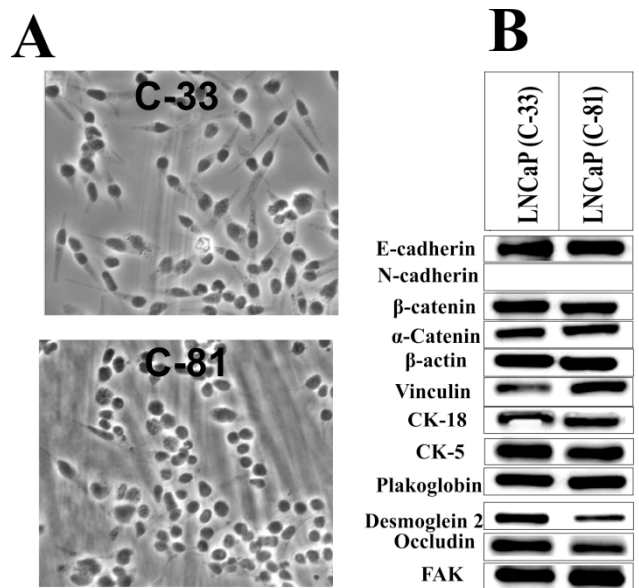

Figure 3. Characterization of LNCaP cell culture model system of PC progression. **A**. Compared to C-33 cells, C-81 cells appear round, adhere less firmly to plastic, and appear to have lost cell-cell adhesion. **B**. The expression of other cell-cell adhesion molecules is not discernibly different between C-33 and C-81 cells. FAK = Focal adhesion kinase. CK = Cytokeratin.

cells (**Figure 3B, top panels, see also Figure 4**). These results suggested that progression from androgen-dependence to independence is likely accompanied by alteration in the strength of cell-cell adhesion — and not by diminished expression of E-cad.   Furthermore, the expression of other cell-cell adhesion and cell-matrix molecules did not seem to be different (**Figure 3B**).

To test if expression of E-cad-W156A mutant attenuates E-cad-mediated cell-cell adhesion, we retrovirally expressed both EGFP- and mCherry-tagged wild-type cadherin (E-cad-WT) and E-cad-W156A mutant in LNCaP-C-33 cells.   The results showed that both WT and mutant E-cad were expressed
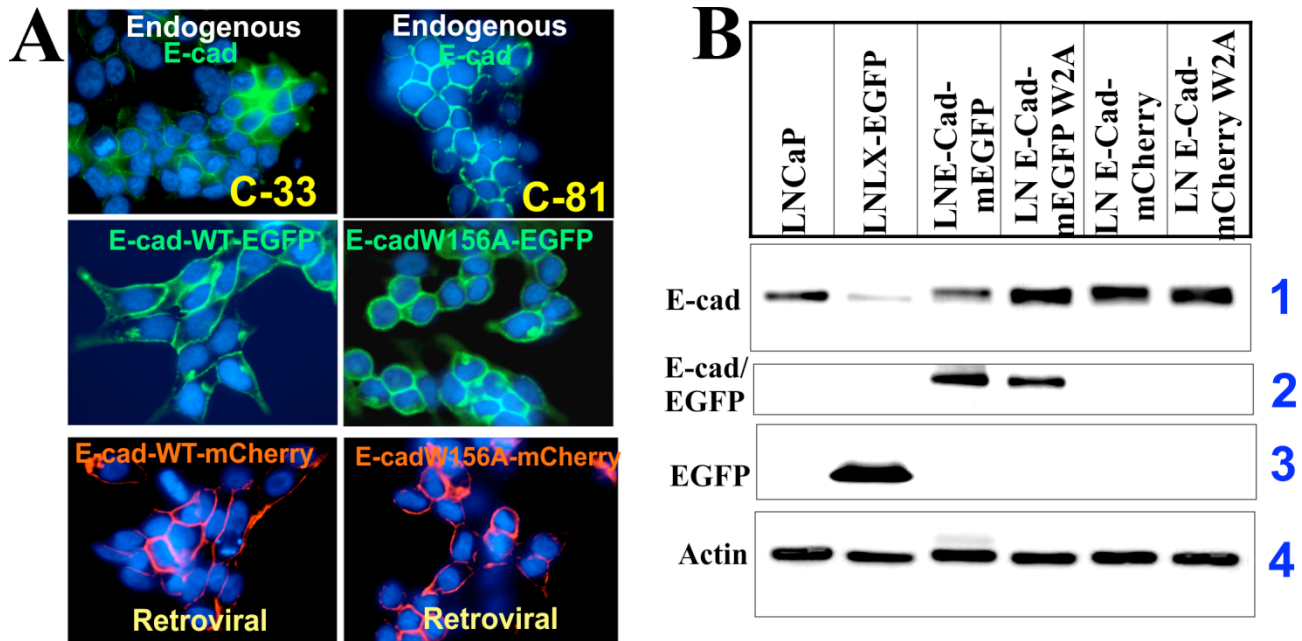

Figure 4. **A.** Top row: Expression of endogenous E-cad in LNCaP-C-33 and LNCaP-C-81 cells. Middle and Bottom rows: LNCaP cells expressing monomeric EGFP (LNLX-EGFP), E-cad-WT-EGFP (LNE-E-Cad-EGFP), E-cad-W156A-EGFP (LNE-E-Cad-EGFP), E-cad-WT-mCherry (LNE-E-Cad-mCherry) and E-cad-W156A-mCherry (LNE-E-Cad-W156A). Note that both EGFP- & mCherry-tagged E-cad and its mutants are expressed at cell-cell contact sites. Endogenous E-cad was detected with E-cad antibody (Green). **B.** Western blot analysis of mEGFP- and mCherry tagged wild-type E-cad and the mutants. The blot was probed with E-cad antibody, and blots 2 and 3 were probed with GFP antibody, which does not recognize mCherry.   Blot 4 was probed with actin as a loading control. E-cad = E-cadherin; E-cad/EGFP = E-cadherin tagged with EGFP or mCherry. LNCaP = Parental LNCaP cells.

appropriately in C-33 cells (**Figure 4A, rows 2 & 3**). Moreover, the morphology of LNCaP-C-33 cells was altered to resemble C-81 cells upon expressing E-cad-W156A mutant whereas expression of E-cad-WT had no effect (**Figure 4, rows 3 and 4, right panels**). Moreover, LNCaP cells expressing E-cad-W156A, apart from becoming rounded, adhered less firmly to the substratum (not shown).   These results suggest that expression of the mutant E-cad-W156A likely disrupts E-cad mediated cell-cell adhesion by acting in a dominant negative manner when introduced into E-cad-expressing LNCaP cells.

PC3M cells are metastatic and express N-cad [24]. α-catenin, a cadherin-associated protein, is also deleted in PC3M cells like the parental PC-3 cells [25]. Hence, PC3M cells cannot form adherens junctions. Linkage of α-catenin to actin filaments is required to form adherens junctions, which also strengthens cell-cell adhesion. Hence, we expressed E-cad–WT and α-catenin (**α-cat**) retrovirally in PC3M cells to test whether their expression affects growth and induces morphological changes. Expression of E-cad–WT had no effect on the growth of PC3M cells, however, expression of α-cat induced mesenchymal to epithelial transformation (**MET**) in PC3M cells (**Figure 5A**). Western blot analysis showed that E-cad and α-cat were robustly expressed (**Figure 5B**). **.**

3)   In the cells described in 2), determine if connexins are assembled into gap junctions using Triton X-100 solubility assays (Mehta and Johnson). (Months 4-16)

PC3M cells express connexin43 but fail to form gap junctions. Hence, we expressed E-cad as well as α-cat to test if the assembly of Cx43 into gap junctions is induced. We found that E-cad expression had no effect on the assembly of Cx43 into gap junctions. However, expression of α-cat induced the trafficking and assembly of Cx43 into gap junctions (**Figure 6, next page**). Cx43, however, still remained detergent-soluble (**Figure 7, next page).**.
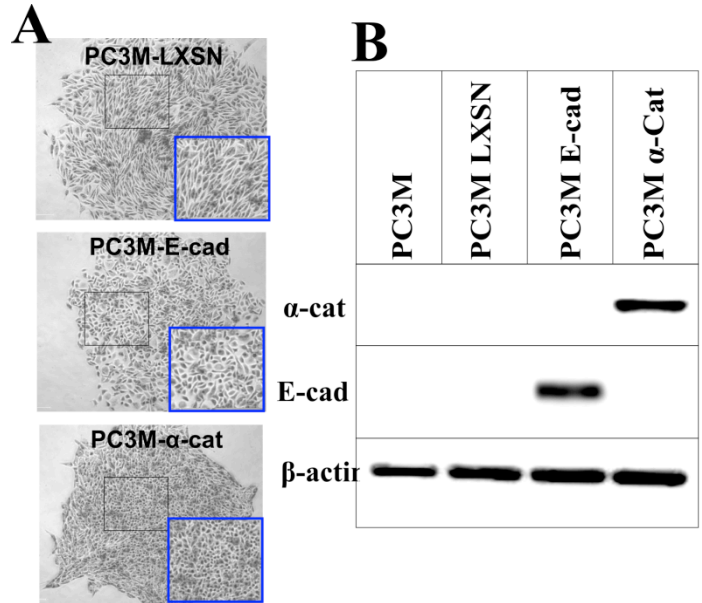

Figure 5. Expression of α-catenin (α-cat) induces MET in PC3M cells. **A.** PC3M cells were infected with the control (PC3M-LXSN), E-cad-WT-harboring (PC3M-E-cad) and α-cat-harboring (PC3M-α-cat) recombinant retroviruses and allowed to form colonies in G418 for two weeks (PC3M-LXSN and PC3M-E-cad) and 3 weeks (PC3M-α-cat). Colonies were fixed and photographed. Images encircled in blue boxes are the enlarged images of areas encircled in black boxes. **B.** Western blot analysis of E-cad and α-cat in infected PC3M cells. Note that E-cad and α-cat are expressed only in PC3M cells infected with E-cad-WT- and α-cat-harboring retroviruses. β-actin is used as a loading control.

The constructs E-cadΔβ-cat and E-cadΔp120 have not yet been introduced into any cell line. These constructs will be introduced into PC3M cells to explore the role of cell-cell adhesion in inducing MET.

4)   In the cells described in 2), determine if cadherins are assembled into adherens junctions using Triton X-100 solubility assays (Mehta and Johnson). (Months 4-16)

We have not initiated these studies.

5)   In the cells described in 2), observe the trafficking of connexins and their assembly into gap junctions (Mehta and Johnson). (Months 6-18)

a)   Perform cell surface biotinylation to detect connexins at the plasma membrane (Mehta).
b)   Determine if connexins co-localize with EEA1, clathrin or caveolin-1 (Mehta and Johnson).

6) Knock down endogenous E-cadherin in LNCaP prostate cancer cells (ATCC) with or without connexin expression (Mehta). (Months 12-20)

a) Determine if motility is altered in cells expressing E-cadherin or connexins (Johnson).

7) Determine if the trafficking of connexins is altered in knock down cells described in 6) (Mehta). (Months 16-24)

We have not assessed the motility of LNCaP cells after expressing E-cad–WT and E-cad-W156A. However, expression of E-cad-W156A mutant altered the morphology of LNCaP cells.

Aim 2: Determine the molecular mechanisms by which E-cadherin and N-cadherin modulate gap junction assembly differentially in human prostate cancer cell lines.

Tasks:
1) Prepare recombinant retroviruses that contain chimeras of E-cadherin and N-cadherin (Johnson). (Months 6-16)
a) Prepare recombinant retrovirus containing chimeras with the extracellular domains switched (Johnson).
b) Prepare recombinant retrovirus containing chimeras with the cytoplasmic domains switched (Johnson).
c) Prepare recombinant retrovirus containing chimeras with segments of the extracellular domains of E-cadherin and N-cadherin swapped (Johnson).

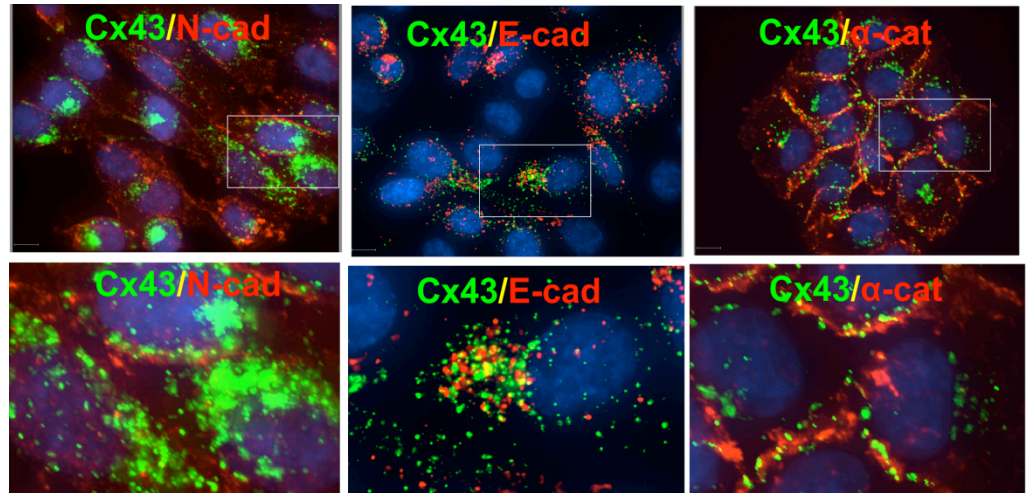We have not expressed chimeras of E-cadherin and N-cadherin in LNCaP cells.

Figure 6. Top row: Expression of endogenous N-cad and Cx43 in PC3M cells infected with the control virus (left panel), endogenous Cx43 and E-cad-harboring retrovirus (middle panel), and endogenous Cx43 and α-cat-harboring retrovirus (right panel). Bottom row: Enlarged images of the boxed areas in top row. Cx43 is in green where as E-cad and N-cad are in red. Nuclei are blue.
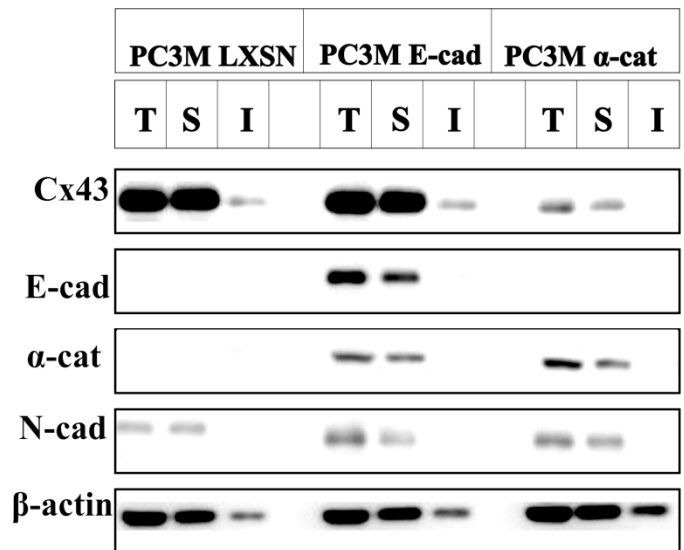

Figure 7. Expression of α-catenin (α-cat) and E-cad does not alter the detergent (TX-100)-solubility of Cx43. PC3M cells were infected with the control (PC3M-LXSN), E-cad-WT-harboring (PC3M E-cad) and α-cat-harboring (PC3M α-cat) recombinant retroviruses were seeded in petri dishes and confluent cells were subjected to TX100-solubility assay, followed by Western blot analysis, which biochemically measures the assembly various cell junction-associated proteins. Note that Cx43, α-cat, E-cad and N-cad remain TX100-soluble even though they are detected at cell-cell contact areas (see Figure 6). TX100 = TritonX-100. T, S, and I refer to total, Tx100-soluble and TX100-insolbule fractions of cell lysates.

2)   Infect LNCaP cells (ATCC) and PZ-HPV-7 cells (ATCC) with the retroviruses described in 1) and retroviruses containing wild-type N-cadherin (Mehta). (Months 12-24)

Expression of N-cad-WT in LNCaP cells and the effect of expression on the morphology was documented in the previous report.   We have not expressed N-cad-W156A to test if it is expressed appropriately and whether it affects the expression of endogenous E-cad in LNCaP cells. The preparation of these constructs has been described [26;27].

3)   In the cells described in 2), determine if connexins are assembled into gap junctions using Triton X-100 solubility assays (Mehta and Johnson). (Months 16-28)

We have not initiated these studies.

4)   In the cells described in 2), determine if cadherins are assembled into adherens junctions using Triton X-100 solubility assays (Mehta and Johnson). (Months 16-28)

We have not initiated these studies.

5)   In the cells described in 2), observe the trafficking of connexins and their assembly into gap junctions. (Months 24-32)
**   a)   Perform cell surface biotinylation to detect connexins at the plasma membrane (Mehta).**
**   b)   Determine if connexins co-localize with EEA1, clathrin or caveolin-1 (Mehta and Johnson).**

We have not initiated this task.

6)   Determine if N-cadherin alters the motility of connexin-expressing LNCaP (ATCC) and cells PZ-HPV-7 (ATCC) cells (Johnson). (Months 28-36)

Please see task 2 of aim 2.

7)   Determine if N-cadherin induces endocytosis of gap junctions in connexin-expressing LNCaP (ATCC) and PZ-HPV-7 (ATCC) cells (Mehta). (Months 28-36)

We have not initiated these studies yet.

Conclusion:

The available data preclude us to draw any conclusions with respect to the proposed studies.

Key Research Accomplishments

1. We have found that expression of a cell-cell adhesion deficient mutant of E-cadherin, in which tryptophan at position 156 in the first extracellular domain is replaced with alanine, acts in a dominant-negative manner when expressed in E-cadherin-expressing human prostate cancer cell line, LNCaP, and abolishes cell-cell adhesion as well as alters their morphology.

2. Expression of α-catenin in metastatic prostate cancer cell line, PC3M, in which this gene is deleted and in which connexins are not assembled into gap junctions, induces mesenchymal to epithelial transformation and partially restores gap junction assembly. These findings highlight the importance of connexins and cadherins in the pathogenesis of prostate cancer.

Reportable Outcomes:

1. The following manuscript was published. The manuscript file is appended with Dr. Mehta's Progress Report. I will also append this manuscript to my Progress Report if you need me to do so.

   Kelsey, LS; Katoch, P; Ray, Mitra, S; Chakraborty, S; Lin M-F; and Mehta, PP. Vitamin D3 rgulates the formation and degradation of gap junctions in androgen-responsive human prostate cancer cells. PLoS ONE, 9, e106437, 2014. Attached.

2. Also the following manuscript was submitted to "Journal of Biological Chemistry". It will be re-submitted in revised form within a week. The manuscript is appended with Dr. Mehta's Progress Report. I will also append this manuscript to my Progress Report if you need me to do so.

   Katoch,P., Ray,A., Kelsey,L., Johnson,K., and Mehta,P.P. (2014) The carboxyl tail of connexin32 regulates gap junction size. J Biol Chem (To be resubmitted after revision). Attached.

Keith R. Johnson, Ph.D.

Reference List

1. Laird,D.W. (2006) Life cycle of connexins in health and disease. *Biochem J*, **394**, 527-543.
2. Saez,J.C., Berthoud,V.M., Branes,M.C., artinez,A.D., Bey., and Beyer,E.C. (2003) Plasma membrane channels formed by connexins: their regulation and functions. *Physiol Rev*, **83**, 1359-1400.
3. Crespin,S., Defamie,N., Cronier,L., and Mesnil,M. (2009) Connexins and carcinogenesis. In Harris,A. and Locke,D. (eds.) *Connexinss: A Guide*., pp 529-42.
4. Naus,C.C. and Laird,D.W. (2010) Implications and challenges of connexin connections to cancer. *Nat Rev Cancer*, **10**, 435-441.
5. Plante,I., Stewart,M.K.G., Barr,K., Allan,A.L., and Laird,D.W. (2010) Cx43 suppresses mammary tumor metastasis to the lung in a Cx43 mutant mouse model of human disease. *Oncogene*, **30**, 1681-1692.
6. McLachlan,E., Shao,Q., Wang,H.l., Langlois,S., and Laird,D.W. (2006) Connexisn act as tumor suppressors in three dimensional mammary cell organoids by regulating differentiation and angiogenesis. *Cancer Res*, **66**, 9886-9894.
7. King TJ, Gurley KE, Prunty J, Shin JL, Kemp CJ, and Lampe PD (2005) Deficiency in the gap junction protein connexin32 alters p27Kip1 tumor suppression and MAPK activation in a tissue-specific manner. *Oncogene*, **24**, 1718-1726.
8. King,T.J. and Lampe,P.D. (2004) Mice deficient for the gap junction protein Connexin32 exhibit increased radiation-induced tumorigenesis associated with elevated mitogen-activated protein kinase (p44/Erk1, p42/Erk2) activation. *Carcinogenesis*, **25**, 669-680.
9. King,T.J. and Bertram,J.S. (2005) Connexins as targets for cancer chemoprevention and chemotherapy. *Biochimica et Biophysica Acta (BBA) - Biomembranes*, **1719**, 146-160.
10. Laird,D.W. (2010) The gap junction proteome and its relationship to disease. *Trends Cell Biol*, **20**, 92-101.
11. Berthoud VM, Minogue PJ, Laing JG, and Beyer EC (2004) Pathways for degradation of connexins and gap junctions. *Cardiovasc.Res.*, **62**, 256-267.
12. Musil,L.S. (2009) Biogenesis and degradation of gap junctions. In Harris,A. and Locke,D. (eds.) *Connexins: A Guide*. Springer, pp 225-40.
13. Falk,M.M., Baker,S.M., Gumpert,A., Segretain,D., and Buckheit,R.W. (2009) Gap junction turnover is achieved by the internalization of small endocytic double-membrane vesicles. *Mol Biol Cell*, **20**, 3342-3352.
14. Jordan,K., Chodock,R., Hand,A., and Laird,D.W. (2001) The origin of annular junctions: a mechanism of gap junction internalization. *J Cell Sci*, **114**, 763-773.
15. Piehl,M., Lehmann,C., Gumpert,A., Denizot,J.P., Segretain,D., and Falk,M.M. (2007) Internalization of Large Double-Membrane Intercellular Vesicles by a Clathrin-dependent Endocytic Process. *Mol.Biol.Cell*, **18**, 337-347.
16. Traub,L.M. (2009) Tickets to ride: selecting cargo for clathrin-regulated internalization. *Nat Rev Mol Cell Biol*, **10**, 583-596.
17. Igawa,T., Lin FF, Lee MS, Karan D, Batra SK, and Lin MF (2002) Establishment and characterization of androgen-independent human prostate cancer LNCaP cell model. *Prostate*, **50**, 222-235.
18. Lin MF, Meng TC, Rao PS, Chang C, Schonthal AH, and Lin FF (1998) Expression of human prostatic

acid phosphatase correlates with androgen-stimulated cell proliferation in prostate cancer cell lines. *J Biol Chem.*, **273**, 5939-5947.

19. Meng TC, Lee MS, and Lin MF (2000) Interaction between protein tyrosine phosphatase and protein tyrosine kinase is involved in androgen-promoted growth of human prostate cancer cells. *Oncogene*, **19**, 2664-2677.

20. Meng TC and Lin MF (1998) Tyrosine phosphorylation of c-ErbB-2 is regulated by the cellular form of prostatic acid phosphatase in human prostate cancer cells. *J Biol Chem.*, **273**, 22096-22104.

21. Govindarajan,R., Song,X.-H., Guo,R.-J., Wheelock,M.J., Johnson,K.R., and Mehta,P.P. (2002) Impaired traffcking of connexins in androgen-independent human prostate cancer cell lines and its mitigation by a-catenin. *J Biol Chem*, **277**, 50087-50097.

22. Mehta,P.P., Perez-Stable,C., Nadji,M., Mian,M., Asotra,K., and Roos,B. (1999) Suppression of human prostate cancer cell growth by forced expression of connexin genes. *Dev Genetics*, **24**, 91-110.

23. Mitra,S., Annamalai,L., Chakraborty,S., Johnson,K., Song,X., Batra,S.K., and Mehta,P.P. (2006) Androgen-regulated Formation and Degradation of Gap Junctions in Androgen-responsive Human Prostate Cancer Cells. *Mol Biol Cell*, **17**, 5400-5416.

24. Pettaway CA, Pathak S, Greene G, Ramirez,E., Wilson,M., Killion,J., and Fidler,I. (1996) Selection of highly metastatic variants of different human prostatic carcinomas using orthotopic implantation in nude mice. *Clin Cancer Res*, **2**, 1627-1636.

25. Ewing CM, Ru N, Morton RA, Robinson JC, Wheelock,M.J., Johnson KR, Barrett JC, and Isaacs WB (1995) Chromosome 5 suppresses tumorigenicity of PC3 prostate cancer cells: correlation with re-expression of a-catenin and restoration of E-cadherin function. *Cancer Res*, **55**, 4813-4817.

26. Nieman,M., Prudoff,R., Johnson,K., and Wheelock,M. (1999) N-cadherin promotes motility in human breast cancer cells regardless of their E-cadherin expression. *J Cell Biol*, **147**, 631-643.

27. Kim JB, Islam S, Kim YJ, Prudoff RS, Sass KM, Wheelock MJ, and Johnson KR (2000) N-Cadherin extracellular repeat 4 mediates epithelial to mesenchymal transition and increased motility. *J Cell Biol*, **151**, 1193-1206.

Appendices:

Attached.

Supporting Data:

None.

PLOS ONE

Vitamin D₃ Regulates the Formation and Degradation of Gap Junctions in Androgen-Responsive Human Prostate Cancer Cells

Linda Kelsey, Parul Katoch, Anuttoma Ray, Shalini Mitra, Souvik Chakraborty, Ming-Fong Lin, Parmender P. Mehta*

Department of Biochemistry and Molecular Biology, University of Nebraska Medical Center, Omaha, Nebraska, United States of America

Abstract

1α-25(OH)₂ vitamin D₃ (1-25D), an active hormonal form of Vitamin D₃, is a well-known chemopreventive and pro-differentiating agent. It has been shown to inhibit the growth of several prostate cancer cell lines. Gap junctions, formed of proteins called connexins (Cx), are ensembles of cell-cell channels, which permit the exchange of small growth regulatory molecules between adjoining cells. Cell-cell communication mediated by gap junctional channels is an important homeostatic control mechanism for regulating cell growth and differentiation. We have investigated the effect of 1-25D on the formation and degradation of gap junctions in an androgen-responsive prostate cancer cell line, LNCaP, which expresses retrovirally-introduced Cx32. Connexin32 is expressed by the luminal and well-differentiated cells of normal prostate and prostate tumors. Our results document that 1-25D enhances the expression of Cx32 and its subsequent assembly into gap junctions. Our results further show that 1-25D prevents androgen-regulated degradation of Cx32, post-translationally, independent of androgen receptor (AR)-mediated signaling. Finally, our findings document that formation of gap junctions sensitizes Cx32-expressing LNCaP cells to the growth inhibitory effects of 1-25D and alters their morphology. These findings suggest that the growth-inhibitory effects of 1-25D in LNCaP cells may be related to its ability to modulate the assembly of Cx32 into gap junctions.

Introduction

The role of Vitamin D₃, and its active hormonal form 1α-25(OH)₂ vitamin D₃ (1-25D), as an anti-neoplastic, pro-differentiating, and pro-apoptotic agent has been established in a wide variety of normal and malignant epithelial cells, including prostate cancer (PCA) [1–4]. The actions of 1-25D are mediated by binding to vitamin D receptor, one of the members of nuclear receptor superfamily, which is expressed in a wide variety of cells, including prostate. The vitamin D receptor heterodimerizes with the RXR receptor and binds to vitamin D receptor response element to alter gene expression [1]. Based upon the observation that PCA mortality rates in the U.S are inversely proportional to the geographically incident ultraviolet radiation exposure from the sun, and that ultraviolet light is essential for vitamin D₃ synthesis in the skin, a role for this vitamin in decreasing the risk of developing PCA has been suggested [5,6]. Numerous *in vitro* studies show consistent growth inhibitory and differentiation-inducing effects of vitamin D₃ on prostate carcinoma cells, and animal studies show that it not only reduces the incidence of PCA by acting as a chemopreventive agent but also suppresses metastasis [7–10].

Gap junction (GJ)s are ensembles of cell-cell channels that signal non-canonically, by permitting the direct exchange of small molecules ($\leq$1500Da) between the cytoplasmic interiors of contiguous cells [11]. The constituent proteins of GJs, called connexins (Cxs), are coded by 21 genes, which have been designated according to their molecular mass [12]. Cell-cell channels are bicellular structures formed by the collaborative effort of two cells. To form a GJ cell-cell channel, Cxs first oligomerize in the endoplasmic reticulum or the trans-Golgi network as a hexamer, called connexon, which docks with the connexon displayed on a contiguous cell [13,14]. Multiple lines of evidence now lend credence to the notion that cell-cell communication mediated by gap junctional channels is an important homeostatic control mechanism for regulating cell growth and differentiation and for curbing tumor promotion. For example, impaired Cx expression, or loss of GJ function, has been implicated in the pathogenesis of several types of cancers and diseases [15–19]. Also, mutations in several Cx genes have been detected in genetic disorders characterized by aberrant cellular proliferation and differentiation [13,20].

Our previous studies showed that the expression of Cx32, which is expressed by the luminal cells of the prostate, coincided with the acquisition of the differentiated state of the luminal cells [21,22]. Moreover, we documented that the progression of PCA from an androgen-dependent state to an invasive, androgen-independent state was characterized by the aberrant trafficking of Cx32 and/or impaired assembly into GJs [22–24]. Furthermore, our studies

showed that forced expression of Cx32 into androgen-responsive human PCA cell line, LNCaP, retarded cell growth *in vivo* and *in vitro* [22]. We have also shown that in LNCaP cells expressing Cx32, formation and degradation of GJs were regulated by the androgens, which controlled the expression level of Cx32 posttranslationally by preventing its degradation by endoplasmic reticulum associated degradation (ERAD) [25]. Androgens are required to maintain the secretory (differentiation-related) function of the luminal epithelial cells of normal prostate as depletion of androgens by surgical or chemical means triggers apoptosis and/or dedifferentiation of these cells [26–29]. Our recent studies have shown that retinoids, which also regulate the proliferation and differentiation of prostate epithelial cells [28,30], also enhance the assembly of Cx32 into GJs [31]. These studies lend credence to the notion that formation and degradation of GJs may be linked to the proliferation and differentiation of luminal prostate epithelial cells.

Like androgens and retinoids, vitamin D₃ is essential for the normal development of the prostate and has also been documented to modulate PCA progression [7,9]. Recent studies have shown that vitamin D suppressed prostatic epithelial neoplasia in Nkx3.1/PTEN transgenic mice [32]. Epidemiologic, cell culture, and clinical studies have implicated antitumor effects of 1-25D for PCA and it has been suggested to be a potent chemopreventive agent [3,4]. However, in contrast to colon cancer [1,33], the potential of effectiveness of 1-25D in the chemoprevention of PCA has remained controversial despite numerous studies in transgenic mouse models of PCA and its use in clinical trials [1,2]. Earlier studies, including ours, have shown that the growth-inhibitory and differentiation-inducing effects of chemopreventive agents might be related to their ability to enhance gap junctional communication [34–38]. The luminal cells of normal prostate express Cx32 and form large GJs and progression of PCA is accompanied by loss of ability to form GJs [22,23]. Formation of GJs has been implicated in maintaining the polarized and differentiated state of epithelial cells [39]. These studies prompted us to examine the effect of 1-25D on the assembly of Cx32 into GJs in androgen-responsive human PCA cell line LNCaP. Because 1-25D has been shown to increase the expression of AR in LNCaP cells [40], we rationalized that it might modulate androgen-regulated formation and degradation of GJs and affect growth of androgen-responsive PCA cells that express Cx32. By using androgen-responsive LNCaP cells, which express retrovirally-introduced Cx32 [25], we show that 1-25D enhances the assembly of Cx32 into GJs. Moreover, we further show that 1-25D prevents androgen-regulated degradation of GJs post-translationally, independent of AR-mediated signaling. Finally, our findings show that formation of GJs sensitizes LNCaP cells to growth-inhibitory effects of 1-25D and alters their morphology.

Materials and Methods

Cell Culture

Androgen-responsive human PCA cell line, LNCaP, was grown as described [41,42]. LNCaP-32 cells, one of the several clones of LNCaP cells expressing retrovirally-transduced rat Cx32, and LNCaP-N cells, one of the several control clones selected in G418 after infection with the control retrovirus, have been described [25,31]. Parental LNCaP cells, hereafter referred to as LNCaP-P cells, were grown in RPMI containing 5% fetal bovine serum in an atmosphere of 5% CO_2/95% air whereas LNCaP-N and LNCaP-32 cells were maintained in RPMI containing 5% fetal bovine serum containing G418 at 200 μg/ml as described [25,31]. Steroid–depleted (charcoal-stripped) serum and phenol-red-free

RPMI were obtained from HyClone Laboratories (Salt Lake City, UT).

Antibodies and Immunostaining

The sources of both monoclonal and polyclonal antibodies against Cx32 have been described previously [24,25,31,43,44]. Mouse anti-occludin (clone OC-3F10) was from Zymed laboratories, Inc. (South San Francisco, CA). Rabbit antibodies against α- and β-catenin and mouse anti-β-actin (clone C-15) were from Sigma (St. Louis, MO). Monoclonal antibodies against E-cadherin (E-cad), α-catenin, β-catenin, generously provided by Drs. Johnson and Wheelock (Eppley Institute), have been described [25,43,44]. A rabbit polyclonal anti-AR receptor antibody was from Santa Cruz Biotech (sc-13062, San Diego, CA). Cells (1.5×10^5), seeded in six well clusters containing glass cover slips and allowed to grow to approximately 50% confluence, were immunostained with various antibodies as described [24,25,31,43–45]. Secondary antibodies (rabbit or mouse), conjugated with Alexa 488 and Alexa 594, were used as appropriate. Images of immunostained cells were acquired with Leica DMRIE microscope (Leica Microsystems, Wetzler, Germany) equipped with Hamamatsu ORCA-ER2 CCD camera (Hamamatsu-City, Japan) and analyzed using image processing software (Volocity, Version 6.3; Improvision, Inc; Perkin Elmer) as described [43–45].

Stock Solutions

Synthetic androgen mibolerone (MB) and a natural androgen dihydro-testosterone (DHT), 1-25D, and Casodex (Bicalutamide) were purchased from BIOMOL (ENZO Life Sciences, Inc., Farmingdale, NY). Stock solutions of MB and DHT were prepared at 1 mM in ethanol and stored at −20°C in small aliquots protected from light. Stock solution of 1-25D (10 μM) was prepared in ethanol and stored in aliquots at −80°C protected from light. Stock solution of Casodex (10 mM) was prepared in DMSO and stored in aliquots at −20°C. They were appropriately diluted in the medium at the time of treatment. All experiments were performed in yellow light as described [36,37].

Androgen Depletion and Other Treatments

Cells were seeded in six well clusters with glass cover slips (1.5×10^5 cells per well) and in 6-cm (2×10^5 cells per dish) and 10-cm dishes (3.5×10^5 cells per dish) in 2, 4 and 10 ml complete medium, respectively. Cells were treated by replenishing with fresh medium containing various reagents at the desired concentration when they attained 50% confluence. Controls were treated with ethanol such that the final concentration of the solvent did not exceed 0.1%. When cells were to be grown under androgen-depleted conditions, normal cell culture medium was replaced with androgen-depleted cell culture medium (phenol-red-free RPMI containing 5% charcoal-stripped serum). The controls received fresh phenol-red-free medium containing normal serum. We used phenol-red-free medium because phenol-red has been documented to have steroidogenic effects on the growth of hormone-responsive cell lines, including LNCaP [46,47].

Western Blot Analysis and Detergent Solubility of Connexin32

Cells (5×10^5) were seeded in 10 cm dishes in replicate in 10 ml of complete medium and grown to confluence in the presence and absence of various reagents. Cell lysis, detergent-solubility assay with 1% Triton X-100 (TX100) and the expression level of Cx32 were analyzed by Western blot analysis as described [25,43,44]. Briefly, after lysis in buffer SSK (10 mM Tris, 1 mM EGTA,
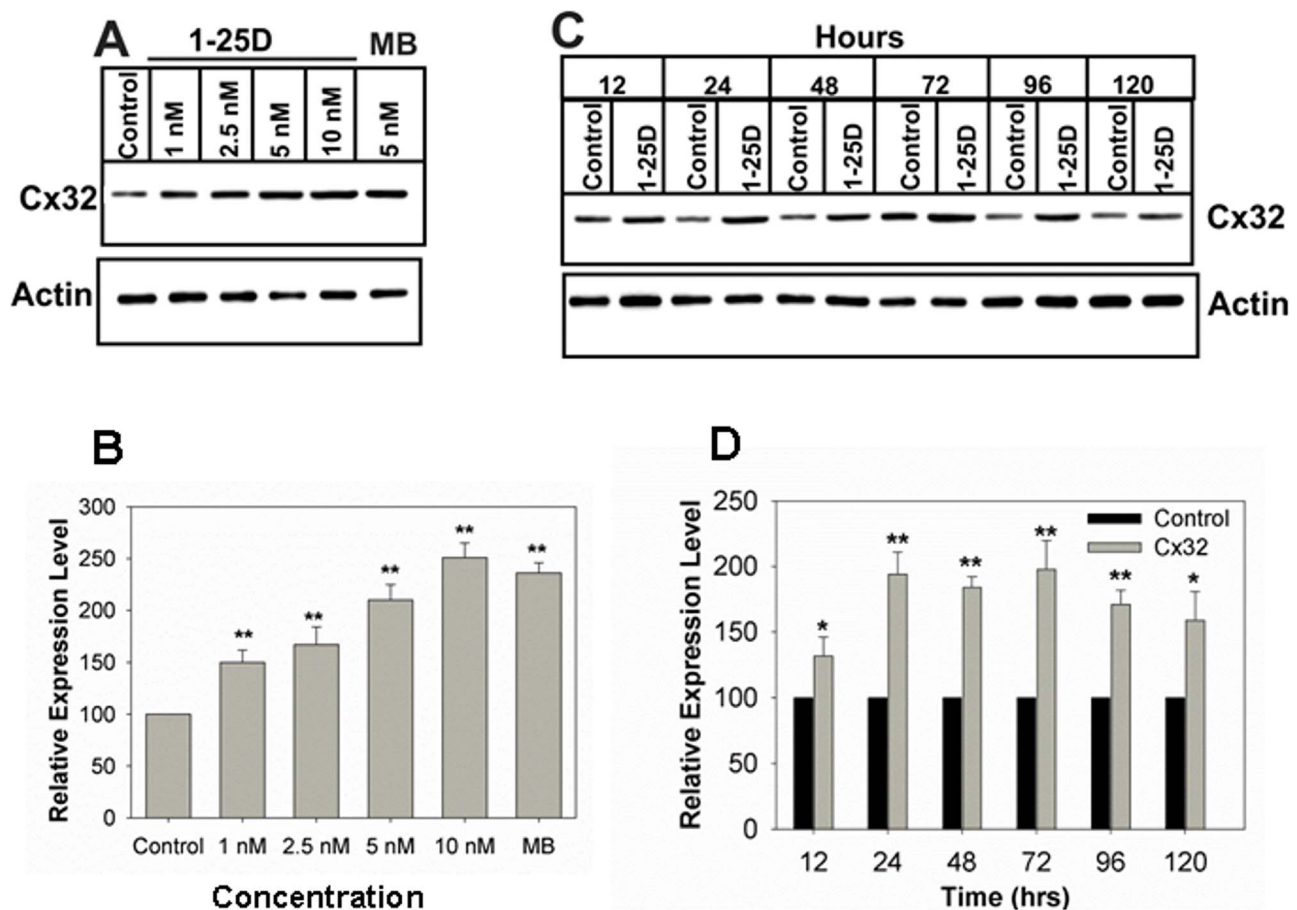
Figure 1. 1-25D increases Cx32 expression level. Cx32-expressing LNCaP-32 cells were treated with the 1-25D, 9-CRA, DHT and MB as indicated. A. Dose-dependent enhancement of Cx32 expression level upon 1-25D treatment for 48 h. **B**. Quantitative analysis of the expression level of the data shown in **A**. Each bar represents the Mean and the Standard Error of the Mean from 4-17 experiments. Note that significant enhancement is observed even at 1 nM. The asterisks (**) indicate P value of ≤0.0001. A two tailed Student's *t* test was used to calculate P value assuming unequal variance. **C**. Kinetics of enhancement of Cx32 expression level upon treatment with 1-25D (10 nM) for the indicated times. Note that enhancement is observed as early as 12 h and plateaus at 72 h. **D**. Quantitative analysis of the expression level of the data shown in C. Each bar represents the Mean and the Standard Error of the Mean from 3-11 experiments. The asterisk (*) indicates P value of ≤0.0016 and asterisks (**) indicate P value of ≤0.0001. A two tailed Student's *t* test was used to calculate P value assuming unequal variance.
doi:10.1371/journal.pone.0106437.g001

1 mM PMSF, 10 mM NaF, 10 mM NEM, 10 mM Na_2VO_4, 10 mM iodoacetamide, 1% TX100, pH 7.4), total, detergent-soluble and -insoluble extracts were separated by ultracentrifugation at 100,000×g for 60 min (35,000 rpm in analytical Beckman ultracentrifuge; Model 17-65 using a SW50.1 rotor). The detergent-insoluble pellets were dissolved in buffer C (70 mM Tris/HCl, pH 6.8, 8 M urea, 10 mM NEM, 10 mM iodoaceta-mide, 2.5% SDS, and 0.1 M DTT). Following normalization based on cell number, the total and TX100-soluble and -insoluble fractions were mixed with 4xSDS-loading buffer to a final concentration of 1x and incubated at room temperature for 1 h before SDS-PAGE analysis. Blots were developed with C-Digit (Li-COR, Lincoln, NE) using SuperSignal WestFemto Maximum Sensitivity Substrate (Thermo Scientific; Rockford, IL).

Communication Assays

Gap junctional communication was assayed by microinjecting Lucifer Yellow (MW 443 Da; Lithium salt), Alexa Fluor 488 (MW 570 Da; A-10436), and Alexa Fluor 594 (MW 760 Da; A-10438) using Eppendorf InjectMan and FemtoJet microinjection systems (models 5271 and 5242, Brinkmann Instrument, Inc. Westbury,

NY) mounted on Leica DMIRE2 microscope. After capturing the images of microinjected cells with the aid of CCD camera (Retiga 2000R, FAST 1394) using QCapture (British Columbia, Canada), the permeability of various fluorescent tracers was quantitated by scoring the number of fluorescent cells at 1 min (Lucifer Yellow), 3 min (Alexa 488) and 15 min (Alexa 594) after microinjection into test cell as described [22,25,43,48].

Colony Formation and Cell Growth Assays

Cell growth was assessed either by colony forming assay or by counting the number of cells as described [22,48]. For colony forming assay, 1×10^3 cells were seeded in 6 cm dishes in triplicate in 3 ml culture medium. After 24 h, one ml medium containing 1-25D, MB or DHT was added to the dishes to give the desired final concentration. Cells were grown for 21 days, with a medium change every 4 days containing the appropriate concentration of the above reagents, when they formed visible colonies. Colonies in dishes were fixed with 3.7% buffered formaldehyde, stained with 0.025% solution of crystal violet in PBS, and photographed. For measuring cell growth, 5×10^4 cells were seeded in 6 cm dishes in replicate and treated with 1-25D described above. Cells were
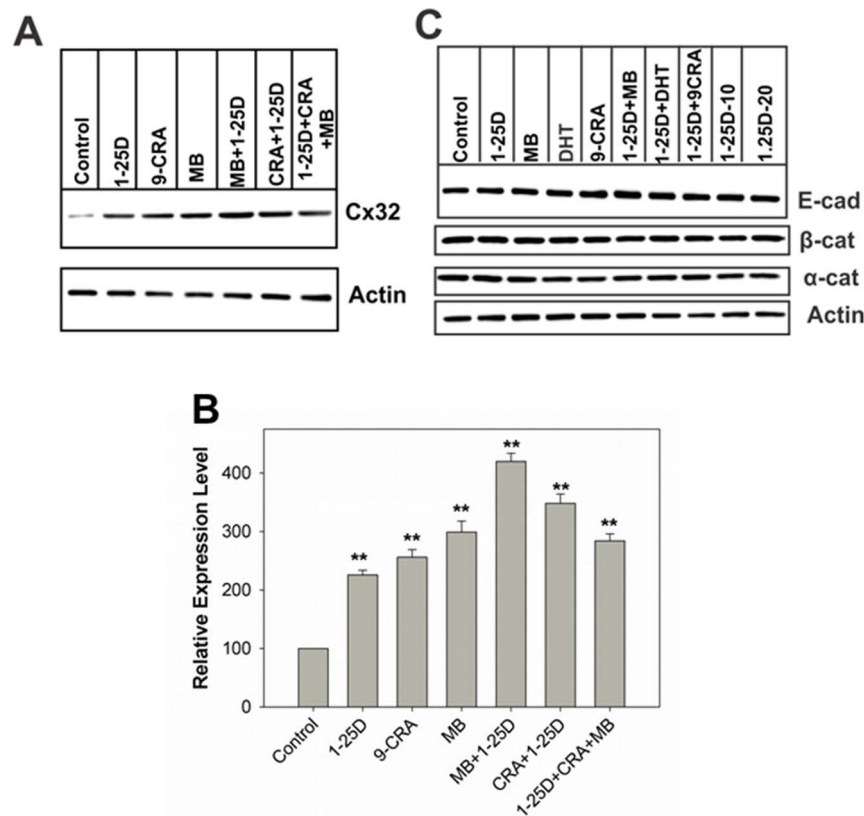
Figure 2. The effect of combined treatment of 1-25D with androgens and retinoids on the expression level of Cx32 and the adherens-junction-associated proteins. Cx32-expressing LNCaP-32 cells were treated with the 1-25D, 9-CRA, DHT and MB as indicated. **A**. Combined treatment with 1-25D with MB or 9-CRA is more effective in increasing Cx32 expression level than treatment with the single agent alone. **B**. Quantitative analysis of the expression level of the data shown in **A**. Each bar represents the Mean and the Standard Error of the Mean from 4-13 experiments. The asterisks (**) indicate P value of ≤0.0001. A two tailed Student's *t* test was used to calculate P value assuming unequal variance. **C**. Effect of 1-25D on adherens junction associated proteins. Expression of adherens junction proteins E-cadherin (E-cad), α-catenin (α-cat), and β-catenin (β-cat) was analyzed by Western blot analysis of total cell lysate (10 µg). Note that there is no effect.
doi:10.1371/journal.pone.0106437.g002

allowed to grow for 10 days with a medium change at day 5. Cells were trypsinized and counted in a hemocytometer.

Results

Vitamin D₃ Enhances Cx32 Expression Level

We used LNCaP-32 cells that express retrovirally-transduced rat Cx32 described previously [25,31]. We previously showed that in LNCaP-32 cells androgens regulated the formation of GJs, post-translationally, by controlling the expression level of Cx32 by inhibiting its ERAD-mediated degradation [25]. Our subsequent studies showed that androgen-regulated degradation of Cx32 was abrogated by all-trans retinoic acid (ATRA) and 9-Cis retinoic acid (9-CRA) [31]. We thus rationalized that 1-25D might act similar to ATRA and 9-CRA. Based on the earlier studies showing the effect of vitamin D on LNCaP cell growth [10,49–52], we treated LNCaP-32 cells with various concentrations of 1-25D to examine its effect on the expression level of Cx32. We found that 1-25D increased Cx32 expression level in a dose-dependent manner (Figure 1A). Significant enhancement was observed even at concentration as low as 1 nM (Figure 1B, left graph). Concentrations higher than 10 nM were toxic to these cells as assessed by the colony formation assay (unpublished data). For subsequent studies we chose 10 nM 1-25D. Time course studies showed that a significant increase in Cx32 expression level

occurred as early as 12 h post-treatment with 1-25D and reached a plateau at 72 h (Figure 1CD, right graph). The effect of 1-25D on Cx32 expression level was as potent as of synthetic androgen, MB, and 9-CRA. Moreover, combined treatment with 1-25D and MB was more effective in increasing Cx32 expression level (Figure 2AB). Vitamin D₃ had previously been shown to affect the expression of level of E-cad, a constituent protein of adherens junctions, in colon cancer cells [33]. To determine if 1-25D also affected the expression level of adherens junction associated proteins, we measured the expression level of E-cad and its associated proteins α- and β-catenins 72 h after treatment with 1-25D. The results showed that 1-25D had no effect on the expression level of E-cad and α- and β-catenins (Figure 2C). As measured by semi-quantitative RT-PCR analysis, 1-25D neither induced the expression of endogenous Cx32 in LNCaP-P or LNCaP-N cells (data not shown) nor altered the expression level of retrovirally-transcribed Cx32 mRNA in LNCaP-32 as documented previously [25].

Vitamin D₃ Enhances Gap Junction Assembly and Junctional Communication

We next examined the effect of 1-25D on the assembly of Cx32 into GJs. We found that, concomitant with an increase in the expression level of Cx32, 1-25D also increased GJ assembly as assessed by immunocytochemical analysis (Figure 3A) and bio-
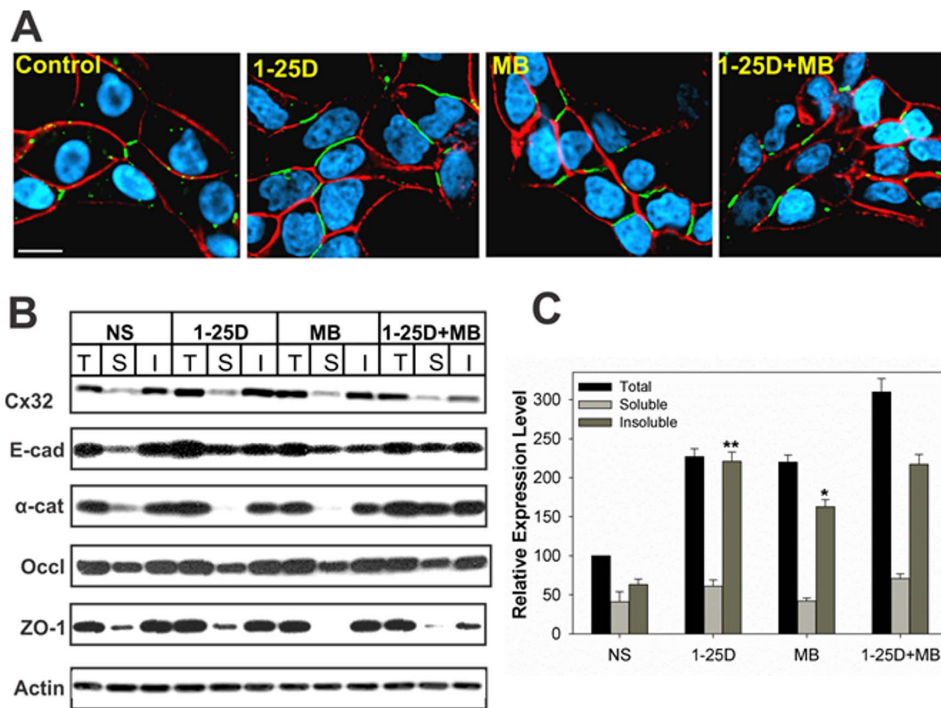
Figure 3. 1-25D enhances the assembly of Cx32 into gap junctions. LNCaP-32 cells, grown either in six well clusters or 10-cm dishes, were treated with 1-25D (10 nM), MB (5 nM) and 1-25D plus MB for 48 h. **A**. Assembly of Cx32 (green) into GJs was assessed immunocytochemically. E-cad is shown in red and the nuclei are in blue. Bar = 20 μM. Note that GJ formation was enhanced upon treatment with 1-25D and MB. **B**. TX100- solubility assay was used to measure the assembly of Cx32 into GJs, of tight junction associated protein, occludin (Occl) and ZO-1, and the adherens junction protein, E-cadherin (E-cad) and α-catenin (α-cat). T = total fraction; S = soluble fraction and I = Insoluble fraction. **C**. Quantitative analysis of the expression level of Cx32 shown in **B**. Each bar represents the Mean and the Standard Error of the Mean from 4-17 experiments. Note that both the total level and the detergent-insoluble fraction of Cx32 increased significantly. Each bar represents the Mean and the Standard Error of the Mean from 3-11 experiments. The asterisk (*) indicates P value of ≤0.0016 and asterisks (**) indicate P value of ≤0.0001. A two tailed Student's *t* test was used to calculate P value assuming unequal variance. Note the absence of effect on adherens junction associated proteins, E-cad, and tight junction associated protein, occludin (Occl).

doi:10.1371/journal.pone.0106437.g003

chemically by Western blot analysis of total, TX100-soluble and –insoluble extracts at 48 h after treatment (Figure 3BC). This biochemical method is based on the principle that Cxs, which are incorporated into GJs, become insoluble in TX100 whereas Cxs that are not incorporated into GJs remain soluble [53]. This assay has been reproducibly shown to measure the assembly of Cxs into GJs as documented by earlier studies [24,25,53]. Moreover, we found that enhancement of GJ assembly was accompanied by a 2-3 fold parallel increase in junctional communication as determined by the junctional transfer of three GJ permeable fluorescent tracers, Lucifer Yellow (MW 443), Alexa 488 (MW 570), and Alexa 594 (MW 760). For example, 1-25D increased junctional transfer of Alexa 594 by 2-3 folds compared to controls (Table 1). The effect of 1-25D on junctional communication was as potent as of synthetic androgen, MB, and the natural androgen DHT (Table 1). To determine if 1-25D affected the assembly of other junctional complexes, we also examined the detergent-solubility of adherens and tight junction associated proteins. The rationale

Table 1. Effect of 1,25D and androgen on the junctional transfer of fluorescent tracers in LNCaP-32 cells.

Junctional Tracer	Expt #	Junctional Transfer [a]			
		NS	NS+1-25D[b]	NS+DHT[b]	NS+MB[b]
Lucifer Yellow (MW 443)	1 2	11.3±2.1(17)[c] 13.1±3.1(19)[c]	27.4±3.1(19)[c] 29.7±5.3(18)[c]	25.6±5.1(21)[c] 29.1±7.3(27)[c]	34.7±5.7(22)[c] 38.1±8.3(20)[c]
Alexa-488 (MW 570)	1 2	14.1±5.3(17)[c] 11.3 ±3.9 (22)c	26.7±4.9(27)[c] 21.3±4.2(24)[c]	26.9.±6.9(23)[c] 23.5±5.1(28)[c]	31.2±7.1(24)[c] 27.3±8.2(29)[c]
Alexa-594 (MW 760)	1 2	6.2±2.1 (20)[c] 7.7±2.7(27)[c]	19.3±3.3(22)[c] 16.5±4.5(29)[c]	15.4±3.8(27)[c] 17.7±5.4(19)[c]	13.7±2.3(23)[c] 14.9±4.1 (26)[c]

LNCaP-32 cells, seeded in 6 cm dishes in replicate, were grown to 65–70% confluence. Junctional transfer was measured after microinjecting fluorescent tracers (see Materials and Methods).
[a]The number of fluorescent cell neighbors (Mean ± SE) 1 min (Lucifer Yellow), 3 min (Alexa-488) and 15 min (Alexa-594) after microinjection into test cell. The total number of injection trials is shown in parentheses.
[b]Cells were treated for 48 h with 1-25D, DHT (10 nM) and MB (2.5 nM).
[c]P≤0.0001 for normal serum versus stripped and treated cells. A two tailed Student's *t* test was used to calculate P value assuming unequal variance.
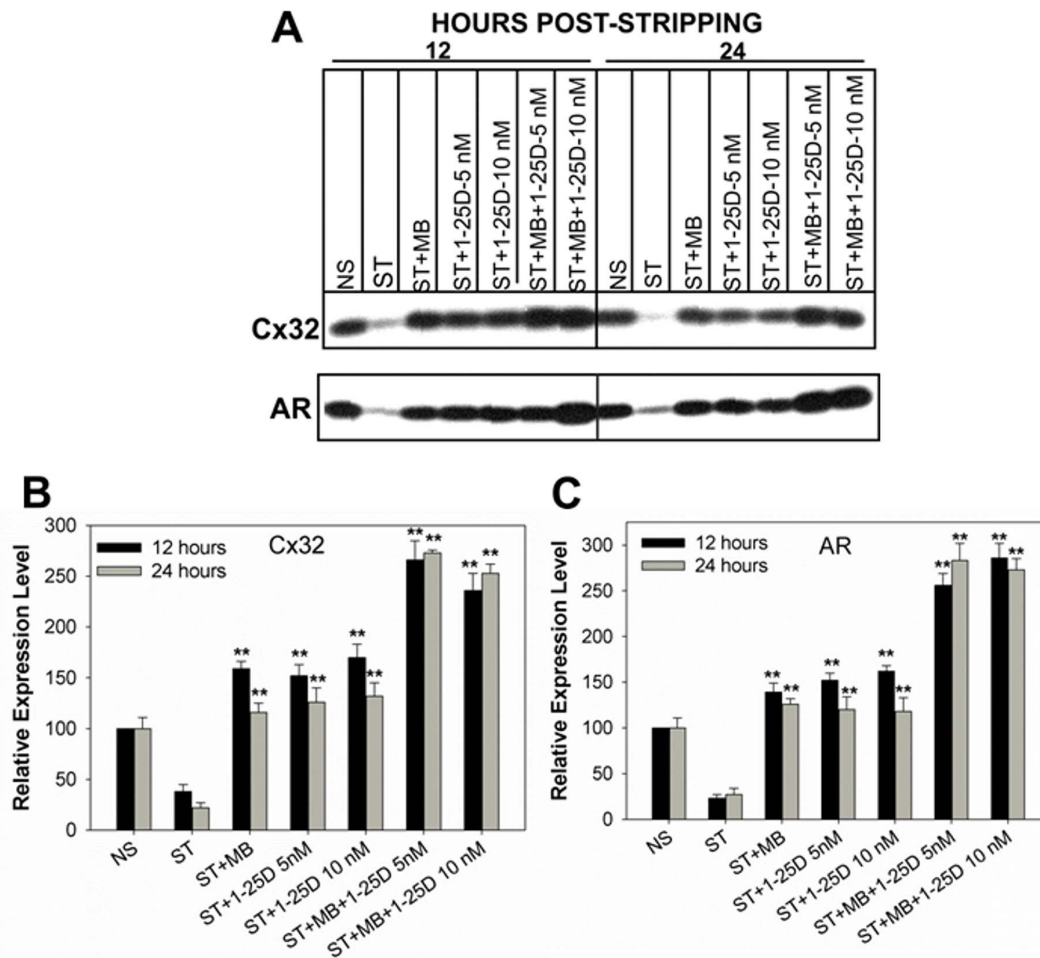doi:10.1371/journal.pone.0106437.t001

Figure 4. 1-25D blocks androgen-regulated degradation of Cx32. LNCaP-32 cells, seeded in 10 cm dishes, were switched to charcoal-stripped (androgen-depleted) medium (ST). Expression level of Cx32 and AR were determined by Western blot analysis (**A**) in the presence and absence of 1-25D (10 nM) and MB (5 nM). Note that Cx32 and AR are degraded upon androgen depletion and degradation is blocked upon 1-25D treatment. **BC**. Quantitative analyses of the expression level of Cx32 (**B**) and AR (**C**) of the data shown in **A**. Each bar represents the Mean and the Standard Error of the Mean from 5-11 experiments. The asterisks (**) indicate P value of ≤0.0001. A two tailed Student's *t* test was used to calculate P value assuming unequal variance.
doi:10.1371/journal.pone.0106437.g004

behind these studies was that E-cad has been shown to facilitate the assembly of Cxs into GJs [43,44,54], and Cx expression has been shown to facilitate the assembly of tight junctions and their constituent proteins [39]. We found that 1-25D had no effect on the solubility of E-cad and its associated proteins, α- and β-catenin, and tight junction associated proteins, ZO-1 and occludin, in TX-100 suggesting that their assembly was not further enhanced into respective cell junctions (Figure 3B). Taken together, these data suggest that 1-25D, like androgens and retinoids, enhances the expression level of Cx32, and its subsequent assembly into GJs, without discernibly altering the expression level of other cell junction associated proteins.

Vitamin D₃ Modulates Androgen-regulated Formation and Degradation of Gap Junctions

Earlier studies with LNCaP-32 cells had shown that androgen depletion caused degradation of Cx32 by ERAD, and that androgens enhanced GJ formation by re-routing the ERAD-targeted pool of Cx32 to the cell surface, making it amenable for GJ assembly [25]. In subsequent studies, we showed that androgen-regulated formation and degradation of GJs was

prevented by 9-CRA and ATRAs [31]. We rationalized that 1-25D might enhance GJ assembly by rescuing the ERAD-targeted pool of Cx32 like 9-CRA and ATRA. Therefore, we examined the expression level of Cx32 and its assembly into GJs upon androgen depletion in the presence and absence of 1-25D in LNCaP-32 cells. For these studies, we used androgen-depleted (charcoal-stripped) and phenol-red-free cell culture medium to grow cells because phenol-red has a weak steroidogenic effect [46]. As was observed in our earlier studies [25], we found that androgen-depletion decreased the expression level of Cx32 within 12 h, which not only was prevented upon addition of MB but also by 1-25D (Figure 4AB). Moreover, combined treatment with MB and 1-25D appeared to be more effective in enhancing the expression level of Cx32 (Figure 4A, upper blot). We also found that androgen depletion decreased the expression level of AR, which was also prevented upon treatment with not only androgens but also with 1-25D (Figure 4A, bottom blot). To substantiate the above data, we further assessed the formation of GJs immunocytochemically (Figure 5A) and functionally by measuring the junctional transfer of Lucifer Yellow, Alexa 488, and Alexa 594 (Table 2). The results showed that GJs were barely observed in
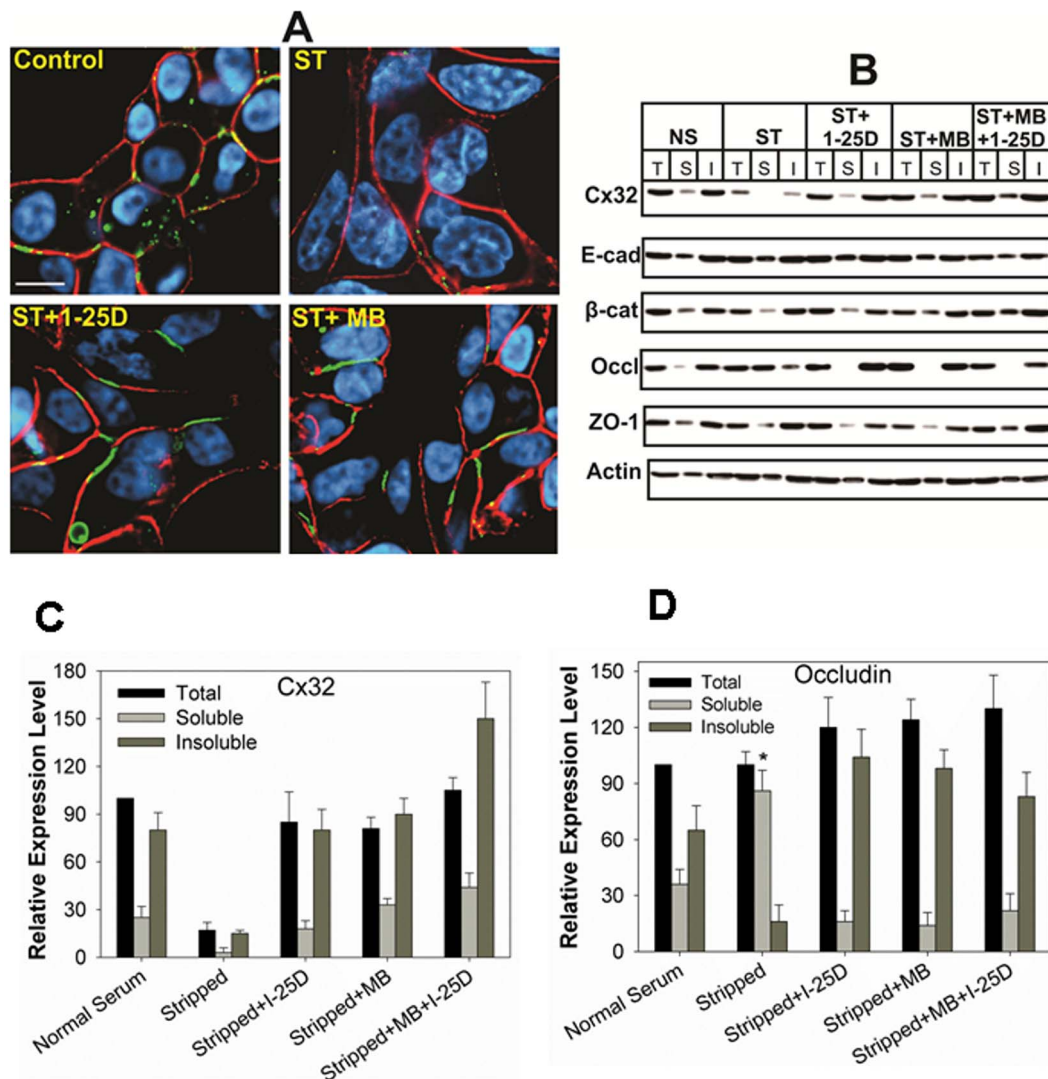
Figure 5. 1-25D blocks androgen-regulated degradation of Cx2 and gap junctions. LNCaP-32 cells, seeded in six well clusters or 10 cm dishes, were switched to charcoal-stripped, androgen-depleted medium (ST). GJ assembly and the expression level of Cx32 were determined by immunocytochemical (**A**) and Western blot (**B**) analyses by TX100-solubility assay in the presence and absence of 1-25D (10 nM) and MB (2.5 nM). In (A), Cx32 is in green and E-cad is red and the nuclei (blue) are stained with DAPI. Scale bar in A = 20 μM. In (B), T = total fraction; S = soluble fraction and I = Insoluble fraction. TX100-soluble and insoluble fractions as well as immunocytochemical assay were performed 24 h post-stripping as described in Materials and Methods. Note that GJs are degraded upon androgen depletion and degradation is blocked upon 1-25D treatment (**A**). Note also that the TX100-soluble fraction of E-cad (E-cad), β-catenin (β-cat) and ZO-1 is not affected. Note also that androgen-depletion increases the soluble fraction of occludin (**B**) without affecting the total occludin levels as quantitated in **D**. The asterisk (*) indicates P value of ≤0.0016 and asterisks (**) indicate P value of ≤0.0001. A two tailed Student's *t* test was used to calculate P value assuming unequal variance.
doi:10.1371/journal.pone.0106437.g005

cells grown in androgen-depleted medium as assessed by the lack of Cx32-specific immunostaining at cell-cell contact areas, while they were readily observed when androgen-depleted medium was supplemented with 1-25D and MB (Figure 5A). Functional assays showed that the junctional transfer of Lucifer Yellow, Alexa 488 and Alexa 594 decreased significantly upon androgen depletion, which was prevented upon replenishing androgen-depleted medium with MB and 1-25D (Table 2), thus substantiating the immunocytochemical data.

The immunocytochemical and junctional transfer data were further corroborated by the TX100-solubility assay (Figure 5BC). We also examined the effect of androgen-depletion on the detergent-solubility of E-cad and β-catenin and tight-junction-associated proteins, ZO-1 and occludin. Consistent with our

earlier studies [25], the results showed that androgen depletion increased the detergent-solubility of occludin but not of ZO-1 and E-cad and β-catenin (Figure 5BD). We also examined the effect of MB and 1-25D either alone or in combination on the formation of GJs in parental LNCaP-P and G418-resistant LNCaP-N cells and found that they had no effect (data not shown). Collectively, these data suggest that 1-25D prevents androgen-regulated degradation of Cx32 and enhances GJ formation in LNCaP-32 cells. Because combined treatment with androgens and 1-25D did not enhance GJ assembly further, it is likely that the assembly was enhanced by rescuing the same pool of Cx32 that was targeted for ERAD upon androgen depletion. Moreover, as was observed in our earlier studies, the assembly and detergent-solubility of Cx32 and

Table 2. Effect of 1-25D and androgens on junctional transfer of fluorescent tracers in LNCaP-32 cells under androgen-depleted conditions.

Treatment	Exp #	Junctional Transfer[a]		
		LY (MW 443)	Alexa 488 (MW 570)	Alexa-594 (MW 760)
NS	1 2	13.3±3.7(31) 12.2±2.5(32)	23.7±4.3(29) 29.1±6.4(23)	17.7±3.9(27) 15.3±5.4(21)
Strip[b]	1 2	1.9±0.6(25)c 2.5±0.9(28)c	2.9±0.3(26)c 2.3±0.7.(22)c	1.1±0.3(21)c 00± 0(17)c
Strip+MB	1 2	27.3±.4.5(37)d 31.7±5.4(26)d	27±3.9(28)d 34.1±6.7(24)d	16.1±2.9(27)d 17.1±3.9(29)d
Strip+1-25D	1 2	29.7±4.9(20)d 30.1±6.1(26)d	33.7±7.6(22)d 30.2±5.5(29)d	14.7±4.1(23)d 15.1±5.3 (22)d
Strip+DHT	1 2	19.2±2.9(26)d 23.1±4.3(20)d	27.2±6.3(27)d 29.8±6.1(23)d	18.1±5.1(33)d 15.6±5.3(26)d

LNCaP-32 cells were seeded as described in Table 1 legend. Cells were switched to charcoal-stripped, androgen-depleted medium (Strip) for 48 h in the presence and absence of 1-25D and synthetic (MB) and the natural (DHT) androgens.
[a]The number of fluorescent cell neighbors (mean ± SE) 1 min (Lucifer Yellow), 3 min (Alexa-488) and 15 min (Alexa-594) after microinjection into test cell. The total number of injection trials is shown in parentheses.
[b]Cells were stripped for 24 h in the presence and absence of 1-25D, DHT (10 nM) and MB (2.5 nM).
[c]P≤0.0001 for normal serum (NS) versus stripped (Strip) for all tracers. A two tailed Student's t test was used to calculate P value assuming unequal variance.
[d]P≤0.0001 for stripped serum (Strip) versus stripped and treated cells for all the tracers. A two tailed Student's t test was used to calculate P value assuming unequal variance.
doi:10.1371/journal.pone.0106437.t002

occludin into cell junctions, or vice versa, appears to be regulated coordinately [25].

1-25D Enhances Gap Junction Formation Independent of Androgen Receptor Function

Our data showed that 1-25D prevented the degradation of AR upon androgen depletion (Figure 4A, bottom blot). Also treatment of LNCaP cells with 1-25D had been shown to enhance AR expression level [40]. Thus, we considered the possibility that the effect of 1-25D on the enhancement of GJ assembly depended on the function of AR alone — and not on the independent effect of 1-25D. To test this notion, we treated LNCaP-32 cells with the anti-androgen, Casodex (Bicalutamide), to block androgen action [55,56]. Both androgen depletion and treatment with Casodex caused degradation of AR (Figure 6A, upper blot, Figure 6B) and abolished the effect of MB and DHT on Cx32 expression level (Figure 6A, bottom blot; Figure 6B) as was observed in our earlier studies [25,31]. However, we found that Casodex had no effect on the enhancement of the expression level of Cx32 resulting from the treatment with 1-25D in androgen-depleted medium (Figure 6AB). To substantiate these data, we next examined the formation of GJs immunocytochemically in cells treated with Casodex in the presence and absence of MB or 1-25D. We found that GJs were not formed when cells were treated with Casodex in normal serum or in androgen-depleted medium containing MB as was observed in our earlier studies (Figure 7) [25,31]. On the other hand, we found that GJs were abundantly formed when cells were treated with Casodex and 1-25D (Figure 7). Altogether, these data suggest that the mechanism by which 1-25D prevents the degradation of Cx32 and enhances GJ formation upon androgen depletion is independent of AR.

Connexin32 Expression Alters the Growth Response of LNCaP Cells to 1-25D

Our earlier studies showed that Cx32 expression potentiated the growth-inhibitory effect of 9-CRA and ATRA in LNCaP cells [31]. To test if 1-25D has similar effect on growth, we measured cell growth of LNCaP-32 cells at concentrations that were barely growth-inhibitory to LNCaP-P cells. We determined cell growth by the colony forming assay as well as by counting the number of cells (Figure 8, Table 3). As assessed visually by the size of the colonies, we found that the growth of LNCaP-32 cells was inhibited by 1-25D whereas the growth of LNCaP-P and LNCaP-N cells was minimally affected (Figure 8AB). These data were substantiated by measuring the growth of LNCaP-32 cells at two different concentrations (Table 3). For example, the growth of LNCaP-P and LNCaP-N cells was inhibited by only 20–25% upon treatment with 1-25D (1nM and 2.5 nM) whereas the growth of LNCaP-32 cells was inhibited by 55–70%. Moreover, we found that higher concentrations of 1-25D (5 and 10 nM) altered the morphology of LNCaP-32 cells profoundly such that LNCaP-32 cells treated with 1-25D appeared flatter and more epithelial-like whereas these changes were minimally observed in LNCaP-P and LNCaP-N cells (Figure 9). Change occurred only in response to 1-25D; and only when cells had been growing in 1-25D-containing medium for at least 4 days and have begun to be contact-inhibited and growth-arrested.

Discussion

The main findings of this study are as follows: 1. 1-25D enhances the expression level of Cx32 and its assembly into functional GJs in androgen-responsive LNCaP cells through inhibition of Cx32's degradation. 2. Formation of GJs sensitizes LNCaP cells to the growth inhibitory effect of 1-25D. We previously showed that 9-CRA and ATRA, the two well-known chemopreventive agents, also enhanced GJ assembly and sensitized these cells to their growth inhibitory effects [31]. Thus, it appears that GJ assembly is also the down-stream target of 1-25D in androgen-responsive LNCaP-32 cells, leading to suppression of growth. Several independent lines of inquiry prompted us to undertake these studies. First, growth inhibitory and chemopreventive effects of retinoids and vitamin D₃ had been previously documented to correlate with their ability to enhance the assembly of Cxs into GJs in other cancer cell types [35–37,57]. Second, the differentiated and polarized state of epithelial cells of the prostate, as well as of several other exocrine glands and tissues, had generally been found to coincide with the expression of Cx32 and its assembly into GJs [22,23,58]. Third, numerous studies had shown that like androgens [28,29], retinoids [57,59–63], and 1-25D were essential for the growth and differentiation of the prostate [4,7,64]. Hence, we rationalized that its expression and
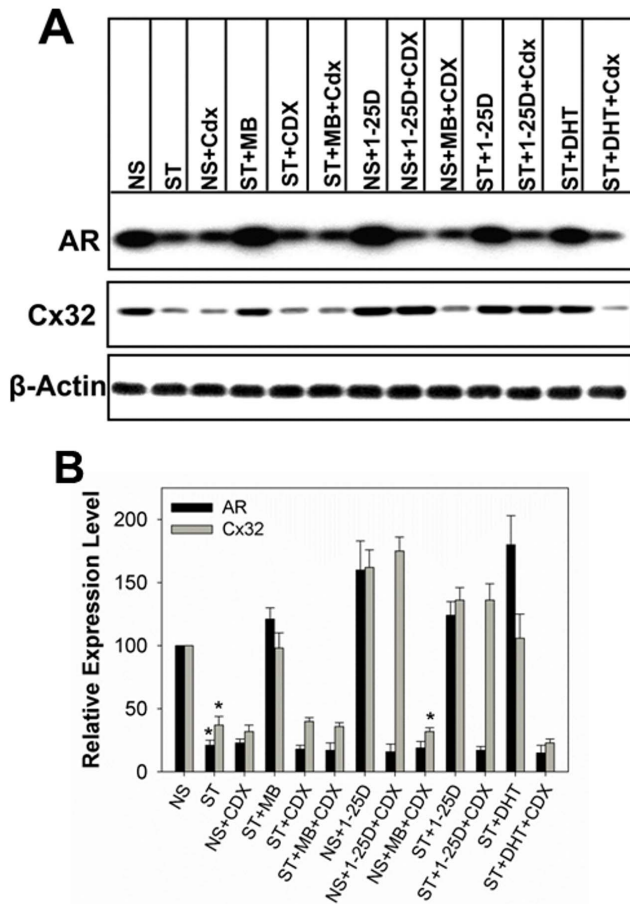
Figure 6. Effect of 1-25D and MB on the expression level of Cx32 and AR in the presence and the absence of Casodex. LNCaP-32 cells, seeded in 6-cm dishes, were grown to 70% confluence. Cells were then grown for additional 24 h in normal medium (NS), androgen-depleted medium alone (ST), normal serum supplemented with Casodex (CDX; NS+CDX), androgen-depleted medium supplemented with MB (ST+MB), MB and Casodex (ST+MB+CDX), 1-25D (ST+1-25D), 1-25D and Casodex (ST+1-25D+CDX) and in normal serum with 1-25D (NS+1-25D). Expression level Cx32 and AR were analyzed by Western blotting (**A**). Note that Cx32 is not degraded in cells treated with 1-25D both in the presence and absence of Casodex whereas it is degraded in normal serum and androgen-depleted but MB supplemented medium containing Casodex. **B**. Quantitative analyses of the expression level of Cx32 and AR of the data shown in **A**. Each bar represents the Mean and the Standard Error of the Mean from 3-9 experiments. The asterisks (*) indicate P value of ≤0.0001. A two tailed Student's *t* test was used to calculate P value assuming unequal variance.
doi:10.1371/journal.pone.0106437.g006

Figure 7. Effect of 1-25D and MB on the formation of gap junctions in the presence and the absence of Casodex. LNCaP-32 cells, seeded on glass cover slips, were grown to 70% confluence. Cells were then grown for additional 24 h in normal medium (NS), androgen-depleted medium alone (ST), normal serum supplemented with Casodex (CDX; NS+CDX), androgen-depleted medium supplemented with MB (ST+MB), MB and Casodex (ST+MB+CDX), 1-25D (ST+1-25D), 1-25D and Casodex (ST+1-25D+CDX) and in normal serum with 1-25D (NS+1-25D). Gap junction formation was assessed immunocytochemically. Note that GJs (green) are not degraded in cells treated with 1-25D both in the presence and absence of Casodex whereas they are degraded in normal serum and androgen-depleted but MB supplemented medium containing Casodex. E-cad is shown in red and the nuclei (blue) are stained with DAPI. Scale Bar = 20 μM.
doi:10.1371/journal.pone.0106437.g007

assembly into GJs might as well as be regulated by 1-25D either alone or in conjunction with the androgens.

How might 1-25D enhance GJ assembly in LNCaP-32 cells? Nearly 50% of newly synthesized Cx32 may be degraded in the endoplasmic reticulum by ERAD [65]. We had previously shown that in LNCaP-32 cells, androgen depletion caused the degradation of nearly 70–80% of Cx32 by ERAD, and degradation was prevented upon replenishment with the androgens, which allowed Cx32 to traffic to the cell surface and assemble into GJs [25]. These studies further showed that androgens neither induced the expression of Cx32 in Cx-null LNCaP-P cells nor increased the expression level of retrovirally-driven Cx32 in LNCaP-32 cells [25,31]. Thus, in LNCaP-32 cells, androgens enhanced the
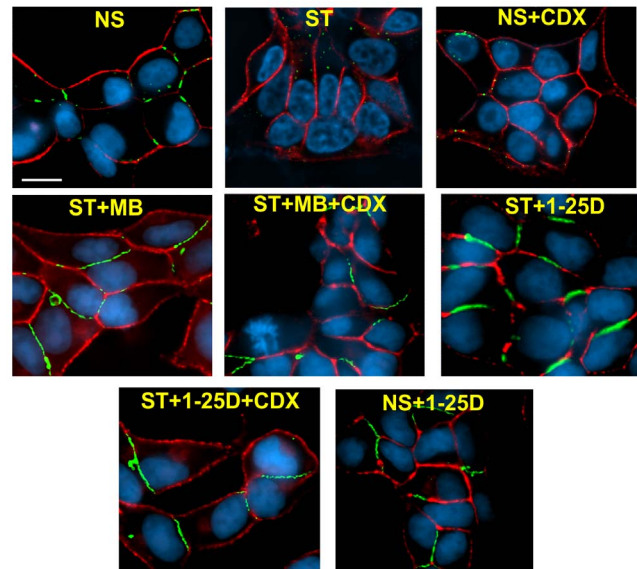
expression level of Cx32 posttranslationally [25]. Although not tested directly, our data seem to suggest that 1-25D also enhances GJ assembly by preventing the androgen-regulated degradation of Cx32 by ERAD posttranslationally both under normal and androgen-depleted conditions. Like androgens, 1-25D neither induced the expression of the endogenous Cx32 in LNCaP-32 cells nor affected retroviral driven Cx32 mRNA transcripts. Our previous studies with LNCaP-32 cells showed that AR-mediated signaling was the sole determining factor in enhancing Cx32 expression level and preventing GJ degradation both under androgen-depleted or androgen-containing medium as Casodex, which inhibits AR-function [66], annulled the effect of androgens on Cx32 expression level and its subsequent assembly into GJs [25]. With regard to 1-25D effect, our data showed that it enhanced the expression level of AR under androgen-depleted conditions (Figure 4). Therefore, it is possible that the effect of 1-25D in the absence of androgens may be indirectly caused by persistent and increased level of AR and its activation by the trace amounts of androgens present in the charcoal-stripped medium. However, 1-25D also enhanced GJ assembly robustly in the presence Casodex in androgen-depleted medium, which robustly decreased AR level and inhibited AR function (Figure 6). One plausible explanation for these findings is that 1-25D activates an AR-dependent mechanism under androgen-depleted conditions to rescue the ERAD-targeted pool of Cx32 yet triggers another signaling pathway to enhance GJ assembly when AR function is inhibited by Casodex both under normal and androgen-depleted conditions. Further studies are required to explore this possibility.
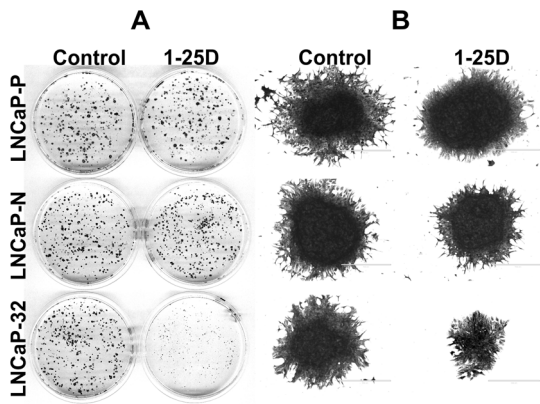
Figure 8. Connexin32 expression and junction formation augments the growth inhibitory effect of 1-25D. LNCaP-P, LNCAP-N and LNCaP-32 cells were seeded at clonal density (2×10^3) and treated with 1-25D (1 nM) after 24 h. Cells were grown for 21 days with a medium change every 4 days when they formed colonies. Colonies were fixed and stained with crystal violet. **A**. Representative dishes showing colonies. **B**. Morphology of the individual colonies at higher magnification. Note the robust decrease in colony size in 1-25D-treated dishes.
doi:10.1371/journal.pone.0106437.g008

Figure 9. 1-25D alters the morphological phenotype of Cx32-expressing LNCaP cells. LNCaP-P, LNCaP-N and LNCaP-32 cells were seeded at a density of 2-3$\times10^4$ per 6-cm dish and treated with the indicated concentrations of 1-25D after 24 hrs. After 5 days, cells were fixed and stained with crystal violet. Note robust morphological changes in LNCaP-32 cells treated with 1-25D.
doi:10.1371/journal.pone.0106437.g009

Of note here are the findings that similar effects were also observed with 9-CRA and ATRA [31].

Cadherins have been shown to facilitate the assembly of Cxs into GJs. However, we failed to observe any effect of 1-25D on the expression and degradation of adherens junction associated proteins, E-cad and its associated proteins α and β catenin under androgen-containing and androgen-depleted conditions (Figures 3 and 5). Therefore, E-cad and its assembly into adherens junctions are not the likely targets of 1-25D in enhancing GJ assembly in contrast to its effect on E-cad expression in human colon carcinoma cells [33]. The assembly of Cx32 into GJs has also been shown to affect tight junction assembly [39,67]. Our previous studies had shown that androgen depletion increased the detergent-solubility of occludin, without significantly altering its expression level, and that the trafficking of occludin to the cell surface and its detergent-solubility was controlled by the assembly of Cx32 into GJs under androgen-depleted conditions [25]. Similar observations were also made in other cell lines [39,68,69]. The present study also showed that androgen-depletion increased the detergent-soluble fraction of occludin without altering its expression level, which was negated when LNCaP-32 cells were treated with 1-25D (Figure 5BD). In this regard, our data suggest that the assembly of Cx32 and occludin might as well be coordinately regulated by 1-25D, and that this may be one of the additional mechanisms by which 1-25D maintains the polarized state of prostate epithelial cells and acts as a differentiating and chemopreventive agent. Further studies are required to substantiate this notion.

1-25D has been shown to induce G0/G1 arrest, differentiation and apoptosis of tumor cells by modulating different signaling pathways to delay tumor progression in different cancer cell types; moreover, it has also been known to potentiate the cytotoxic effects of many chemotherapeutic agents [1–3]. Several studies have shown that vitamin D inhibits the growth of PCA cell lines, including LNCaP, in both AR-dependent and –independent manner [10,49,50,70,71]. We found that the expression of Cx32 potentiated the growth inhibitory effect of 1-25D such that suppression of growth was observed at doses which had no
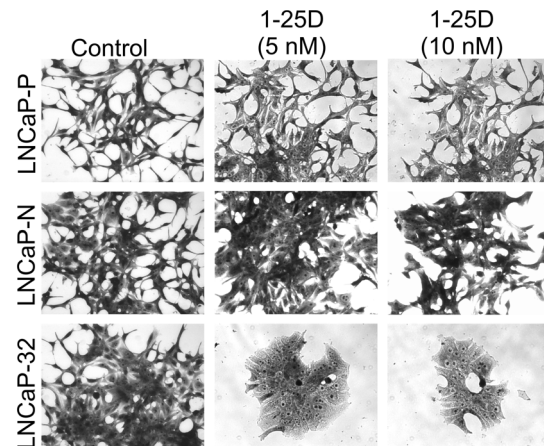
significant effect on the growth of Cx-null LNCaP cells (Figure 8, Table 3). For example, 1-25D at 1nM barely inhibited the growth of LNCaP-P and LNCaP-N cells but inhibited the growth of LNCaP-32 by more than 50% (see Table 3). Earlier studies had shown that LNCaP cells were sensitized to undergo apoptosis by tumor necrosis factor α, TRAIL, and anti-Fas antibodies when Cx43 was expressed via adenoviruses to which Cx-null LNCaP cells were resistant [72]. Moreover, expression of Cx32 not only inhibits the growth of cells but also induces differentiation in breast cancer cell lines as well as in LNCaP cells [22,73,74].

What might be the possible explanation for the growth-suppressive effects of 1-25D with regard to the assembly of Cx32 into GJs? The signaling pathways that are activated or suppressed upon formation and degradation of GJs to impact cell growth and differentiation are not well-understood [16,17,75–79]. Elegant studies in Cx32 knockout mice revealed increased activation of mitogen-activated protein kinases and decreased level of tumor suppressor p27Kip1 [80–82]. While it is well-known that 1-25D suppresses the growth of several human PCA cell lines, the effect appear not to depend on the expression level of vitamin D receptor. For example, only LNCaP cells were found to be exquisitely sensitive to the growth inhibitory effect of 1-25D whereas other PCA cell lines, such as PC-3, DU-145 and ALVA-31, were barely sensitive despite the fact that all cell types expressed nearly similar levels of vitamin D receptor [50,71,83,84]. Also, in LNCaP cells the growth suppression by 1-25D was mediated via increased expression of cyclin-dependent kinase inhibitors p21waf1/cip1 and p27kip1 as well as through hyper-phosphorylation of retinoblastoma protein, resulting in G0/G1 arrest [50]. Given the fact that Cx expression also has an impact on cell cycle [79,85], it is possible that transmission of growth-regulatory signals through channels composed of Cx32 activates signaling pathways that increase the expression of gene-regulatory proteins involved in the control of cell cycle progression as proposed [18,79]. Given the multiple effects of 1-25D on different tumor cell types, it is at present difficult to envisage how its chemopreventive, pro-differentiating and growth-inhibitory effects are related to its ability to regulate formation and degradation of GJs [16–18,77,79,86]. More elaborate studies are underway to explore the molecular basis of the augmentation of

Table 3. Cx32 expression sensitizes LNCaP cells to growth inhibitory effect of 1-25D.

Treatment	LNCaP-P	LNCaP-N	LNCaP-32
Experiment # 1			
Control	7.9±1.5 (100±19)a	7.1±1.1 (100±15)a	6.5±1.6 (100±25)b
MB (2.5 nM)	6.1±1.4 (77±23)a	6.2±1.2 (87±19)a	3.7±0.8 (57±22)b
1-25D (1 nM)	6.8±1.3 (86±19)a	6.8±1.1 (96±16)a	2.9±0.3 (45±10)b
1-25D (2.5 nM)	5.9±0.9 (75±15)a	6.3±1.0 (89±16)a	1.9±0.4 (29±21)b
Experiment #2			
Control	7.7±1.8 (100±23)a	7.1±1.7 (100±24)a	6.7±1.5 (100±22)b
MB (2.5 nM)	6.7±1.1 (87±16)a	6.3±1.2 (89±19)a	3.8±0.6 (57±16)b
1-25D (1 nM)	6.2±0.6 (81±10)a	6.6±1.3 (93±20)a	2.8±0.8 (42±29)b
1-25D (2.5 nM)	6.6±0.9 (86±14)a	6.2±1.5 (87±24)a	2.2±0.7 (33±32)b
Experiment # 3			
Control	8.3±1.5 (100±18)a	7.4±1.9 (100±26)a	6.9±1.0 (100±14)b
MB (2.5 nM)	7.2±1.0 (87±14)a	6.6±1.4 (89±21)a	3.2±0.7 (46±22)b
1-25D (1 nM)	6.8±1.3 (82±16)a	6.8±1.1 (92±16)a	2.6±0.9 (38±34)b
1-25D (2.5 nM)	6.9±1.1 (86±16)a	6.4±1.2 (86±19)a	2.3±0.5 (33±22)b

LNCaP-P, LNCaP-N and LNCaP-32 cells were seeded in 6-cm dishes in replicate (5×10⁴ cells/dish) and treated with 1-25D (1 nM or 2.5 nM) and MB (2.5 nM). Cells were grown for 10 days with a medium change at day 2 and 5. Cells were trypsinized and counted as described in Materials and Methods. The values represent Mean number of cells per dish ×10⁵ ± SE of the Mean. Values in the parentheses represent Means of % Growth ± SE of the Mean.
aP≥0.12.
bP≤0.05.
doi:10.1371/journal.pone.0106437.t003

growth-suppressive effect of 1-25D in LNCaP cells upon formation of GJs.

An intriguing observation made during this study was that 1-25D caused a radical change in the morphology of LNCaP-32 cells compared to Cx-null LNCaP-P and LNCaP-N cells such that the treated cells became flatter and acquired an epithelial morphology (Figure 9). Expression of Cx32 by itself had no conspicuous effect on the morphology and the change occurred only in response to 1-25D; and only when cells had been growing in 1-25D-containing medium for at least 4 days and have begun to be contact-inhibited and growth-arrested. One possible explanation for these data is that the formation of large GJs in response to 1-25D permits a more elaborate remodeling of the cortical actin network, which has emerged as a key regulator of cell morphology [87,88]. This notion is supported by studies that utilized embryonic fibroblasts from Cx43 knockout mice in wound-healing studies. Fibroblasts from Cx43 knockout mice showed cell polarity defects as characterized by the failure of the microtubule organizing center to reorient with the direction of wound closure as well as failure of actin stress fibers to appropriately align at the wound edge [89]. Whether expression of Cx32 in LNCaP cells also governs cell shape in response to 1-25D through modulation of actin-cortex or microtubule network remains to be explored in future studies.

Several pre-clinical and clinical trials have suggested that a decrease in vitamin D₃ levels contributes to the development and possibly to the progression of human PCA [1,2,90,91]. Connexin32 is expressed by the luminal epithelial cells of normal prostate and is aberrantly assembled in the epithelial cells of prostate tumors [22,23]. Because GJs have been implicated in maintaining the polarized and differentiated state of epithelial cells [39], we propose that the chemopreventive effects 1-25D in PCA may result from its ability to enhance the formation of GJs. Our results show that GJ assembly is the down-stream target of signaling initiated by 1-25D and that the formation of GJs sensitizes PCA cells to its growth modulatory influence. Because loss of cell junctions is a hallmark of PCA progression [29] and might occur as early as during prostatic intraepithelial neoplasia [92,93], understanding basic cell and molecular biological mechanisms by which 1-25D might govern the formation of GJs will provide new insights with regard to signaling pathways utilized to maintain the polarized and the differentiated state of epithelial cells in prostate tumors. This should open innovative avenues for designing new therapeutic approaches to delay the onset of malignancy as loss of polarization is the earliest changes that may initiate PCA progression [92].

Acknowledgments

Author Contributions

Conceived and designed the experiments: PM SC SM. Performed the experiments: LK PK AR SM SC. Analyzed the data: LK PK AR SM SC PM ML. Contributed reagents/materials/analysis tools: SM SC ML. Wrote the paper: PM.

References

1. Fleet JC, Desmet M, Johnson R, Li Y (2012) Vitamin D and cancer: a review of molecular mechanisms. Biochemical Journal 441: 61–76.
2. Deeb KK, Trump DL, Johnson CS (2007) Vitamin D signalling pathways in cancer: potential for anticancer therapeutics. Nat Rev Cancer 7: 684–700.
3. Swami S, Krishnan AV, Feldman D (2011) Vitamin D metabolism and action in the prostate: Implications for health and disease. Molecular and Cellular Endocrinology 347: 61–69.

4. Krishnan AV, Feldman D (2010) Molecular pathways mediating the anti-inflammatory effects of calcitriol: implications for prostate cancer chemoprevention and treatment. Endocr Relat Cancer 17: R19–R38.

5. Schwartz GG, Hulka BS (1990) Is vitam D deficiency a risk factor for prostate cancer? Anticancer Res 10: 1307–1311.

6. Schwartz GG, Hill CC, Oeler TA, Becich MJ, Bahnson RR (1995) 1,25-Dihydroxy-16-ene-23-yne-vitaminD3 and prostate cancer proliferation in vivo. Urology 46: 365–369.

7. Konety BR, Schwartz GG, Acierno JS, Becich MJ, Getzenberg (1996) The role of vitamin D in normal prostate growth and differentiation. Cell Growth Diff 7: 1563–1570.

8. Lokeshwar BL (1999) Inhibition of prostate cancer metastasis in vivo: a comparison of 1,25-dihydroxy vitamin D (calcitrol) and EB1089. Cancer Epidemiol Biomark Prev 8: 241.

9. Peehl D, Feldman D (2003) The role of vitamin D and retinoids in controlling prostate cancer progression. Endocr Relat Cancer 10: 131–140.

10. Yang ES, Maiorino CA, Roos BA, Knight SR, Burnstein KL (2002) Vitamin D-mediated growth inhibition of an androgen-ablated LNCaP cell line model of human prostate cancer. Mol Cell Endocrinol 186: 69–79.

11. Goodenough DA, Paul DL (2009) Gap Junctions. Cold Spring Harbor Perspectives Biology 1: a002576.

12. Beyer EC, Berthoud VM (2009) The Family of Connexin Genes. In: Harris A, Locke D, editors. Connexins: A Guide. Springer. pp. 3–26.

13. Laird DW (2006) Life cycle of connexins in health and disease. Biochem J 394: 527–543.

14. Thevenin AF, Kowal TJ, Fong JT, Kells RM, Fisher CG, et al. (2013) Proteins and Mechanisms Regulating Gap-Junction Assembly, Internalization, and Degradation. Physiology 28: 93–116.

15. Crespin S, Defamie N, Cronier L, Mesnil M (2009) Connexins and carcinogenesis. In: Harris A, Locke D, editors. Connexinss: A Guide. pp. 529–542.

16. Naus CC, Laird DW (2010) Implications and challenges of connexin connections to cancer. Nat Rev Cancer 10: 435–441.

17. Trosko J (2006) From adult stem cells to cancer stem cells: Oct-4 Gene, cell-cell communication, and hormones during tumor promotion. Ann NY Acad Sci 1089: 36–58.

18. Trosko J (2007) Gap Junctional Intercellular Communication as a Biological "Rosetta Stone" in Understanding, in a Systems Biological Manner, Stem Cell Behavior, Mechanisms of Epigenetic Toxicology, Chemoprevention and Chemotherapy. J Memb Biol 218: 93–100.

19. Wei CJ, Xu X, Lo CW (2004) Connexins and cell signaling in development and disease. Ann Rev Cell Dev Biol 20: 811–838.

20. Xu J, Nicholson BJ (2013) The role of connexins in ear and skin physiology-Functional insights from disease-associated mutations. Biochimica et Biophysica Acta (BBA) - Biomembranes 1828: 167–178.

21. Habermann H, Chang WY, Birch L, Mehta P, Prins GS (2001) Developmental Exposure to Estrogens Alters Epithelial Cell Adhesion and Gap Junction Proteins in the Adult Rat Prostate. Endocrinology 142: 359–369.

22. Mehta PP, Perez-Stable C, Nadji M, Mian M, Asotra K, et al. (1999) Suppression of human prostate cancer cell growth by forced expression of connexin genes. Dev Genetics 24: 91–110.

23. Habermann H, Ray V, Prins G (2002) Alterations in gap junction protein expression in human benign prostatic hyperplasia and prostate cancer. J Urol 167: 655–660.

24. Govindarajan R, Song X-H, Guo R-J, Wheelock MJ, Johnson KR, et al. (2002) Impaired traffcking of connexins in androgen-independent human prostate cancer cell lines and its mitigation by α-catenin. J Biol Chem 277: 50087–50097.

25. Mitra S, Annamalai L, Chakraborty S, Johnson K, Song X, et al PP (2006) Androgen-regulated Formation and Degradation of Gap Junctions in Androgen-responsive Human Prostate Cancer Cells. Mol Biol Cell 17: 5400–5416.

26. Abate-Shen C, Shen M (2000) Molecular genetics of prostate cancer. Genes Dev 14: 2410–2434.

27. Cunha G, Donjacour A, Cooke P, Mee S, Bigsby R, et al. (1987) The endocrinology and developmental biology of the prostate. Endocr Rev 8: 338–362.

28. Marker P, Donjacour A, Dahiya R, Cunha G (2003) Hormonal, cellular, and molecular control of prostatic development. Dev Biol 253: 165–174.

29. Shen MM, Abate-Shen C (2010) Molecular genetics of prostate cancer: new prospects for old challenges. Genes & Development 24: 1967–2000.

30. Aboseif S, Dahiya R, Narayan P, Cunha G (1997) Effect of retinoic acid on prostate development. Prostate 31: 161–167.

31. Kelsey L, Katoch P, Johnson K, Batra SK, Mehta P (2012) Retinoids regulate the formation and degradation of gap junctions in androgen-responsive human prostate cancer cells. PLoS ONE 7: E32846.

32. Banach-Petrosky W, Ouyang X, Gao H, Nader K, Ji Y, et al. (2006) Vitamin D Inhibits the Formation of Prostatic Intraepithelial Neoplasia in Nkx3.1; Pten Mutant Mice. Clinical Cancer Research 12: 5895–5901.

33. Palmer HG, Gonzalez-Sancho JM, Espada J, Berciano MT, Puig I, et al. (2001) Vitamin D(3) promotes the differentiation of colon carcinoma cells by the induction of E-cadherin and the inhibition of beta-catenin signaling. J Cell Biol 154: 369–387.

34. Bertram J (1999) Carotenoids and Gene Regulation. Nutr Rev 57: 182–191.

35. King TJ, Bertram JS (2005) Connexins as targets for cancer chemoprevention and chemotherapy. Biochimica et Biophysica Acta (BBA) - Biomembranes 1719: 146–160.

36. Mehta P, Loewenstein W (1991) Differential regulation of communication by retinoic acid in homologous and heterologous junctions between normal and transformed cells. J Cell Biol 113: 371–379.

37. Mehta P, Bertram J, Loewenstein W (1989) The actions of retinoids on cellular growth correlate with their actions on gap junctional communication. J Cell Biol 108: 1053–1065.

38. Trosko J, Chang C-C (2001) Mechanism of up-regulated gap junctional intercellular communication during chemoprevention and chemotherapy of cancer. Mutat Res 480: 219–229.

39. Kojima T, Murata M, Go H, Spray DC, Sawada N (2007) Connexins induce and maintain tight junctions in epithelial cells. J Membr Biol 217: 13–19.

40. Zhao X, Ly L, Peehl D, Feldman D (1999) Induction of androgen receptor by 1alpha,25-dihydroxyvitamin D3 and 9-cis retinoic acid in LNCaP human prostate cancer cells. Endocrinology 140: 1205–1212.

41. Igawa T, Lin FF, Lee MS, Karan D, Batra SK, et al. (2002) Establishment and characterization of androgen-independent human prostate cancer LNCaP cell model. Prostate 50: 222–235.

42. Lin MF, Meng TC, Rao PS, Chang C, Schonthal AH, et al. (1998) Expression of human prostatic acid phosphatase correlates with androgen-stimulated cell proliferation in prostate cancer cell lines. J Biol Chem 273: 5939–5947.

43. Chakraborty S, Mitra S, Falk MM, Caplan S, Wheelock MJ, et al. (2010) E-cadherin differentially regulates the assembly of connexin43 and connexin32 into gap junctions in human squamous carcinoma cells. J Biol Chem 285: 10761–10776.

44. Govindarajan R, Chakraborty S, Falk MM, Johnson KR, Wheelock MJ, et al. (2010) Assembly of connexin43 is differentially regulated by E-cadherin and N-cadherin in rat liver epithelial cells. Mol Biol Cell 21: 4089–4107.

45. Johnson KE, Mitra S, Katoch P, Kelsey LS, Johnson KR, et al. (2013) Phosphorylation on Ser-279 and Ser-282 of connexin43 regulates endocytosis and gap junction assembly in pancreatic cancer cells. Mol Biol Cell 24: 715–733.

46. Glover JF, Irwin JT, Darbre PD (1988) Interaction of Phenol Red with Estrogenic and Antiestrogenic Action on Growth of Human Breast Cancer Cells ZR-75-1 and T-47-D. Cancer Research 48: 3693–3697.

47. Lin M-F, Lee MS, Garcia-Arenas R, Lin F-F (2000) Differential responsivenesss of prostatic acid phosphatae and prostate-specific antigen mRNA to androgen in prostate cancer cells. Cell Biology International 24: 681–689.

48. Mehta P, Bertram J, Loewenstein W (1986) Growth inhibition of transformed cells correlates with their junctional communication with normal cells. Cell 44: 187–196.

49. Yang ES, Burnstein KL (2003) Vitamin D Inhibits G1 to S Progression in LNCaP Prostate Cancer Cells through p27Kip1 Stabilization and Cdk2 Mislocalization to the Cytoplasm. J Biol Chem 278: 46862–46868.

50. Zhuang S-H, Burnstein KL (1998) Antiproliferative effect of 1α, 25-dihydroxyvitamin D3 in human prostate cancer cell line LNCaP involves reduction of cyclin-dependent kinase 2 activity and persistent G1 accumulation. Endocirnology 139: 1197–1207.

51. Lokeshwar B (1999) Inhibition of prostate cancer metastasis in vivo: a comparison of 1,25-dihydroxy vitamin D (calcitrol) and EB1089. Cancer Epidemiol Biomark Prev 8: 241–248.

52. Zhao X, Peehl D, Navone N, Feldman D (2000) 1alpha,25-dihydroxyvitamin D3 inhibits prostate cancer cell growth by androgen-dependent and androgen-independent mechanisms. Endocrinology 141: 2548–2556.

53. VanSlyke JK, Musil LS (2000) Analysis of connexin intracellular transport and assembly. Methods 20: 156–164.

54. Musil L, Cunningham.BA, Edelman G, Goodenough D (1990) Differential phosphorylation of the gap junction protein connexin43 in junctional communicaton-competent and -deficient cell lines. J Cell Biol 111: 2077–2088.

55. Kemppainen J, Wilson J (1996) Agonist and antigonis activities of hydroxy-fluamide and casodex related to androgen receptor stabilization. Urology 48: 157–163.

56. Farla P, Hersmus R, Trapman J, Houtsmuller AB (2005) Antiandrogens prevent stable DNA-binding of the androgen receptor. Journal of Cell Science 118: 4187–4198.

57. Trosko J (2006) Dietary modulation of the multistage, multimechanisms of human carcinogenesis: effects on initiated stem cells and cell-cell communication. Nutr Cancer 94: 102–110.

58. Bosco D, Haefliger JA, Meda P (2011) Connexins: Key Mediators of Endocrine Function. Physiol Rev 91: 1393–1445.

59. Vezina C, Allgeier SMT, Fritz W, Moore R, Strerath M, et al. (2008) Retinoic acid induces prostatic bud formation. Dev Dyn 237: 1321–1333.

60. Lasnitzki I (1976) Reversal of methylchoantherene-induced changes in mouse prostates in vitro by retinoic acid and its analogues. British Journal of Cancer 34: 239–248.

61. Lasnitzki I, Goodman D (1974) Inhibition of the effects of methylcholanthrene on mouse prostate in organ culture by vitamin A and its analogs. Cancer Res 34: 1564–1571.

62. Christov KT, Moon RC, Lantvit DD, Boone CW, Steele VE, et al. (2002) 9-cis-retinoic acid but not 4-(hydroxyphenyl)retinamide inhibits prostate intraepithelial neoplasia in Noble rats. Cancer Res 62: 5178–5182.

63. Manual M, Ghyselink NB, Chambon P (2006) Functions of the retinoid nuclear receptors: Lessons from the genetic and pharmacological dissections of the

retinoic acid signaling pathway during mouse embryogenesis. Ann Rev Pharm Tox 46: 451–480.

64. Swami S, Krishnan AV, Wang JY, Jensen K, Horst R, et al. (2012) Dietary Vitamin D3 and 1,25-Dihydroxyvitamin D3 (Calcitriol) Exhibit Equivalent Anticancer Activity in Mouse Xenograft Models of Breast and Prostate Cancer. Endocrinology 153: 2576–2587.

65. VanSlyke JK, Deschenes SM, Musil LS (2001) Intracellular transport, assembly, and degradation of wild-type and disease-linked mutant gap junction proteins. Mol Biol Cell 11: 1933–1946.

66. Iversen P (2002) Antiandrogen monotherapy: indications and results. Urology 60: 64–71.

67. Kokai Y, Murata M, Go M, Spray DC, Sawada N (2011) Connexins induce and maintain tight junctions in epithelial cells. J Membr Biol 217: 13–19.

68. Kojima T, Kokai Y, Chiba H, Yamamoto M, Mochizuki Y, et al. (2001) Cx32 but Not Cx26 Is Associated with Tight Junctions in Primary Cultures of Rat Hepatocytes. Experimental Cell Research 263: 193–201.

69. Kojima T, Spray DC, Kokai Y, Chiba H, Mochizuki Y, et al. (2002) Cx32 formation and/or Cx32-mediated intercellular communication induces expression and function of tight junctions in hepatocytic cell line. Exp Cell Res 276: 40–51.

70. Shen R, Sumitomo M, Dai J, Harris A, Kaminetzky D, et al. (2000) Androgen-Induced Growth Inhibition of Androgen Receptor Expressing Androgen-Independent Prostate Cancer Cells Is Mediated by Increased Levels of Neutral Endopeptidase. Endocrinology 141: 1699.

71. Zhuang S-H, Schwartz GG, Cameron D, Burnstein KL (1997) Vitamin D receptor content and transcriptional activity do not fully predict antiproliferative effects of vitamin D in human prostate cancer cell lines. Mol Cell Endo 83–90.

72. Wang M, Berthoud VM, Beyer EC (2007) Connexin43 increases the sensitivity of prostate cancer cells to TNF{alpha}-induced apoptosis. Journal of Cell Science 120: 320–329.

73. Hirschi KK, Xu C, Tsukamoto T, Sager R (1996) Gap junction genes Cx26 and Cx43 individually suppress the cancer phenotype of human mammary carcinoma cells and restore differentiation potential. Cell Growth Diff 7: 861–870.

74. Mao AJ, Bechberger J, Lidington D, Galipeau J, Laird DW, et al. (2000) Neuronal Differentiation and Growth Control of Neuro-2a Cells After Retroviral Gene Delivery of Connexin43. The Journal of Biological Chemistry 275: 34407–34414.

75. Langlois SP, Cowan KN, Shao Q, Cowan BJ, Laird DW (2010) The Tumor-Suppressive Function of Connexin43 in Keratinocytes Is Mediated in Part via Interaction with Caveolin-1. Cancer Research 70: 4222–4232.

76. Langlois S, Maher AC, Manias JL, Shao Q, Kidder GM, et al. (2007) Connexin Levels Regulate Keratinocyte Differentiation in the Epidermis. J Biol Chem 282: 30171–30180.

77. McLachlan E, Shao Q, Wang Hl, Langlois S, Laird DW (2006) Connexisn act as tumor suppressors in three dimensional mammary cell organoids by regulating differentiation and angiogenesis. Cancer Res 66: 9886–9894.

78. Plante I, Stewart MKG, Barr K, Allan AL, Laird DW (2010) Cx43 suppresses mammary tumor metastasis to the lung in a Cx43 mutant mouse model of human disease. Oncogene 30: 1681–1692.

79. Kardami E, Dang X, Iacobas DA, Nickel BE, Jeyaraman M, et al. (2007) The role of connexins in controlling cell growth and gene expression. Progress in Biophysics and Molecular Biology 94: 245–264.

80. King TJ, Lampe PD (2005) Altered tumor biology and tumorigenesis in irradiated and chemical carcinogen-treated single and combined connexin32/p27Kip1-deficient mice. Communication and Cell Adhesion 293–305.

81. King TJ, Lampe PD (2004) Mice deficient for the gap junction protein Connexin32 exhibit increased radiation-induced tumorigenesis associated with elevated mitogen-activated protein kinase (p44/Erk1, p42/Erk2) activation. Carcinogenesis 25: 669–680.

82. King TJ, Gurley KE, Prunty J, Shin JL, Kemp CJ, et al. (2005) Deficiency in the gap junction protein connexin32 alters p27Kip1 tumor suppression and MAPK activation in a tissue-specific manner. Oncogene 24: 1718–1726.

83. Blutt S, Allegretto EA, Pike JW, Weigel NL (1997) 1,25-dihydroxyvitamin D₃ and 9-cis-retinoic acid act synergistically to inhibit the growth of LNCaP prostate cells and cause accumulation of cells in G₁. Endocirnology 138: 1491–1497.

84. Skowronski RJ, Peehl DM, Feldman D (1993) Vitamin D and prostate cancer: 1,25 Dihydroxyvitamin D₃ receptors and actions in human prostate cancer cell lines. Endocirnology 132: 1952–1960.

85. Chen S-C, Pelletier DB, Ao P, Boynton AL (1995) Connexin43 reverses the phenotype of transformed cells and alters their expression of cyclin/cyclin-dependent kinases. Cell Growth Diff 6: 681–690.

86. Laird DW (2010) The gap junction proteome and its relationship to disease. Trends Cell Biol 20: 92–101.

87. Paluch E, Heisenberg CP (2009) Biology and Physics of Cell Shape Changes in Development. Current Biology 19: R790–R799.

88. Salbreux G, Charras G, Paluch E (2012) Actin cortex mechanics and cellular morphogenesis. Trends In Cell Biology 22: 536–545.

89. Francis R, Xu X, Park H-D, Wei J-C, Chang S, et al. (2012) Connexin43 modulates cell polarity and directional cell migration by regulating microtubule dynamics. PLoS ONE 6: 1–14.

90. Schwartz G, Hulka BS (1990) Is vitamin D deficiency a risk factor for prostate cancer? Anticancer Res 10: 1307–1311.

91. Ahn J, Peters U, Albanes D, Purdue MP, Abnet CC, et al. (2008) Serum Vitamin D Concentration and Prostate Cancer Risk: A Nested CaseΓÇôControl Study. Journal of the National Cancer Institute 100: 796–804.

92. Bostwick DG, Qian J (2004) High-grade prostatic intraepithelial neoplasia. Mod Pathol 17: 360–379.

93. Bostwick DG (1992) Prostatic intraepithelial neoplasia (PIN): current concepts. J Cell Biochem 16H: 10–19.

The Carboxyl Tail of Connexin32 Regulates Gap Junction Assembly in Human Prostate and Pancreatic
Cancer Cells

**Parul Katoch, Shalini Mitra, Anuttoma Ray, Linda Kelsey, Brett J. Roberts, James K. Wahl III,
Keith R. Johnson and Parmender P. Mehta[1]**

Running Title: *Carboxyl Tail of Connexin32 and Gap Junction Assembly*

Department of Biochemistry and Molecular Biology, Department of Oral Biology, Eppley Institute for Research
in Cancer and Allied Diseases, Fred and Pamela Buffett Cancer Center, University of Nebraska Medical
Center, Omaha, NE 68198

To whom correspondence should be addressed: Parmender P. Mehta; Department of Biochemistry and
Molecular Biology, Fred and Pamela Buffett Cancer Center, University of Nebraska Medical Center, Omaha,
NE 68198. Tel. (402)-559-3826; Fax. (402)-559-6650; Email: pmehta@unmc.edu

Keywords: Gap junctions, connexin, cytoplasmic tail, pancreatic cancer, prostate cancer, LNCaP, BxPC3

_____
_____
_____

Background: The cytoplasmic tails of
connexins are highly divergent yet their role in gap
junction assembly has not been elucidated..

Result: Gap junctions of tail-deleted
connexin32 remain small as they fail to grow.

Conclusion: The tail is not required for gap
junction formation but is essential for the growth.

Significance: The cytoplasmic tail of
connexin32 plays an important role in regulating
assembly.

ABSTRACT

Connexins, the constituent proteins of gap
junctions, are transmembrane proteins. A connexin
(Cx) traverses the membrane four times, and has
one intracellular and two extracellular loops, with the
amino and carboxyl termini facing the cytoplasm. The
transmembrane and the extracellular loop domains
are highly conserved among different Cxs whereas
the carboxyl termini, called the cytoplasmic tails, are
highly divergent. We explored the role of the
cytoplasmic tail of Cx32 in regulating gap junction
assembly. Our results demonstrate that compared to
the full-length Cx32, the cytoplasmic-tail-deleted
Cx32 is assembled into smaller gap junctions in
pancreatic and human prostatic cancer cell lines.
Our results further document that the expression of
full-length Cx32 in cells expressing tail-deleted Cx32,
increases the size of gap junctions whereas the
expression of tail-deleted Cx32 in cells expressing
full length Cx32 has the opposite effect. Moreover,
we show that the tail is required for the clustering of
cell-cell channels, and that in cells expressing the
tail-deleted Cx32, expression of the cytoplasmic tail
alone is sufficient to enhance assembly. Our live-cell
imaging data demonstrate that compared to the
mobility of gap junction plaques formed of full-length
Cx32, the plaques composed of tail-deleted Cx32 are
highly motile. These findings suggest that the
cytoplasmic tail is not required to initiate the
assembly of gap junctions but for its subsequent
growth and stability. Our findings reveal an important
role for the cytoplasmic tail of Cx32 in regulating the
growth of a gap junctional plaque.

INTRODUCTION

Gap junctions are ensembles of cell-cell
channels through which molecules up to 1 kDa can
directly pass between the cytoplasmic interiors of
adjoining cells (1,2). Cell-cell channels are formed of
connexins, which are designated according to the
molecular mass. The Cxs are encoded by a family of
21 distinct genes in humans, and some members of
the family are expressed in tissue-specific manner,
while others are expressed redundantly (2). Knock
out studies of Cx genes have unveiled diverse roles
of cell-cell communication in maintaining tissue
homeostasis (3). Their roles have been
substantiated by human genetic diseases, such as

occulodental digital dysplasia, palmoplanta keratoderma, and keratitits-icthyosis-deafness syndrome, in which mutations in Cx genes have been detected (3,4). Despite tissue-specific expression of some Cxs, gap junctions in all tissues appear as disc-shaped structures consisting of several regularly spaced particles in freeze-fracture replicas. To form a cell-cell channel, six Cxs first oligomerize into a hexamer, called a connexon, which is transported to the cell surface and docks with a connexon in an adjacent cell. A gap junction is formed when several such cell-cell channels cluster (1). Thus, a key step in the assembly of gap junctions is the aggregation of cell-cell channels at one particular spot at areas of cell-cell contact, a process that has not yet been elaborated (5).

A Cx is a transmembrane protein which traverses the membrane four times, and has one intracellular and two extracellular loops, with the amino and carboxyl termini facing the cytoplasm. The transmembrane and the extracellular loop domains are highly conserved among different Cxs whereas the carboxyl termini, often called the cytoplasmic tails, are highly divergent (2,5). The role of the two extracellular loop domains of Cxs in the formation of cell-to-cell channels and the cytoplasmic tails in regulating the opening and closing of cell-cell channels has been well-documented (6-9). The cytoplasmic tails of many Cxs have also been shown to interact directly or indirectly with several proteins. While these interactions have been postulated to control the assembly of Cxs into gap junctions, the molecular mechanisms involved have remained unexplored (10). In particular, it is not clear what the exact role of a Cx's cytoplasmic tail in regulating the assembly of gap junctions is and at which step it is involved. For example, the interaction of a scaffolding protein, ZO-1, which binds to the PDZ-binding domain of several Cxs, facilitates the assembly of Cx43, an ubiquitously expressed Cx, into gap junctions yet has the opposite effect on the assembly of Cx50, which is expressed in lens epithelial cells (11,12). Thus, it is highly likely that besides ZO-1 other proteins documented to interact with Cxs might inhibit or enhance gap junction assembly and disassembly in a tissue-specific and cell-context dependent manner. Moreover, most studies with Cx-interacting proteins have been performed with Cx43 (5) and not with Cxs that are expressed in a tissue-specific manner (2). Tissue-specific as well as redundant expression of some Cxs, combined with the fact that most tissues and cell types express more than one Cx subtype(1,13,14), implies that the assembly of each Cx subtype into gap junctions is likely regulated spatiotemporally in a cell-context and physiological-state dependent manner by distinct mechanisms to prevent fortuitous gap junction formation and internalization. The cytoplasmic tails of Cxs seem to be the likely targets for such type of regulation as they are the most divergent among different members of Cx gene family(2).

Among all the Cxs, the expression of Cx32 is observed in the well-differentiated acinar cells of exocrine glands, such as prostate and pancreas(14). Our previous studies showed that the retrovirus-mediated expression of Cx32 into Cx-null, androgen-sensitive prostate cancer cell line, LNCaP, induced the formation of gap junctions, restored junctional communication, inhibited growth *in vitro*, and retarded malignancy *in vivo* (15). We further showed that androgens — the key players that govern prostate morphogenesis and oncogenesis (16) — regulated the formation and degradation of gap junctions by controlling the expression level of Cx32 posttranslationally(17). In these studies, we had fortuitously observed that the retrovirally-expressed cytoplasmic-tail-deleted Cx32 appeared to assemble into small gap junctions compared to those formed by the expression of the full-length Cx32 (17). Moreover, our previous study with cadherin-null human squamous carcinoma cells had also shown that the assembly of Cx32 into gap junctions was facilitated when cells acquired a partially polarized state and that the cytoplasmic-tail of Cx32 (Cx32-CT) was required to initiate the formation of a gap junction plaque and/or its subsequent growth in these cells (18). These studies prompted us to explore the role of Cx32-CT in the assembly of gap junctions.

We demonstrate here that compared to full-length Cx32, the cytoplasmic-tail-deleted Cx32 is assembled into smaller gap junctions despite normal trafficking to the cell surface in pancreatic and human prostatic cancer cell lines. We also document that the expression of full-length Cx32 in cells stably expressing cytoplasmic-tail-deleted Cx32 increases the size of gap junctions whereas the expression of cytoplasmic-tail-deleted Cx32 in cells expressing full-length Cx32 has the opposite effect. Moreover, our

results show that the cytoplasmic tail is required for the clustering of cell-cell channels. Furthermore, we also show that in cells expressing cytoplasmic-tail-deleted Cx32, the expression of cell-surface-targeted cytoplasmic tail alone is sufficient to enhance gap junction assembly. Finally, our live-cell imaging data document that compared to the mobility of plaques formed of full-length Cx32, the gap junction-like puncta composed of cytoplasmic-tail-deleted Cx32 are highly motile. Our findings suggest that the cytoplasmic tail is not required to initiate the assembly of Cx32 into gap junctions but for its subsequent growth and stability.

MATERIALS AND METHODS

Cell Culture

The human pancreatic cancer cell line, BxPC3 (CRL-1687), and a prostate cancer cell line, LNCaP (ATCC CRL 1740), were grown, respectively, in RPMI 1640 and DMEM (GIBCO, Grand Island, NY) containing 7% fetal bovine serum (Sigma Aldrich, St. Louis, MO) in an atmosphere of 5% CO_2 at 37°C. Stock cultures were maintained weekly by seeding $5x10^5$ cells per 10 cm dish in 10 ml of complete culture medium with a medium change at day 3 or 4 as described (17,19). New stocks were initiated after 10 passage numbers. The two retroviral packaging cell lines, EcoPack and PTi67, were grown as described previously (15,17). BxPC3 and LNCaP cells were infected with various recombinant retroviruses and pooled polyclonal cultures from approximately 2000 colonies were grown and maintained in RPMI containing G418 (200 µg/ml) (see Recombinant DNA Constructs and Retrovirus Production and Infection).

Antibodies and Immunostaining

Rabbit polyclonal and mouse monoclonal antibodies against Cx32 and mouse anti-β-catenin, and rabbit anti-β-actin have been described previously (17,18,20). We also used rabbit polyclonal antibodies raised against the carboxyl tail (Sigma; C-3470) and cytoplasmic loop of Cx32 (Signal, C-3595). For immunostaining $5x10^5$ BxPC3 and $4x10^5$ LNCaP cells were seeded on glass cover slips in six-well clusters and allowed to grow for 3 days, after which they were fixed with 2% paraformaldehyde and immunostained as described

(18-20). Anti-rabbit and anti-mouse secondary antibodies, conjugated with Alexa 488 or Alexa 594 (Invitrogen), were used as appropriate. After mounting immunostained cells on glass slides in SlowFade antifade medium (Invitrogen), images were acquired with a Leica DMRIE microscope (Leica Microsystems, Wetzler, Germany) equipped with a Hamamatsu ORCA-ER2 CCD camera (Hamamatsu City, Japan) using a 63x oil objective (NA 1.35). Several z-stacked images taken 0.3 µm apart were used to measure colocalization using the commercial image analysis program Volocity 6.0.3 (Improvision, Lexington, MA) as described (18,19) .

Recombinant DNA Constructs and Retrovirus Production and Infection

Construction of retroviral vectors containing wild-type rat Cx32 (Cx32-WT) and the cytoplasmic-tail-deleted Cx32 (Cx32Δ220) has been described (17). Briefly, the Cx32Δ220 was engineered by PCR-based cloning technique and cloned into the retroviral vector LXSN. The PCR amplification was performed using the forward primer: 5'-GCC<u>GAATTC</u>ATGAACTGGACAGGTC-3', and reverse primer containing a premature stop codon (TGA, Umber) at amino acid position 221: 5'-CCG<u>GAATTC</u>TCAACGGCGGGCACAG-3'. The mutant was generated by site-directed mutagenesis using a QuikChange kit (Stratagene, La Jolla, CA) according to the manufacturer's instructions. Cx32-WT and Cx32Δ220 were fused in frame with enhanced green fluorescent protein using pEGFP-N1 (Clontech, Mountain View CA). The Cx32-CT-Myr construct (containing amino acid residues 220-283) was constructed by PCR cloning as follows: Cx32-CT was first cloned in frame with pmTurqouise-C3 to create pmTurquoiseCx32Δ220. The entire pmTurquoiseCx32Δ220 was amplified by PCR with Nco1 and BamH1 sites added at the 3' and 5' ends, respectively. This Nco1 and BamH1 fragment was cloned into a modified pSPUTK vector which added 5' myristoylation and 2 Myc tags. The assembled cassette was removed and subcloned in pcDNA3.1 (+) as a HindIII and BamH1 fragment. All constructs were verified by DNA sequencing (ACGT Inc, Wheeling, IL). Plasmids Cx32-WT-Myc and Cx32Δ220-Myc, with Myc fused to the carboxyl termini, were constructed by PCR cloning as described for Cx43 (19). The construction of retroviral vector harboring Cx32-WT tagged with

EGFP (Cx32-WT-EGFP) and Cx32-WT-mApple, tagged with red fluorescent protein (mApple), has been described (19). To construct retroviral vector Cx32Δ220-EGFP, we used the standard recombinant DNA methodology described in our earlier studies (19).

The retroviral vectors were used to produce recombinant retroviruses in EcoPack and PTi67 packaging cell lines as described previously (18-20). The recombinant retroviruses produced from the pooled polyclonal cultures of PTi67 cells were assayed for virus titer by colony forming units as described (21). BxPC3 and LNCaP cells were multiply (2-4 times) infected with the recombinant retroviruses and selected in G418 (400 µg/ml) for 2–3 weeks in complete medium. Pooled cultures from about 2000 colonies obtained from 3-4 dishes were expanded, frozen, and maintained in selection media containing G418 (200 µg/ml). Pooled polyclonal cultures were used within 2-4 passages for immunocytochemical and biochemical analyses.

Detergent Extraction and Western Blot Analysis

BxPC3 (3×10^6) and LNCaP (2×10^6) cells, seeded in replicate 10 cm dishes in 10 ml of complete medium, were grown for 72 h. The procedures for cell lysis, detergent-solubility assay with 1% Triton X-100 (TX100), and Western blot analysis have been described previously (17,18,20). Normalization was based on equal cell number for the analysis of detergent-soluble and -insoluble fractions by SDS-PAGE in cell lysates.

Cell Surface Biotinylation Assay

BxPC3 (5×10^5) and LNCaP (4×10^5) cells were seeded in 6 cm dishes in replicates and grown to 70-80% confluence. Biotinylation reaction, using freshly prepared EZ-LinkSulfo-NHS-SS Biotin reagent (Pierce; Rockford, IL) at 0.5 mg/ml in phosphate buffered saline (PBS) supplemented with 1 mM $CaCl_2$ and 1 mM $MgCl_2$ (PBS-PLUS), was performed at 4°C for 1 h. Cells were lysed after quenching the reaction with PBS-PLUS containing 20 mM glycine as described previously (18,20,22). The affinity precipitation of biotinylated proteins was from 200 µg of total protein using 100 µl of streptavidin-agarose beads (Pierce, Rockford, IL) on a rotator overnight at 4°C. SDS-PAGE followed by Western blotting was used to resolve the streptavidin-bound biotinylated proteins after elution as described previously (18,20,22). The kinetics of degradation of cell-surface-associated Cx32-WT and Cx32Δ220 was determined essentially as described previously (19,20). The protein concentration was determined using the BCA reagent (Pierce).

Cell Transfection

Twenty-four hours prior to transfection, BxPC3 (1.5×10^6) and LNCaP (10^6) cells were seeded on glass cover slips in 6-well clusters. Cells were transfected with various plasmids in duplicate using Fugene (Roche Diagnostics) according to the manufacturer's instructions. For transfections, 2 µg of plasmid DNA was used per well. For co-transfection of two plasmids, pmCherry or pEGFP (0.5 µg) and the plasmid DNA (1.5 µg), containing the gene whose expression was to be detected, were mixed. Expression was analyzed 24 h post-transfection after fixing and immunostaining cells with the desired antibodies as described (17).

Communication Assays

Gap junctional communication was assayed by microinjecting the fluorescent tracers Lucifer Yellow (MW 443 Da; Lithium salt); Alexa 488 (MW 570 Da; A-10436), or Alexa 594 (MW 760 Da; A-10438) (18,20,22,23). Alexa dyes were purchased from Molecular Probes (Carlsbad, CA) and stock solutions (10 mM) for microinjection were prepared in water. Eppendorf InjectMan and FemtoJet microinjection systems (models 5271 and 5242, Brinkmann Instrument, Inc. Westbury, NY), mounted on a Leica DMIRE2 microscope were used to microinject the fluorescent tracers. Junctional transfer of fluorescent tracers was assessed by counting the number of fluorescent cells (excluding the injected one) either at 1 min (Lucifer Yellow), 3 min (Alexa 488) or 15 min (Alexa 594) after microinjection into test cells as described (15,17,18,24).

Co-cultures

For the coculture experiments shown in Figure 6, parental LNCaP cells and LNCaP cells expressing retrovirally-introduced Cx32-WT-EGFP, Cx32-WT-mApple, Cx32Δ220, Cx32Δ220-EGFP, or EGFP were suspended in RPMI and then mixed

together at various ratios ranging from 1:1 to 1:3. Cells were allowed to aggregate in suspension for 4 h at 37°C in an atmosphere of 5% CO_2 and 1-3 $\times 10^5$ cells/well were plated in six well clusters. After 24 h, cocultures were immunostained for Cx32 using an antibody raised against the cytoplasmic loop or immunostained with an antibody raised against the cytoplasmic tail of Cx32, which does not recognize Cx32Δ220.

Live Cell Imaging and Fluorescent Recovery after Photo-bleaching (FRAP)

Bx32-WT-EGFP, Bx32Δ220-EGFP, LN32-WT-EGFP and LN32Δ220-EGFP cells (1.5 $\times 10^5$) were seeded in LabTek FluoroDish and allowed to grow to confluence. Confluent monolayers of cells were imaged using a 100 x oil objective (NA 1.4) and a broad-band GFP filter. Cells were imaged at 37°C in an atmosphere of 5% CO_2/95% air in a live-cell imaging chamber mounted on an Olympus IX81 Spinning Disc Confocal motorized inverted microscope (Olympus America Inc; Center Valley, PA). The microscope was controlled by IX2-UCB U-HSTR2 motorized system with a focus drift compensatory device IX1-ZDC. Images were captured using a Hamamatsu ORCA ER2 CCD camera and processed by imaging software Slidebook version 5.0 (Intelligent Imaging Innovations, Denver, CO). Z-stacks of 1 μm were acquired every two minutes for 120 min. The z-stacks were projected into 1 single Z-projection, which were superimposed on to a phase-contrast image.

For FRAP analysis, Bx32-WT-EGFP and Bx32Δ220-EGFP cells were photo-bleached as described (25). For measuring recovery within gap junction plaques, only puncta at the areas of cell-cell contact were photo-bleached whereas the recovery in non-junctional areas was determined in single cells in regions of cells where only diffuse GFP fluorescence was observed and there were no vesicular puncta. Recovery was measured using a Marianas Live Cell microscopy system (Intelligent Imaging Innovations Inc, Denver, Co.) equipped with a Stanford Research Laser Ablation System (model NL100). After the cells were photo-bleached, we captured z-stack images every 10 seconds for 15-20 minutes. As described in our earlier studies (25), prior to quantitation of relative fluorescence intensity,

raw images were de-convolved and collapsed into a projection image. For comparing multiple FRAP experiments, we collected normalized FRAP data using SlideBook (Version 5.0). For determining the relative fluorescence intensity value, we set the pre-bleach and post-bleach values, respectively, as 100 % and 0%. The graphs shown in Figure 11 represent the plotted relative fluorescence intensity and error bars represent the 95% confidence interval.

For tracking of gap junction puncta, we used the following method. After image acquisition, time lapses were corrected for photobleaching and images were manually enhanced using SlideBook (Version 5.0). To visualize the tracks of gap junction like puncta at the cell-cell contact areas, we only chose puncta that were visually assessed by two independent observers to be at the cell-cell contact sites. We plotted the distance traveled over time for each puncta as long as the particle could be visually traced as assessed by its disappearance from the focal plane. The distance measurement was approximated in a quasi-1 dimensional manner using the punctum's position before its disappearance with respect to the punctum's initial point of origin. All puncta were assigned a trajectory profile based on their appearance and disappearance from the focal plane during the detection period. All analyses were carried out by the two blinded observers.

RESULTS

Cytoplasmic-Tail-deleted Cx32 Assembles into Smaller Gap Junctions

Earlier studies had shown that the truncation of Cx32-CT up to amino acid 219 had no effect on the trafficking of connexons to the plasma membrane (26). We also showed that the cytoplasmic-tail-deleted Cx32, abbreviated as Cx32Δ220, formed smaller gap junctions in human prostate cancer cell line, LNCaP, compared to full-length Cx32, hereafter abbreviated as Cx32-WT (17). Moreover, we further showed that in human squamous carcinoma cell line, A431D, Cx32-WT assembled into gap junctions only when cells acquired a partially polarized state whereas Cx32Δ220 did not (18). These observations hinted that the Cx32-CT was involved in some aspect of gap junction plaque growth and/or initiation.

To define the role of Cx32-CT further, we retrovirally expressed Cx32-WT and Cx32Δ220 in LNCaP and BxPC3 cell lines in parallel, and obtained pooled polyclonal cultures from each cell line. The pooled polyclonal cultures of LNCaP and BxPC3 cells expressing Cx32-WT and Cx32Δ220 are designated as LN32-WT, Bx32-WT, LN32Δ220 and Bx32Δ220 cells, respectively. Western blot analysis showed that Cx32-WT and Cx32Δ220 were expressed robustly in LNCaP and BxPC3 cells (Figure 1AB). However, immunocytochemical analysis revealed that in both cell types Cx32Δ220 formed only smaller junctions whereas Cx32-WT formed both large and small gap junctions (Figure 1C; compare the size of gap junction puncta in the left panels with the right panels). We therefore measured the surface areas of 350-500 individual gap junctional puncta in LNCaP and BxPC3 cells expressing Cx32-WT and Cx32Δ220 (Figure 2A). As described earlier, the size of each fluorescent spot or a punctum at the cell-cell interface, as delineated by E-cadherin or β-catenin staining, was presumed to represent a single gap junction plaque (18,27). As assessed by measuring the surface areas of individual puncta, we found that compared to LN32-WT and Bx32-WT cells, LN32Δ220 and Bx32Δ220 cells formed 20-35 fold smaller gap junctions (Figure 2A). Moreover, the frequency of larger gap junctions was decreased in LN32Δ220 cells, with a concomitant increase in the frequency of smaller gap junctions (data not shown). Furthermore, when we counted the number of gap junctions per interface, we found that the number of intracellular puncta were more in cells expressing Cx32Δ220 compared to cells expressing Cx32-WT (data not shown). In addition, as assessed visually, the number of intracellular puncta appeared to be more in cells expressing Cx32Δ220 compared to cells expressing Cx32-WT (Figure 1C, bottom right panel). Similar observations were made in LNCaP cells although intracellular puncta are not as evident in images due to their location in different focal planes.

To determine if Cx32Δ220 formed functional gap junctions, we microinjected gap junction-permeable fluorescent tracers in LN32-WT and LN32Δ220 cells. We found that the junctional transfer of all fluorescent tracers was reduced in cells expressing Cx32Δ220 (Figure 2B; Table 1). To assess the relevance of our findings in LNCaP and BxPC3 cells to other cell types, we also retrovirally expressed Cx32-WT and Cx32Δ220 in HEK293T and HeLa cells as well as in another human pancreatic cancer cell line HPAF-II. We found that compared to Cx32-WT, Cx32Δ220 was assembled into smaller gap junctions in all cell types examined (data not shown). Thus, Cx32Δ220 assembled into smaller gap junctions in a variety of cell types. Overall, the above data suggest that although both the size of gap junction plaques and function composed of cytoplasmic-tail-deleted Cx32Δ220 are compromised, Cx32-CT is not required for initiating the formation of gap junctions.

Detergent Solubility of Cx32-WT and Cx32Δ220

To substantiate the immunocytochemical data, we determined gap junction assembly biochemically by measuring the solubility of Cx32-WT and Cx32Δ220 in Triton-X (TX)100 (28). We found that a proportion of Cx32-WT and Cx32Δ220 was detected in detergent-insoluble and -soluble fractions in both LNCaP and BxPC3 cells (Figure 3AB). The detergent-solubility of β-catenin, an adherens junction-associated protein, was used as a control for these experiments. For example, we found that in three independent experiments between 55-60% of total Cx32-WT was in TX100-insoluble fraction in LN32-WT and Bx32-WT cells while this fraction ranged between 20-30% for LN32Δ220 and Bx32Δ220 cells. However, this difference in detergent-soluble and –insoluble fraction between Cx32-WT and Cx32Δ220 in LNCaP and BxPC3 cells was not statistically significant because of large variation in soluble and insoluble fractions.

Cx32-WT and Cx32Δ220 Traffic and Degrade Normally

To determine whether Cx32Δ220 traffics normally to the cell surface, we used cell surface biotinylation. The data showed that Cx32Δ220 was biotinylated as efficiently as Cx32-WT in both cell types (Figure 4A). For example, in both cell types between 5-10% of input Cx32-WT and Cx32Δ220 was biotinylated (Figure 4A). To investigate if cell surface-associated Cx32Δ220 degrades more rapidly compared to Cx32-WT, we determined their kinetics of degradation after biotinylation. We found that the cell surface-biotinylated Cx32Δ220 degraded with kinetics similar to Cx32-WT (Figure 4 BC). The data from two independent experiments, which varied by

less than 10%, are plotted in Figure 4D. These findings suggest that the assembly of Cx32Δ220 into smaller gap junctions is not caused by its impaired trafficking to the cell surface or its rapid internalization and degradation prior to assembly but by some mechanism that interferes with the growth of the gap junction plaques after they have been assembled.

Expression of Cx32-WT Rescues the Small Junction Phenotype of Cx32Δ220

Because Cx32Δ220 trafficked normally to the cell surface, and degraded with kinetics similar to Cx32-WT, we asked if small junction phenotype of Cx32Δ220 could be rescued by providing the Cx32-CT in *Cis* (as a part of Cx32-WT). Earlier studies had shown that the defective gap junction assembly of Cx43 in human pancreatic cancer cell lines was restored upon expressing endocytosis-deficient mutants of Cx43 in cells expressing endogenous full-length Cx43, and that restoration was caused by the formation of heteromers between them (19). We rationalized that Cx32-WT, by forming heteromers with Cx32Δ220, might increase the frequency of large gap junctions by providing Cx32-CT in *Cis.* To test this notion, we transiently expressed Myc-tagged Cx32-WT in LN32Δ220 and Bx32Δ220 cells and, conversely, Myc-tagged Cx32Δ220 in LN32-WT and Bx32-WT cells. Formation of gap junctions was examined immunocytochemically. We found that the expression of Myc-tagged Cx32-WT increased the size of gap junctions formed by Cx32Δ220 in both LN32Δ220 and Bx32Δ220 cells (Figure 5AD). Expression of Myc-tagged Cx32Δ220 in LN32Δ220 and Bx32Δ220 cells had not effect (data not shown). As determined by measuring 347 individual gap junction puncta at the cell-cell interfaces, we found that the mean surface area of rescued Cx32Δ220 gap junctions was 12-25 folds larger compared to the area of gap junctions formed by the Cx32Δ220 alone (Figure 5D).

In the next series of experiments we examined if expression of Myc-tagged Cx32Δ220 in LN32-WT and Bx32-WT cells would attenuate the assembly of Cx32-WT into gap junctions. The results showed that the assembly of Cx32-WT was inhibited upon expressing Cx32Δ220-Myc (Figure 5B). Expression of Myc-tagged Cx32-WT in LN32-WT and Bx32-WT had no effect (data not shown). As

assessed visually, we also found that the rescue of Cx32Δ220 gap junctions was accompanied with a concomitant decrease in the number of intracellular puncta (Figure 5A) whereas inhibition of Cx32-WT assembly was accompanied with a concomitant increase in intracellular puncta (Figure 5B). To test whether the preponderance of Cx32Δ220 or the ratio of Cx32-WT and Cx32Δ220 in a connexon controls gap junction assembly, we transiently expressed Cx32-WT and Cx32Δ220-EGFP at various ratios in HEK293T cells and examined assembly immunocytochemically (Figure 6). We chose HEK293T cells because they are highly transfectable and do not express Cx32 endogenously. For these experiments we used an antibody raised against the Cx32-CT, which would not recognize Cx32Δ220-EGFP. As assessed by an increase in the size of gap junctions formed by Cx32Δ220-EGFP and a concomitant decrease in the number of smaller gap junction puncta, we found that the rescue occurred only when the expression of Cx32-WT was high (Figure 6). Collectively, the data presented in Figures 5 and 6 suggest that Cx32-CT enhances gap junction assembly.

Expression of Cx32-CT in Trans Affects Cx32Δ220 Junction Assembly

To explore whether expression of Cx32-CT by itself in *Trans* would modulate the size of gap junctions formed by Cx32Δ220 or Cx32-WT, we rationalized that the Cx32-CT interacts and/or recruits proteins that determine the Cx32Δ220 plaque growth and that the recruitment and interaction occur at the cell surface. To test this, we engineered a Cx32-CT construct (representing amino acid residues 220-283) in which a myristoylation sequence was added at the amino terminus of Cx32-CT to target it to the plasma membrane; moreover, the Cx32-CT was also tagged with cyan fluorescent protein mTurquoise (see Materials and Methods). This construct is designated as Cx32-CT-Turquoise-Myr. As a control, we also engineered an mCherry-Myr construct in which the myristoylation sequence was added to the amino terminus of red fluorescent protein mCherry. Both engineered constructs were also tagged with Myc (see Materials and Methods). Transient transfection of Cx32-CT-Turquoise-Myr and mCherry-Myr in HEK293 cells, followed by Western blot analysis, showed that both Cx32-CT-Turquoise-Myr and mCherry-Myr ran at the predicted

MW and were appropriately targeted to the cell surface (data not shown).

To test if expression of Cx32-CT in *Trans* would modulate gap junction size, we transiently expressed Cx32-CT-Turquoise-Myr and mCherry-Myr in LN32-WT, LN32Δ220, Bx32-WT and Bx32Δ220 cells and examined gap junction assembly immunocytochemically. As assessed by the size of the puncta at cell-cell interfaces, we found that while the expression of Cx32-CT-Turquoise-Myr had no effect on the assembly of Cx32-WT in LN32-WT and Bx32-WT cells, small gap junction phenotype of LN-32Δ220 and Bx32Δ220 cells was partially rescued (Figure 7). When we measured the surface areas of 350-670 individual gap junction puncta in transfected LN32Δ220 and Bx32Δ220 cells, there was a consistent 2-2.5-fold increase in the size (surface area) of gap junction puncta in LN32Δ220 and Bx32Δ220 cells expressing Cx32-CT-Myr compared to those expressing mCherry-Myr (Figure 7B). Moreover, we also found that the number of intracellular puncta in Cx32-CT-Turquoise-Myr expressing cells was significantly decreased (Table 2). These data suggest that Cx32-CT recruits some factor(s) to the cell surface as it traffics along the secretory pathway and/or upon arrival at the cell surface, which facilitates the growth of gap junctions composed of Cx32Δ220.

Segregation of LN32-WT and LN32Δ220 Cells in Coculture

To examine if small gap junction phenotype of cells expressing Cx32Δ220 is also rescued upon co-culturing with cells expressing Cx32-WT cells, we retrovirally introduced EGFP, Cx32Δ220-EGFP, and Cx32-WT-mApple (tagged with red fluorescent protein mApple) in LNCaP cells and established pooled cultures termed as LN-EGFP, LN-32Δ220-EGFP, and LN32-WT-mApple cells, respectively. We chose LNCaP cells for these studies because only E-cadherin is expressed abundantly in these cells (17) compared to BxPC3 cells, which express E-, P- and N-cadherin (29). LN32-WT and LN32-WT-mApple cells were mixed with LN32Δ220 or LN32Δ220-EGFP cells in various ratios, allowed to aggregate in suspension for 4 h and seeded in six well clusters for 24 h to permit gap junction assembly (see Materials and Methods). We then examined if the size of gap junctions formed of LN32-WT or LN32Δ220, tagged

or untagged, was affected by immunostaining cocultures with the antibody raised against the carboxyl tail of Cx32-WT that would not recognize Cx32Δ220 or Cx32Δ220-EGFP (Figure 8). As a control, LN32-WT cells were also cocultured with LN-EGFP cells at different ratios. We found that as was observed in previous studies with other cell types (30), LN32-WT cells segregated from LN-EGFP cells in cocultures (Figure 8, bottom row). Remarkably, we also found that LNCaP cells expressing Cx32-WT and Cx32Δ220, untagged or tagged with mApple or EGFP, also segregated in coculture, and heterologous gap junctions formed of LN32-WT and LN32Δ220 were not observed (Figure 8, top two rows). In contrast, we failed to observe any segregation in cocultures of LN-EGFP and parental LN-WT cells (Figure 8, third row). Western blot and immunocytochemical analyses showed that expression of Cx32-WT, Cx32Δ220, and EGFP had no effect on the expression of E-cadherin (data not shown). These results suggest that the expression of Cx32-WT and Cx32Δ220, untagged or tagged with mApple or EGFP, in LNCaP cells overrides the cell-cell adhesion mediated by E-cadherin, allowing them to segregate into two different cell populations dependent upon Cx32-WT and Cx32Δ220 expression.

Carboxyl Tail of Cx32 is Essential for the Clustering of Cell-Cell Channels

Earlier studies had shown that clustering of cell-cell channels composed of Cx43 was induced when intracellular levels of cAMP were elevated (31-34). Moreover, other studies had shown that elevating intracellular cAMP levels enhanced gap junctional communication by stabilizing Cx32 in rat hepatocytes (35,36). Based upon these results, we rationalized that Cx32-CT is required for the clustering of cell-cell channels. Hence, we expected Cx32Δ220 not to cluster in response to forskolin, which elevates intracellular levels of cAMP by activating adenylyl cyclase (37). Therefore, we treated LN32-WT, LN32Δ220, Bx32-WT and Bx32Δ220 with forskolin for 8 h based on our earlier studies with the other cell lines (38-40). The results showed the following: 1. Cell-cell channels composed of Cx32-WT clustered and/or redistributed to form large gap junctions in LN32-WT cells (Figure 9). 2. Cx32Δ220 did not cluster in response to forskolin in

LN32Δ220 cells (Figure 9). Similar results were obtained with Bx32-WT and Bx32Δ220 cells although the effect was not robust as forskolin was toxic to these cells (data not shown). These results suggest that Cx32-CT is required for the clustering and/or redistribution of cell-cell channels and gap junction assembly.

Movement of Gap Junction Plaques Composed of Cx32-WT and Cx32Δ220

Next we investigated the dynamic behavior of gap junctions composed of Cx32-WT and Cx32Δ220 in LNCaP and BxPC3 cells. To test this we retrovirally expressed Cx32-WT-EGFP and Cx32Δ220-EGFP in LNCaP and BxPC3 cells. Like their untagged counterparts, Cx32-WT-EGFP and Cx32Δ220-EGFP were assembled into large and small gap junctions, respectively. Live-cell imaging was performed on confluent cells to allow unambiguous detection of gap junction plaques at the areas of cell-cell contract as well as to minimize artifacts that might result from the movement of contacting cells during the imaging period (see Materials and Methods). For most studies related to live-cell imaging, we utilized BxPC3 cells as they were thin and hence were easy to image compared to LNCaP cells. The results showed that gap junction plaques composed of Cx32Δ220-EGFP were highly dynamic compared to those composed of Cx32-WT-EGFP (Movies S1 and S2). By individually tracking the movement and disappearance of puncta at cell-cell contact areas, we found that most Cx32Δ220-EGFP puncta moved within 10 min whereas most Cx32-WT-EGFP gap junction puncta did not disappear even up to 2 h (Figure 10, movies S1 and S2). Also, the average speed of Cx32Δ220-EGFP puncta was twice that of Cx32-WT-EGFP puncta (Figure 11A). Moreover, Cx32Δ220-EGFP puncta moved abruptly whereas the movement of Cx32-WT-EGFP puncta was saltatory (Movies S1 and S2, Figure 11B). Furthermore, by analyzing the behavior of both large and small puncta of Cx32-WT-EGFP and several puncta of Cx32Δ220-EGFP, we also found that small puncta formed by the Cx32-WT-EGFP, comparable in size to those formed of Cx32Δ220-EGFP, moved slowly and in a saltatory manner like larger puncta of Cx32-WT-EGFP (Figure 11AB, see also Movies S1 and S2).

To assess if the mobility of Cx32Δ220-EGFP was different from Cx32-WT-EGFP, we photobleached gap junction plaques (contacting cells) and the non-junctional areas (single cells) and measured recovery by FRAP analysis (Figure 11CD, see Materials and Methods). The results showed that the mobility fraction of Cx32-WT-EGFP and Cx32Δ220-EGFP in gap junction plaques was low and was not different (Figure 11C). We also found that the mobility fraction of both the WT and the cytoplasmic- tail-deleted Cx32 in non-junctional areas was comparable to that observed in gap junction plaques (Figure 11D). Earlier live-cell imaging studies had indicated that the smaller gap junction-like puncta could fuse to give rise to larger puncta (41). Therefore, we also examined if larger plaques arose from the smaller plaques by fusion, a process that could be facilitated by the Cx32-CT. As assessed by analyzing the behavior of several large and small puncta composed of Cx32-WT-EGFP and Cx32Δ220-EGFP, we found that small puncta rarely fused with one another (Table 3, movies S1 and S2). Collectively, these data suggest that the Cx32-CT does not regulate the mobility of Cx32-WT and Cx32Δ220-EGFP both in the plaques and in nonfunctional regions.

DISCUSSION

The cytoplasmic tails of Cxs are highly divergent in amino acid composition, and the phosphorylation of the tails by a variety of kinases has been documented to be important in regulating the permeability of gap junctional channels (42). The cytoplasmic tails of Cxs have also been shown to interact with many cytoskeletal and cell-junction-associated proteins (12). It is thought that, besides regulating the permeability of channels, these interactions govern the assembly of Cxs into gap junctions either directly or indirectly (12). Evidence favoring the role of cytoplasmic tails in controlling gap junction assembly has been obtained through colocalization and coimmunoprecipitation studies (12), and most studies have been performed with Cx43, which is ubiquitously expressed (2,5). The extent to which the assembly of a particular Cx into gap junctions upon arrival at the cell surface is determined by factors intrinsic to the Cx itself or by extrinsic factors, such as the direct or indirect interaction of a Cx's cytoplasmic tail with the

cytoskeleton and the cell-surface-associated proteins, has not yet been explored mechanistically for many other Cxs (4,12). The first major conclusion of our study is that the size of gap junction plaques composed of cytoplasmic-tail-deleted Cx32Δ220 is drastically diminished, and that the tail is not required for initiating the formation of a gap junction plaque but for its subsequent growth. The second major conclusion of our studies is that gap junctions composed of cytoplasmic-tail-deleted Cx32 are highly unstable and that the tail of Cx32 is able to fine-tune the growth of a gap junction plaque when provided either as a part of a connexon or in *Trans* as a separate molecular entity. Our findings, thus, reveal a stringent role for the cytoplasmic tail of Cx32 in imposing or relieving local constraints at the site of cell-cell contact to restrict or permit the growth of a nascent gap junctional plaque.

Our results showed that Cx32Δ220 not only trafficked normally to the cell surface but also degraded with kinetics similar to Cx32-WT (Figure 4). Despite this, it formed 10-35 fold smaller gap junctions (Figure 1C and 2A). These data rule out impaired trafficking and/or enhanced degradation as one possible mechanism for the decrease in the size of gap junctions composed of Cx32Δ220. Moreover, Cx32Δ220 was also assembled into functional gap junctions (Figure 1D, Table 1), suggesting that the cytoplasmic-tail-deleted connexons were able to dock and assemble into miniscule functional gap junctions, and implying that the distinct puncta seen at the light microscopic level at the cell-cell contact sites likely represent junctional plaques rather than aggregates of undocked connexons (Figure 1C). Thus, the fact that the tail-deleted Cx32 is able to assemble into functional gap junctions suggests that the formation of a nascent plaque is independent of the function of the cytoplasmic tail, while the subsequent growth of the plaque is tail-dependent. In this regard, it is noteworthy to mention that the cytoplasmic-tail-deleted Cx43 mutants, Cx43Δ244 and Cx43Δ258, were also assembled into gap junctions; however, the plaque growth composed of these mutants was not affected and compromised (43,44). In fact, the average diameter of the plaques formed by the cytoplasmic-tail-deleted Cx43Δ258 was larger than those formed by the full-length Cx43 (43). Given the fact that the expression of Cx32 is restricted to the polarized and differentiated cells of the exocrine glands, our results imply that the assembly of gap

junctions composed of Cx32 is regulated differently from those composed of Cx43.

A salient as well as an intriguing aspect of our data is that the size of gap junctions composed of Cx32Δ220 was also increased 2-2.5-fold by expressing the membrane-targeted form of Cx32-CT (Cx32-CT-Myr) in *Trans* (Figure 5). Moreover, increase in size of Cx32Δ220 puncta upon expressing Cx32-CT-Myr also decreased the number of intracellular puncta (Table 2). One possible explanation for these data is that Cx32-CT-Myr either sequesters proteins at the cell surface that inhibit plaque growth and/or recruits additional proteins that facilitate growth. This possibility is supported by the Cx32-mediated recruitment of disc large protein, Dlg, to the cell surface in hepatocytes possibly through direct or indirect interaction (45,46). Lack of robust effect of Cx32-CT-Myr alone in incrementing Cx32Δ220 plaque growth compared to that observed upon expressing Cx32-WT may be due the time required by Cx32-CT-Myr, which is delivered randomly to the cell surface, to arrive near the connexons or plaques as compared to when Cx32-CT is available as a part of the connexon itself.

Earlier live-cell imaging studies had indicated that the smaller gap junction-like puncta could fuse to give rise to larger puncta (41). Therefore, we also rationalized that the larger plaques might arise from the fusion of the smaller plaques, a process that could be facilitated by the Cx32-CT. However, our live-cell imaging data revealed that this mechanism was less likely as small puncta were rarely seen to fuse with one another (Movies S1 and S2, Table 3). Moreover, while our live-cell imaging data showed substantially decreased mobility of larger plaques formed of Cx32-WT-EGFP, we also found that gap junction-like puncta composed of Cx32Δ220-EGFP were highly mobile and moved faster and abruptly (Figure 11B). Moreover, we also found that small gap junction-like puncta formed by the Cx32-WT-EGFP, comparable in size to those formed by Cx32Δ220-EGFP, were as stable as larger puncta (Figure 11A, Movies S1 and S2). Furthermore, our FRAP analysis showed that the mobility of both Cx32Δ220-EGFP and Cx32-WT-EGFP within gap junctional plaques (in contacting cells) and in non-junctional membranes (in single cells) was not discernibly different (Figure 11CD). These results rule out differential diffusion of Cx32-WT and

Cx32Δ220 connexons at the cell surface as one mechanism to account for the drastic difference in the size of gap junction plaques. In this regard it is noteworthy to mention that the mobility of gap junction-like puncta composed of cytoplasmic tail-deleted Cx43 was not different from Cx43-WT (44).

The findings that the small size of gap junctional plaques composed of Cx32Δ220 could be rescued upon co-expressing Cx32-WT and vice versa (Figure 5), combined with the fact that the tail had no effect on the mobility of Cx32, raise intriguing possibilities with regard to the molecular mechanisms involved in the genesis of larger plaques and the role played by the Cx32-CT in plaque growth. Evidence to date supports the notion that once a plaque has been nucleated, the subsequent growth of a plaque occurs upon recruitment of connexons to its periphery either by diffusion (44,47-49) or upon direct delivery of connexons to its vicinity (50). Moreover, it is highly likely that the docking of connexons to form functional cell-cell channels occurs either in the vicinity of the plaque or during docking near the plaque itself, with a concomitant incorporation of the channels into the plaque (51,52). What might then be the possible explanation for the failure of Cx32Δ220 to assemble into larger gap junctions?

The molecular collisions among several transmembrane proteins have recently been postulated to be regulated by the partitioning of the entire plasma membrane by the actin-based membrane cytoskeleton and/or its associated proteins into several subdomains (53). Anchoring of transmembrane proteins to the cytoskeleton proteins either directly or indirectly via a scaffolding protein is likely to hinder or prevent its diffusion in the plane of the plasma membrane compared to a protein that is not anchored (54-56). Tethering of a Cx's cytoplasmic tail to the cytoskeleton either directly or indirectly via a scaffolding protein could attenuate its delivery to the plaque via diffusion or stimulate plaque growth by anchoring connexons near the plaque and increase the probability of their docking with the connexons in the adjacent cells, with concomitant incorporation of the channels into the plaque. A similar mechanism may be evoked to explain the increased motility of small gap junctions composed of Cx32Δ220 and increased stability of plaques composed of Cx32-WT. In addition, the cytoplasmic tail might recruit some factors to the sites of nascent plaques to stabilize membrane subdomains near its vicinity to permit docking of connexons and the subsequent incorporation of channels in the plaque.

Several lines of evidence provide support for this notion. For example, earlier studies showed that when interaction between the cytoplasmic tail of Cx43 and ZO-1 — a scaffolding protein that links Cx43's cytoplasmic tail to the cytoskeleton — was disrupted, connexon recruitment and/or incorporation to the plaque periphery was facilitated, leading to an increase in the size of gap junction plaque (52). On the other hand, deletion of the PDZ-binding domain of Cx50, a Cx expressed in the lens epithelial cells and shown to interact with ZO-1 (57), inhibited gap junction assembly (11). Hence, it is possible that the cytoplasmic tail is required for anchoring Cx32 to cytoskeletal proteins near the plaque to facilitate docking of connexons between the contiguous cells and the subsequent incorporation of the channels into nascent plaque. Support for this comes from our data showing increase in the size of gap junctions composed of Cx32Δ220 upon transient expression of Cx32-WT (Figure 5A), decrease in the size of gap junctions composed of Cx32-WT upon transient expression of Cx32Δ220 (Figure 5B), and failure of Cx32Δ220, but not Cx32-WT, to cluster to form larger gap junctions upon elevation of intracellular levels of cAMP (Figure 9). However, unlike Cx43, only few proteins have been discovered to interact with Cx32 (12).

Based on the above arguments, we propose that the cytoplasmic tail of Cx32 is not required to nucleate a plaque but for the stability of the plaque once it has been initiated, possibly by permitting its linkage to the cytoskeleton by mass action resulting from the clustering of channels after the plaques have been nucleated. The nascent plaques formed by the cytoplasmic-tail-deleted Cx32Δ220 are unstable because they are unable to establish a firm linkage with the cytoskeleton directly or indirectly via the associated proteins. We also propose that the mobility of Cx32-WT in non-junctional areas away from the plaque is not dependent on the anchoring of the tail to the cytoskeleton. The Cx32Δ220 plaques remain small because they are dislodged before a significant number of connexons are recruited to the plaque periphery. This explanation is in accord with the increased stability of both the small and the large

plaques formed of Cx32-WT. Moreover, this explanation is also consistent with the lack of formation of gap junctions between cells expressing Cx32-WT and Cx32Δ220. Earlier studies showed that in pig thyrocytes, which expressed endogenous Cx43 and Cx32, as well as in Cx43-expressing human embryonic kidney cells in which Cx26 was transiently expressed, while both Cxs were assembled into gap junctions the plaques composed of each Cx subtype resided in two different plasma membrane sub-domains (58,59). Our results with Cx32Δ220 may provide rational explanation for the segregation of plaques composed of Cx43 and Cx32 in different subdomains of the plasma membrane as well as for the increased motility of Cx26-GFP, a tail-less Cx, in gap junction-like clusters (48). Altogether, our results suggest that the assembly of Cx32 is regulated differently than that of Cx43 and substantiate the conclusion drawn from earlier studies, which showed that the assembly of Cx32 and Cx43 into gap junctions was differentially regulated in cadherin-null human squamous carcinoma cells (18).

What might be the possible physiological relevance of the cytoplasmic-tail-mediated facilitation of gap junction assembly with regard to the growth of a plaque? The number of cell-cell channels in a given gap junction plaque varies substantially and may range from 50 to over 10,000; moreover, there is a wide range of variation in the size of gap junctions formed between the two contiguous cells (8,60). Furthermore, hormone-induced clustering of cell-cell channels to increase the size of gap junctions is frequently observed (61). Clustering of cell-cell channels is a prerequisite for their opening and that the larger gap junctional plaques have more open channels compared to the smaller plaques (51). It is tempting to speculate that while post-translational modifications in the cytoplasmic tail of a Cx are used to acutely regulate gating of cell-cell channels, the engagement and the disengagement of a Cx's tail with the cytoskeletal proteins via the cytoplasmic tail are used for the chronic regulation of permeability of channels with slower, spatio-temporal characteristics. Alternatively, the cytoplasmic-tail-mediated increase in gap junction plaque size and stability may facilitate the assembly of other junctional complexes, which are required to maintain the polarized and differentiated state of epithelial cells (62,63). More elaborate studies are needed to assess further the physiological significance of our findings with respect to functional role of gap junctional communication.

References

1. Goodenough, D. A., and Paul, D. L. (2009) Gap junctions. *Cold Spring Harb.Perspect.Biol.* **1**, a002576
2. Beyer, E. C., and Berthoud, V. M. (2009) The Family of Connexin Genes. in *Connexins: A Guide* (Harris, A., and Locke, D. eds.), Springer. pp 3-26
3. Dobrowolski, R., and Willecke, K. (2009) Connexin-caused genetic diseases and corresponding mouse models. *Antioxidant and Redox Signaling* **11**, 283-296
4. Laird, D. W. (2010) The gap junction proteome and its relationship to disease. *Trends In Cell Biology* **20**, 92-101
5. Laird, D. W. (2006) Life cycle of connexins in health and disease. *Biochem J* **394**, 527-543
6. Foote, C. I., Zhou, L., Zhu, X., and Nicholson, B. J. (1998) The parttern of disulfide linkages in the extracellular loop regions of connexin 32 suggests a model for the docking interface of gap junctions. *J Cell Biol* **140**, 1187-1197
7. Zhou, L., Kasperek, E. M., and Nicholson, B. J. (1999) Dissection of the molecular basis of pp60(v-src) induced gating of connexin 43 gap junction channels. *J.Cell Biol* **144**, 1033-1045
8. Sosinsky, G. E., and Nicholson, B. J. (2005) Structural organization of gap junction channels. *Biochimica et Biophysica Acta (BBA) - Biomembranes* **1711**, 99-125
9. Harris, A. L. (2007) Connexin channel permeability to cytoplasmic molecules. *Progress in biophysics and molecular biology* **94**, 120-143
10. George, C. H., Kendall, J. M., and Evans, H. W. (1999) Intracellular trafficking pathways in the assembly of connexins into gap junctions. *J.Biol.Chem.* **274**, 8678-8685
11. Chai, Z., Goodenough, D. A., and Paul, D. L. (2011) Cx50 requires an intact PDZ-binding motif and ZO-1 for the formation of functional intercellular channels. *Molecular biology of the cell* **22**, 4503-4512
12. Herve, J. C., Derangeon, M., Sarrouilhe, D., Giepmans, B. N., and Bourmeyster, N. (2012) Gap junctional channels are parts of multiprotein complexes. *Biochim Biophys Acta* **1818**, 1844-1865
13. Wei, C. J., Xu, X., and Lo, C. W. (2004) Connexins and cell signaling in development and disease.
14. Bosco, D., Haefliger, J. A., and Meda, P. (2011) Connexins: Key Mediators of Endocrine Function. *Physiol.Rev.* **91**, 1393-1445
15. Mehta, P. P., Perez-Stable, C., Nadji, M., Mian, M., Asotra, K., and Roos, B. A. (1999) Suppression of human prostate cancer cell growth by forced expression of connexin genes. *Dev Genetics* **24**, 91-110
16. Shen, M. M., and Abate-Shen, C. (2010) Molecular genetics of prostate cancer: new prospects for old challenges. *Genes & Development* **24**, 1967-2000
17. Mitra, S., Annamalai, L., Chakraborty, S., Johnson, K., Song, X., Batra, S. K., and Mehta, P. P. (2006) Androgen-regulated Formation and Degradation of Gap Junctions in Androgen-responsive Human Prostate Cancer Cells. *Mol Biol Cell* **17**, 5400-5416
18. Chakraborty, S., Mitra, S., Falk, M. M., Caplan, S., Wheelock, M. J., Johnson, K. R., and Mehta, P. P. (2010) E-cadherin differentially regulates the assembly of connexin43 and connexin32 into gap junctions in human squamous carcinoma cells. *J Biol Chem* **285,** 10761-10776
19. Johnson, K. E., Mitra, S., Katoch, P., Kelsey, L. S., Johnson, K. R., and Mehta, P. P. (2013) Phosphorylation on Ser-279 and Ser-282 of connexin43 regulates endocytosis and gap junction assembly in pancreatic cancer cells. *Molecular biology of the cell* **24**, 715-733
20. Govindarajan, R., Chakraborty, S., Falk, M. M., Johnson, K. R., Wheelock, M. J., and Mehta, P. P. (2010) Assembly of connexin43 is differentially regulated by E-cadherin and N-cadherin in rat liver epithelial cells. *Mol Biol Cell* **21**, 4089-4107
21. Mehta, P. P., Hotz-Wagenblatt, A., Rose, B., Shalloway, D., and Loewenstein, W. R. (1991) Incorporation of the gene for a cell-to-cell channel proteins into transformed cells leads to normalization of growth. *J Membr Biol* **124**, 207-225
22. Govindarajan, R., Song, X. H., Guo, R. J., Wheelock, M. J., Johnson, K. R., and Mehta, P. P. (2002) Impaired trafficking of connexins in androgen-independent human prostate cancer cell lines and its mitigation by a-catenin. *J Biol Chem* **277**, 50087-50097

23. Kelsey, L., Katoch, P., johnson, K. E., Batra, S. K., and Mehta, P. (2012) Retinoids regulate the formation and degradation of gap junctions in androgen-responsive human prostate cancer cells. *PLoS ONE* **7**, E32846

24. Mehta, P. P., Bertram, J. S., and Loewenstein, W. R. (1986) Growth inhibition of transformed cells correlates with their junctional communication with normal cells. *Cell* **44**, 187-196

25. Roberts, B. J., Reddy, R., and Wahl, J. K., 3rd. (2013) Stratifin (14-3-3 sigma) limits plakophilin-3 exchange with the desmosomal plaque. *PloS one* **8**, e77012

26. Martin, P. E., Steggles, J., Wilson, C., Ahmad, S., and Evans, W. H. (2000) Targeting motifs and functional parameters governing the assembly of connexins into gap junctions. *Biochem.J* **349**, 281-287

27. Gourdie, R. G., Green, C. R., and Severs, N. J. (1991) Gap junction distribution in adult mammalian myocardium revealed by an anti-peptide antibody and laser scanning confocal microscopy. *Journal of cell science* **99**, 41-55

28. VanSlyke, J. K., and Musil, L. S. (2000) Analysis of connexin intracellular transport and assembly. *Methods* **20**, 156-164

29. Maeda, M., Johnson, K. R., and Wheelock, M. J. (2005) Cadherin switching: essential for behavioral but not morphological changes during an epithelium-to-mesenchyme transition. *J Cell Sci* **118**, 873-887

30. Cotrina, M. L., and Nedergaard, M. (2009) Physiological and pathological functions of P2X7 receptor in the spinal cord. *Purinergic signalling* **5**, 223-232

31. Atkinson, M. M., Lampe, P. D., Lin, H. H., Kollander, R., Li, X. R., and Kiang, D. T. (1995) Cyclic AMP modifies the cellular distribution of connexin43 and induces a persistent increase in the junctional permeability of mouse mammary tumor cells. *J Cell Sci* **108**, 3079-3090

32. Paulson, A., Lampe, P., Meyer, R., TenBroek, E., Atkinson, M., Walseth, T., and Johnson, R. (2000) Cyclic AMP and LDL trigger a rapid enhancement in gap junction assembly through a stimulation of connexin trafficking. *Journal of cell science* **113**, 3037-3049

33. Mehta, P. P., Lokeshwar, B. L., Schiller, P. C., Bendix, M. V., Ostenson, R. C., Howard, G. A., and Roos, B. A. (1996) Gap-junctional communication in normal and neoplastic prostate epithelial cells and its regulation by cAMP. *Mol Carcinogen* **15**, 18-32

34. Mehta, P. P., Yamamoto, M., and Rose, B. (1992) Transcription of the gene for the gap junctional protein connexin43 and expression of functional cell-to-cell channels are regulated by cAMP. *Mol Biol Cell* **3**, 839-850

35. Saez, J.C, Angus, C. N., Andrew, J. C., David, C. S., Elliot, L. H., Paul, G., and Michael, V. L. B. (1990) Phosphorylation of connexin 32, a hepatocyte gap-junction protein, by cAMP-dependent protein kinase, protein kinase C and Ca2+ /calmodulin-dependent protein kinase II. *European Journal of Biochemistry* **192,** 263-273

36. Sáez, J., Gregory, W., Watanabe, T., Dermietzel, R., Hertzberg, E., Reid, L., Bennett, M., and Spray, D. (1989) cAMP delays disappearance of gap junctions between pairs of rat hepatocytes in primary culture. *The American journal of physiology* **257**, 1-11

37. Seamon, K. B., and Daly, J. W. (1981) Forskolin: a unique diterpene activator of cyclic AMP-generating systems. *Journal of cyclic nucleotide research* **7**, 201-224

38. Wang, Y., and Mehta, P. P. (1995) Facilitation of gap junctional communiation and gap junction formation by inhibition of glycosylation. *Euro J Cell Biol* **67**, 285-296

39. Wang, Y., Mehta, P. P., and Rose, B. (1995) Inhibition of Glycosylation Induces Formation of Open Connexin-43 Cell-to-Cell Channels and Phosphorylation and Triton X-100 Insolubility of Connexin-43. *J.Biol.Chem.* **270**, 26581-26585

40. Wang, Y., and Rose, B. (1995) Clustering of Cx43 cell-to-cell channels into gap junction plaques: regulation by cAMP and microfilaments. *J.Cell Sci.* **108**, 3501-3508

41. Holm, I., Mikhailov, A., Jilson, T., and Rose, B. (1999) Dynamics of gap junctions observed in living cells with connexin43-GFP chimeric protein. *Eur J Cell Biol* **78**, 856-866

42. Solan, J. L., and Lampe, P. D. (2009) Biochemistry of connexins. in *Connexins: A Guide* (Harris, A., and Locke, D. eds.), Springer. pp 263-286

43. Maass, K., Ghanem, A., Kim, J. S., Saathoff, M., Urschel, S., Kirfel, G., Grummer, R., Kretz, M., Lewalter, T., Tiemann, K., Winterhager, E., Herzog, V., and Willecke, K. (2004) Defective Epidermal Barrier in Neonatal Mice Lacking the C-Terminal Region of Connexin43. *Molecular biology of the cell* **15**, 4597-4608

44. Simek, J., Churko, J., Shao, Q., and Laird, D. W. (2009) Cx43 has distinct mobility within plasma-membrane domains, indicative of progressive formation of gap-junction plaques. *Journal of cell science*, jcs

45. Duffy, H. S., Iacobas, I., Hotchkiss, K., Hirst-Jensen, B. J., Bosco, A., Dandachi, N., Dermietzel, R., Sorgen, P. L., and Spray, D. C. (2007) The Gap Junction Protein Connexin32 Interacts with the Src Homology 3/Hook Domain of Discs Large Homolog 1. *J.Biol.Chem.* **282**, 9789-9796

46. Stauch, K., Kieken, F., and Sorgen, P. (2012) Characterization of the Structure and Intermolecular Interactions between the Connexin 32 Carboxyl-terminal Domain and the Protein Partners Synapse-associated Protein 97 and Calmodulin. *J.Biol.Chem.* **287**, 27771-27788

47. Lauf, U., Giepmans, B. N. G., Lopez, P., Braconnot, S., Chen, S. C., and Falk, M. M. (2002) Dynamic trafficking and delivery of connexons to the plasma membrane and accretion to gap junctions in living cells. *PNAS* **99**, 10446-10451

48. Thomas, T., Jordan, K., Simek, J., Shao, Q., Jedeszko, C., Walton, P., and Laird, D. W. (2005) Mechanisms of Cx43 and Cx26 transport to the plasma membrane and gap junction regeneration. *J Cell Sci* **118**, 4451-4462

49. Gaietta, G., Deerinck, T., Adams, S., Bouwer, J., Tour, O., Laird, D., Sosinsky, G., Tsien, R., and Ellisman, M. (2002) Multicolor and electron microscopic imaging of connexin trafficking. *Science (New York, N.Y.)* **296**, 503-507

50. Shaw, R. M., Fay, A. J., Puthenveedu, M. A., von Zastrow, M., Jan, Y. N., and Jan, L. Y. (2007) Microtubule Plus-End-Tracking Proteins Target Gap Junctions Directly from the Cell Interior to Adherens Junctions. *Cell* **128**, 547-560

51. Bukauskas, F. F., Jordan, K., Bukauskiene, A., Bennett, M. V. L., Lampe, P. D., Laird, D. W., and Verselis, V. K. (2000) Clustering of connexin 43-enhanced green fluorescent protein gap junction channels and functional coulpling in living cells. *Proc Natl Acad Sci USA* **97**, 2556-2561

52. Rhett, J. M., Jourdan, J., and Gourdie, R. G. (2011) Connexin 43 connexon to gap junction transition is regulated by zonula occludens-1. *Molecular biology of the cell* **22**, 1516-1528

53. Kusumi, A., Fujiwara, T. K., Morone, N., Yoshida, K. J., Chadda, R., Xie, M., Kasai, R. S., and Suzuki, K. G. (2012) Membrane mechanisms for signal transduction: the coupling of the meso-scale raft domains to membrane-skeleton-induced compartments and dynamic protein complexes. *Seminars in cell & developmental biology* **23**, 126-144

54. Sheetz, M. P., Schindler, M., and Koppel, D. E. (1980) Lateral mobility of integral membrane proteins is increased in spherocytic erythrocytes. *Nature* **285**, 510-511

55. Tomishige, M., Sako, Y., and Kusumi, A. (1998) Regulation mechanism of the lateral diffusion of band 3 in erythrocyte membranes by the membrane skeleton. *The Journal of cell biology* **142**, 989-1000

56. Jaqaman, K., Kuwata, H., Touret, N., Collins, R., Trimble, W. S., Danuser, G., and Grinstein, S. (2011) Cytoskeletal control of CD36 diffusion promotes its receptor and signaling function. *Cell* **146**, 593-606

57. Nielsen, P. A., Baruch, A., Shestopalov, V. I., Giepmans, B. N., Dunia, I., Benedetti, E. L., and Kumar, N. M. (2003) Lens connexins alpha3Cx46 and alpha8Cx50 interact with zonula occludens protein-1 (ZO-1). *Mol Biol Cell* **14**, 2470-2481

58. Guerrier, A., Fonlup, t. P., Morand, I., Rabilloud, R., Audebet, C., Krutovskikh, V., Gros, D., Rousset, B., and Munari-Silem, Y. (1995) Gap junctions and cell polarity: connexin32 and connexin43 expressed in polarized thyroid epithelial cells assemble into gap junctions, which are located in distinct regions of the lateral plasma membrane domain. *J Cell Sci* **108**, 2609-2617

59. Gemel, J., Valiunas, V., Brink, P. R., and Beyer, E. C. (2004) Connexin43 and connexin26 form gap junctions, but not heteromeric channels in co-expressing cells. *J Cell Sci* **117**, 2469-2480

60. Sosinsky, G. E., Gaietta, G., and Giepmans, B. N. G. (2009) Gap junction morphology and dynamics in situ. in *Connexins: A Guide* (Harris, A., and Locke, D. eds.), Springer. pp 241-261

61. Stagg, R. B., and Fletcher, W. H. (1990) The hormone-induced regulation of contact-dependent cell-cell communication by phosphorylation. *Endocr Rev* **11**, 302-325
62. Mellman, I., and Nelson, W. J. (2008) Coordinated protein sorting, targeting and distribution in polarized cells. *Nat Rev Mol Cell Biol* **9**, 833-845
63. Bryant, D. M., and Mostov, K. E. (2008) From cells to organs: building polarized tissue. *Nat Rev Mol Cell Biol* **9**, 887-901

Figure Legends

Figure 1. **Cytoplasmic-tail-deleted Cx32 assembles into smaller gap junctions.**

LNCaP and BxPC3 cells were infected with the control and Cx32-harboring recombinant retroviruses and Cx32 expression level and gap junction assembly were determined by Western blot (**A,B**) and immunocytochemical (**C**) analyses. **A**. Note that only cells infected with Cx32-harboring retroviruses express Cx32-WT (32-WT) and Cx32Δ220 (32Δ220) in LNCaP (**A**) and BxPC3 (**B**) cells. The numbers on the left indicate the position of the molecular weight markers. **C**. Note that Cx32-WT-expressing LNCaP (upper row, left panels) and BxPC3 (lower row, left panels) cells form large gap junctions (red) whereas Cx32Δ220-expressing LNCaP (upper row, right panels) and BxPC3 cells (bottom row, right panels) form miniscule gap junctions (red). The enlarged images of the boxed areas in upper and lower panels are shown towards left. Immunostaining for E-cadherin (E-Cad, green) was used to delineate the cell-cell interfaces. The nuclei (blue) were stained with DAPI.

Figure 2. Cytoplasmic-tail-deleted Cx32 assembles into smaller but functional gap junctions.

Cx32-WT and Cx32Δ220 expressing LNCaP and BxPC3 cells, seeded on glass cover slips, were immunostained for Cx32. **A.** Areas (Mean ± SE) of 350 distinct gap junction puncta, from 3 single optical sections from 3 independent experiments after iterative volume de-convolution of the captured images, were determined using the measurement module of Volocity. The area is represented in μm^2 (see Materials and Methods). Note the 20-35-fold decrease in the mean gap junction plaque area in cells expressing Cx32Δ220. The differences in areas between Cx32-WT and Cx32Δ220 expressing cells were statistically highly significant ($P \leq 0.001$). **B**. LNCaP cells expressing Cx32-WT and Cx32Δ220 were microinjected with Alexa-488 (Green, MW 570) and Alexa-594 (red, MW 760). Note extensive transfer of both tracers in LNCaP cells expressing Cx32-WT and weaker transfer in cells expressing Cx32Δ220. The microinjected cells are marked by the arrows.

Figure 3. Detergent-solubility of Cx32-WT and Cx32Δ220 in LNCaP and BxPC3 cells.

Cells were grown in 10-cm dishes for 5-7 days when they became confluent (80%). TX100-solubility assay was used to measure the assembly of Cx32-WT and Cx32Δ220 into gap junctions. TX100-solubility of β-catenin (β-cat), an adherens junction associated protein, was used as a control. Note that both Cx32-WT and Cx32Δ220 are found in TX100-soluble and -insoluble fractions.

Figure 4. Cx32-WT and Cx32Δ220 traffic and degrade normally in LNCaP and BxPC3 cells.

A. The cell surface proteins of LNCaP and BxPC3 were biotinylated, and were pulled down by immobilized streptavidin and immunoblotted for Cx32. Biotinylation of E-cadherin (E-cad) was used as a positive control. A non-biotinylated dish was kept as a control (-). For input, 10 μg of total cell lysate was used. Note that both Cx32-WT and Cx32Δ220 and E-cad are efficiently biotinylated. **B**. Cell surface associated Cx32-WT and

Cx32Δ220 degrade with similar kinetics in LNCaP and BxPC3 cells. Cells were biotinylated at 4ºC and were incubated for various times at 37 ºC before streptavidin pull-down and Western blot analysis (see Materials and Methods). Representative blots for Cx32-WT and Cx32Δ220 from LNCaP (**B**) and BxPC3 (**C**) cells are shown. **D**. The blots were quantified using C-digit and the values from 2 independent experiments were plotted graphically with Sigma plot using the best fit function. Note that biotinylated Cx32-WT and Cx32Δ220 degrade with similar kinetics in both cell lines. The values in the two independent experiments varied by ≤10% and hence only symbols from one experiment are shown.

Figure 5. Cytoplasmic tail of Cx32 controls gap junction size.

A. Myc-tagged Cx32-WT (Cx32-WT-Myc) was transiently expressed in LN32Δ220 (top row) and Bx32Δ220 (bottom row) cells expressing Cx32Δ220 stably. After 24 h, cells were immunostained for Myc (green) and Cx32 (red) using antibody raised against the Cx32-CT (amino acids 265-279). Note the formation of large gap junction plaques in cells expressing Cx32-WT-Myc. **B**. Myc-tagged Cx32Δ220 (Cx32Δ220-Myc) was transiently expressed in LN32-WT (top row) and Bx32-WT (bottom row) cells expressing Cx32-WT stably. After 24 h, cells were immunostained for Myc (red) and Cx32 (green). Note loss of gap junction plaque in cells expressing Cx32Δ220-Myc. **C**. Gap junction size in cells expressing Cx32-WT (32-WT, green) and Cx32Δ220 (Δ220, red) in LNCaP (top row) and BxPC3 (bottom row) transiently transfected with pmCherry and pAcGFP (not shown). **D**. Mean surface area of the rescued gap junctions in LN32Δ220 (LNCaP) and Bx32Δ220 (BxPC3) cells. Surface areas (Mean ±SE) of 350 distinct gap junction puncta, from 3 single optical sections from 3 independent experiments after iterative volume de-convolution of the captured images, were determined using the measurement module of Volocity. The area is represented in μm^2 (see Materials and Methods). Note the 15-20 fold increase in the mean gap junction plaque area in cells expressing Cx32-WT-Myc. The nuclei (blue) were stained with DAPI.

Figure 6. An optimal expression of Cx32-WT and Cx32Δ220 is required to restore gap junction assembly.

HEK293T cells were transiently transfected with Cx32-WT and Cx32Δ220-EGFP at different ratios as indicated by the red and green circles. Transfected cells were fixed and immunostained for Cx32 (red) using antibody against the Cx32-CT. Note that cells expressing high levels of Cx32-WT are assembled into larger gap junctions.

Figure 7. Cx32-CT partially restores gap junction assembly.

A. LN32-WT, LN32Δ220, Bx32-WT and Bx32Δ220 were transiently co-transfected with mCherry, mCherry-Myr (CH-MYR), and Cx32-CT-Turquoise-Myr (32-CT-TQ-MYR). Twenty four hours after transfection, cells were fixed and immunostained for Cx32 (green). Note that only the expression of Cx32-CT-TQ-Myr increases the size of gap junction-like puncta. The color of the blue channels indicating the expression of Cx32-CT-TQ-MYR was converted into red to simplify the figure. **B.** Areas (Mean ±SE) of 350 distinct gap junction puncta, from 3 single optical sections from 3 independent experiments after iterative volume de-convolution of the captured images, were determined using the measurement module of Volocity. The area is represented in μm^2 (see

Materials and Methods). Note the 2-3 fold increase in the mean gap junction plaque area in cells expressing Cx32-CT-TQ-MYR.

Figure 8. LNCaP cells expressing Cx32-WT and Cx32Δ220 do not form gap junctions.

LN-WT, LN-EGFP, LN32-WT, LN-EGFP, LN32-WT-mAPL, LN32Δ220, and LN32Δ220-EGFP cells expressing cells were cocultured at various ratios (Materials and Methods). **Top row**: Formation of gap junctions between LN32-WT and LN-32Δ220-EGFP was examined after immunostaining cocultures with the antibody against the carboxyl tail of Cx32-WT (red).   Note that LN32-WT cells segregate from LN32Δ220-EGFP (green) cells. **Bottom row**: LN32-WT cells in coculture with LN-EGFP cells were immunostained for Cx32. Note that LN32-WT (red) cells segregate from LN-EGFP (green) cells in cocultures. **Second row**: LN32-WT-mAPL cells were cocultured with LN32Δ220-EGFP cells and formation of heterologous gap junctions was examined. Note segregation of LN32-WT-mAPL (red) cells from LN32Δ220-EGFP (green) cells and lack of gap junction formation between them. **Third row**: LN-WT cells were cocultured with LN-EGFP cells and immunostained for E-cadherin (red). Note that there is no segregation of LN-WT and LN-EGFP (green) cells. The nuclei (blue) were stained with DAPI.

Figure 9: Cx32Δ220 fails to cluster in response to forskolin.

LN32-WT and LN32Δ220 cells were treated with forskolin for 8 h and gap junction assembly was examined immunocytochemically. White arrows point to gap junctions (red). Note that forskolin increases the size of gap junctions of Cx32-WT but not of Cx32Δ220. The cell-cell interfaces were delineated by immunostaining for E-cadherin (E-Cad, green). The nuclei (blue) were stained with DAPI.

Figure 10. Gap junctions composed of Cx32Δ220 are more motile than those formed of Cx32-WT.

 Selected time lapse images of BxPC3 cells expressing EGFP-tagged Cx32-WT (Bx32-WT-EGFP) and Cx32Δ220 (Bx32Δ220-EGFP) are shown. The traced gap junction puncta are indicated by the yellow arrows. The numbers in white indicate lapsed time in minutes. Note the rapid disappearance of Cx32Δ220-EGFP puncta compared to Cx32-WT-EGFP puncta. See also movies S1 and S2.

Figure 11. Motility of gap junctions and connexons composed of Cx32-WT and Cx32Δ220.

        Average speed of gap junction puncta composed of Cx32-WT-EGFP and Cx32Δ220-EGFP in BxPC3 cells (n=10). Note that the average speed of gap junction puncta composed Cx32Δ220 is nearly twice of puncta composed of Cx32-WT.   Note also that the Cx32-WT puncta comparable in size to the Cx32Δ220 puncta also move slowly. **B**. Motile behavior of gap junction puncta composed of Cx32-WT-EGFP and Cx32Δ220-EGFP in BxPC3 cells as determined by tracking individual puncta (n=5; only two are shown). Each movement step is indicated by the red dot on the traced line (see Materials and Methods). **CD.** Analysis of the mobility fraction of Cx32-WT-EGFP (Cx32-WT) and Cx32Δ220-EGFP (Cx32-T220) by FRAP analysis within gap junctional plaques (Gap Junctional) in contacting cells (**C**) and in non-gap junctional (Non-Junctional)

regions in single cells (**D**). Note that there is no difference in the mobile fraction of Cx32-WT and Cx32Δ220 in gap junction plaques and at non-junctional regions. For FRAP analysis, 10 junctional and non-junctional regions were photobleached for each cell line.

TABLES

Table 1. Junctional transfer of fluorescent tracers in LN32-WT and LN32Δ220 cells.

Junctional Tracer	Experiment Number	Junctional Transfer [a]	
		LN32	**LN32Δ220**
Lucifer Yellow	1	26 ± 4(18)	7 ± 2(14)
	2	29 ± 6(16)	6 ±2 (13)
Alexa-488	1	22 ± 5(16)	6 ± 2(14)
	2	23 ±6 (14)	8 ± 3(18)
Alexa-594	1	13 ±3 (14)	4 ± 1(22)
	2	11 ± 4(17)	3 ± 1(29)

Cells, seeded in 6 cm dishes in replicate, were grown for 4-7 days to 70 % confluence. Junctional transfer was measured after microinjecting fluorescent tracers (see Materials and Methods).

a: The number of fluorescent cell neighbors (mean ± SE) 1 min (Lucifer Yellow), 3 min (Alexa-488) and 15 min (Alexa-594) after microinjection into test cell. The total number of injection trials is shown in the parentheses

Table 2. Expression of membrane-targeted Cx32-CT decreases number of intracellular puncta.

Transfection	LN32-WT	LN32Δ220	Bx32-WT	Bx32Δ220
mCherry-Myr	10.7 ± 4.1 (30)	18.7 ± 3.3 (25)	18.2 ± 3.8 (25)	18.6 ± 3.6 (42)
32-CT-mTurquoise-Myr	3.3 ± 1.0 (57)	8.1 ± 3.6 (62)	7.0 ± 4.3 (62)	6.2 ± 3.8 (57)

LNCaP and BxPC3 cells stably expressing Cx32-WT (LN32-WT, Bx32-WT)) and Cx32Δ220 (LN32Δ220, Bx32Δ220) were transfected with membrane-targeted mCherry-Myr or Cx32-CTmTruquoise-Myr and number of intracellular puncta was determined 24 h after transfection as described in Materials and Methods. Numbers represent the Mean ± S.E. In parenthesis is the number of transfected cells counted. Transfected cells were from 10 different fields in two independent experiments.

Table 3. Larger gap junctions do not arise from the fusion of microscopically detectable smaller gap junctions

BxPC3 Cells Expressing	# of Puncta Tracked	# Puncta Never Fused (%)	# Puncta Fused but Separated	# Puncta Fused
Bx32-WT-EGFP	205 (5)[a]	188	8 (4)[b]	17 (8)[b]
Bx32Δ220-EGFP	193 (5)[a]	186	5 (2.6)	7 (3.6)[b]
LN32Δ220-EGFP	105 (4)	101	6 (5.7)	8 (5.7)[b]

Live cell imaging of BxPC3 and LNCaP cells expressing EGFP tagged Cx32-WT and Cx32Δ220 was performed and puncta that appeared at the cell-cell contact were individually tracked as described in Materials and Methods. a= Number of movies analyzed. b= % of Total.

Reference List

1. Nielsen, P. A., Baruch, A., Shestopalov, V. I., Giepmans, B. N. G., Dunia, I., Benedetti, E. L., and Kumar, N. M. (2003) Lens Connexins ¦3Cx46 and ¦8Cx50 Interact with Zonula Occludens Protein-1 (ZO-1) *Mol. Biol. Cell* **14,** 2470-2481

A

LNCaP | 32-WT | 32Δ220

32.5
25
16.5

ß-actin

B

BxPC3 | 32-WT | 32Δ220

32.5
25
16.5

ß-actin

C Cx32-WT/E-Cad   Cx32Δ220/E-Cad

LNCaP

BxPC3
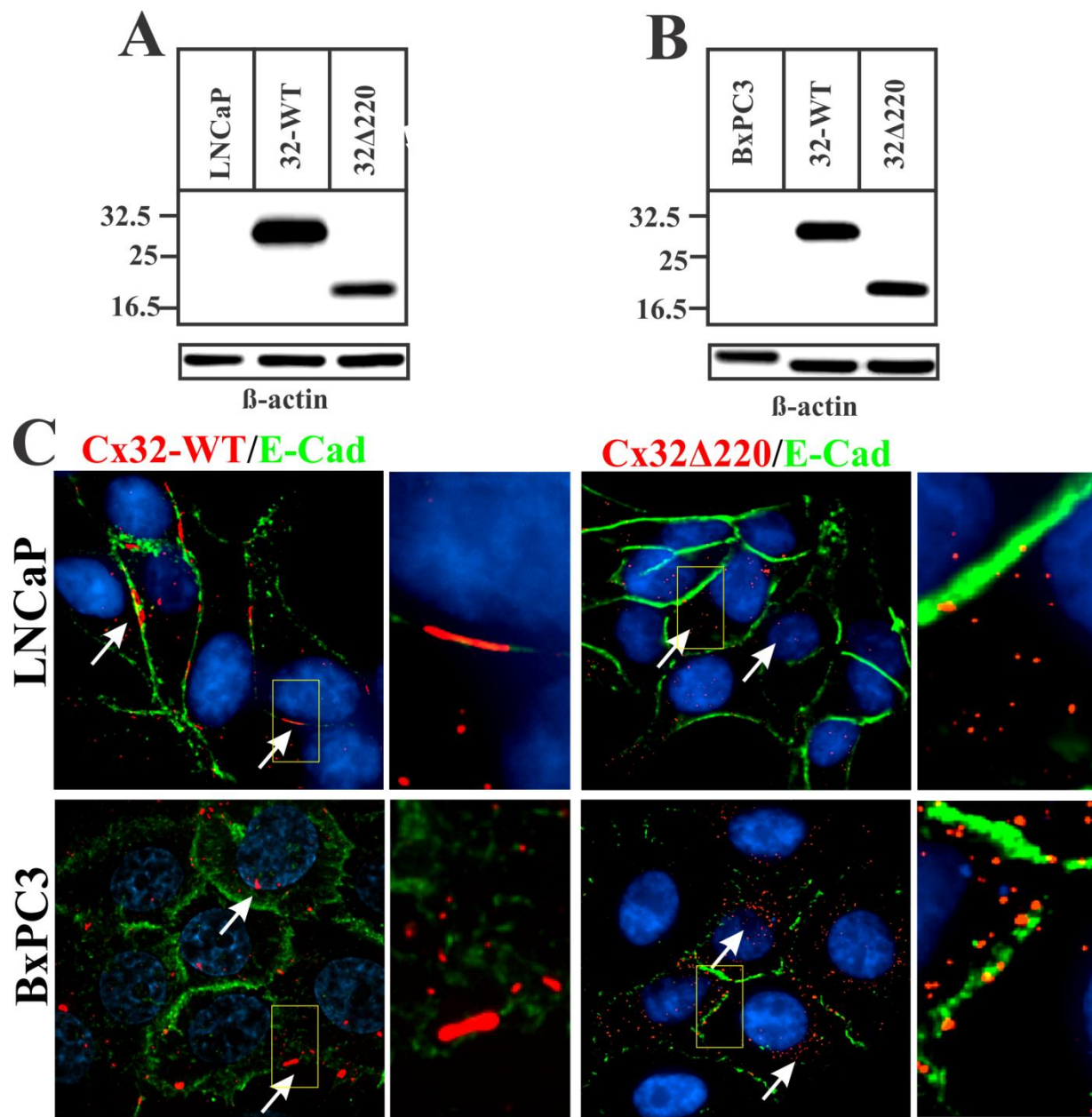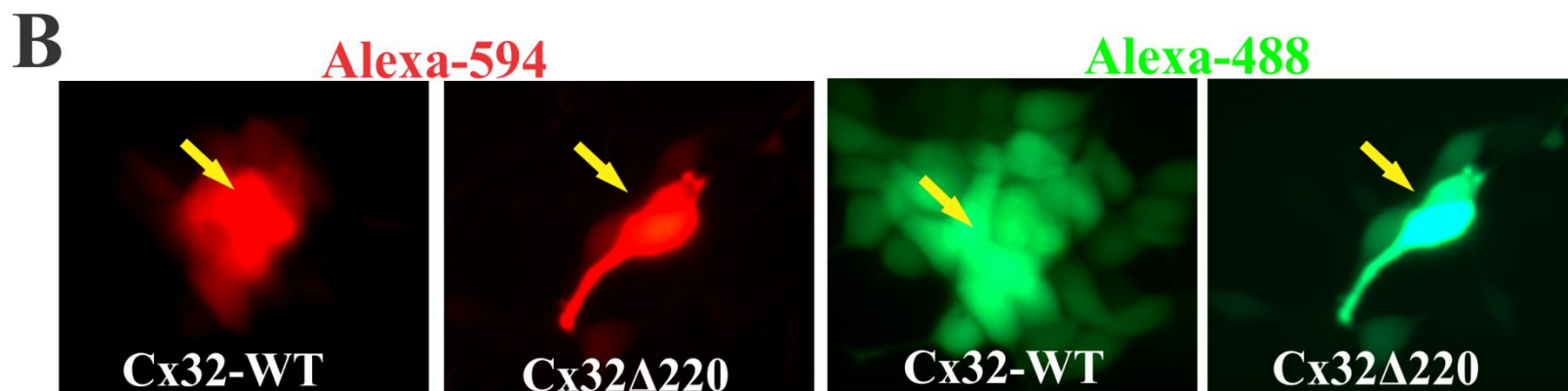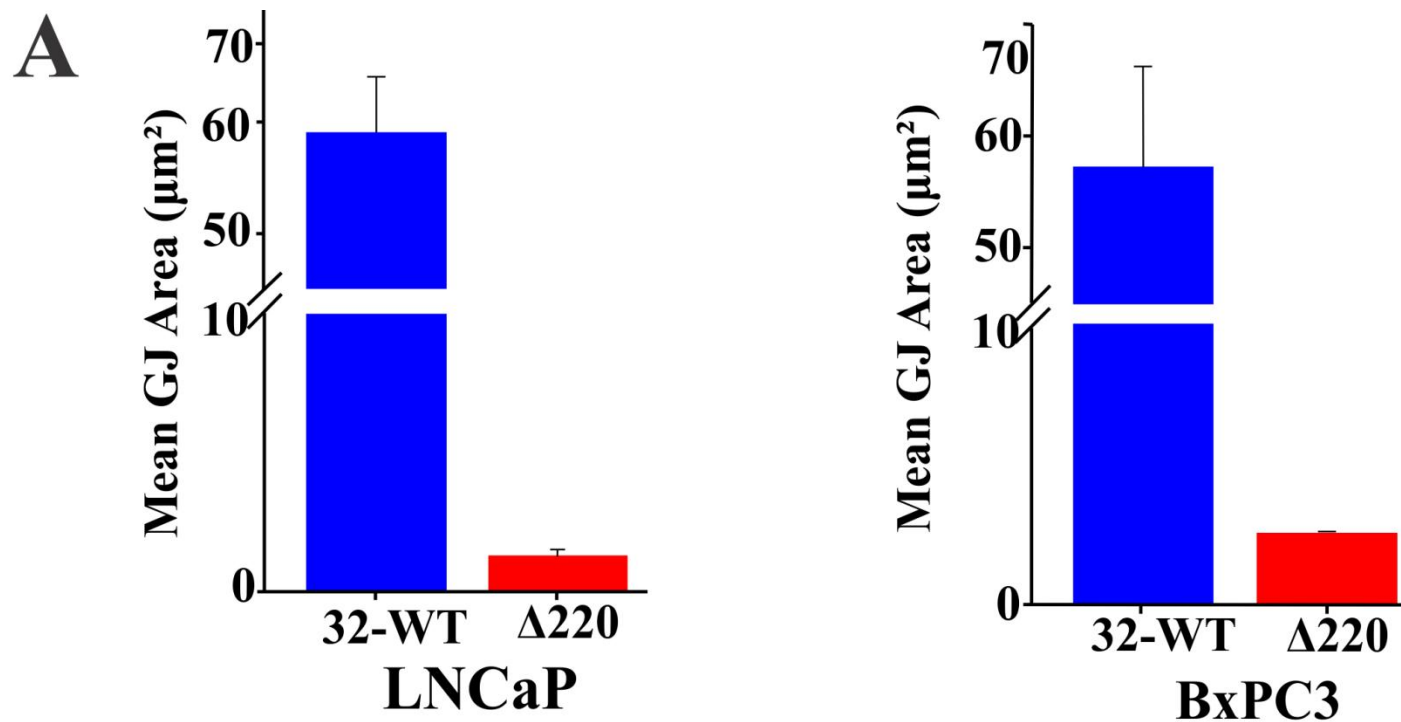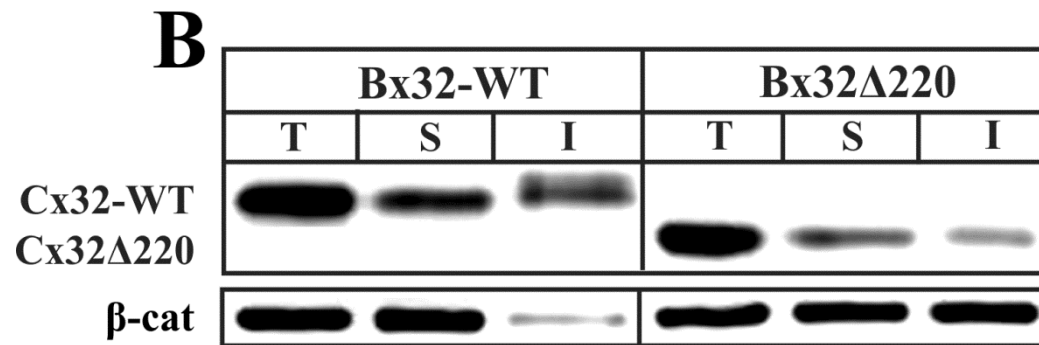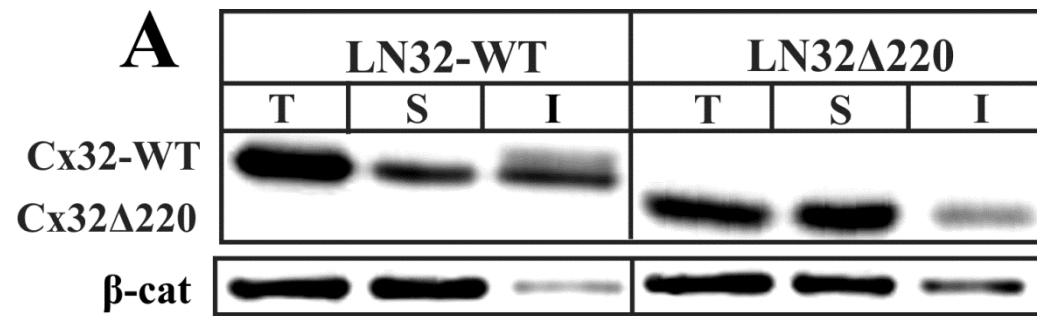
Figure 1

Figure 2

Figure 3
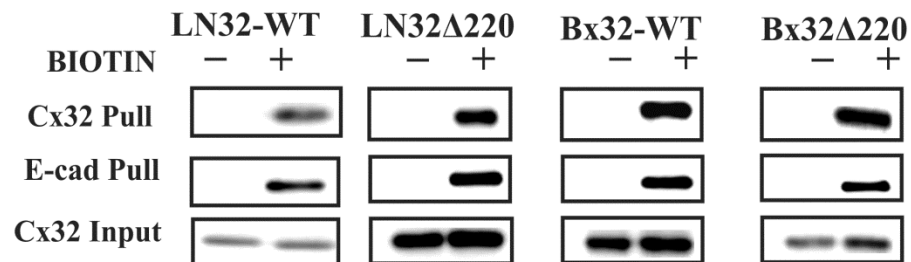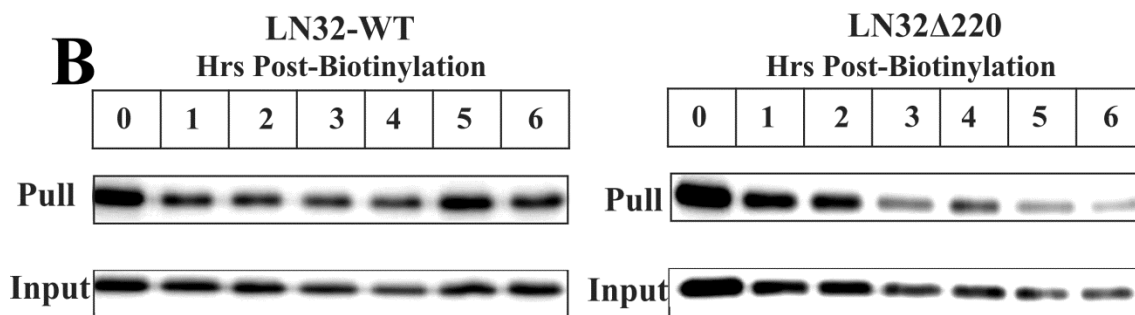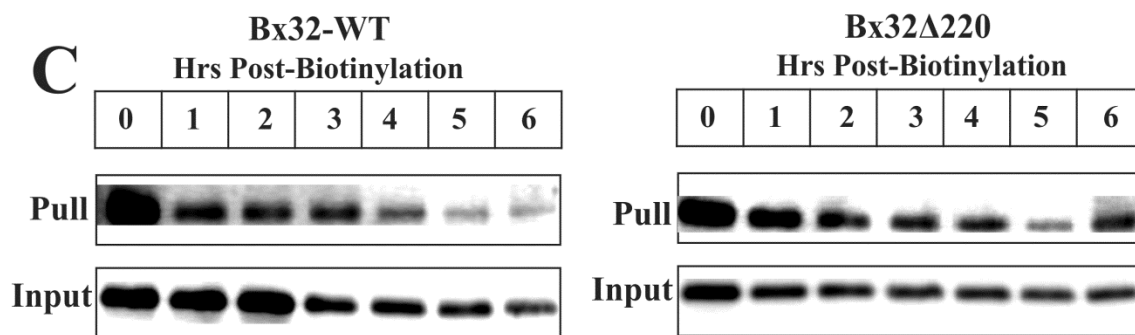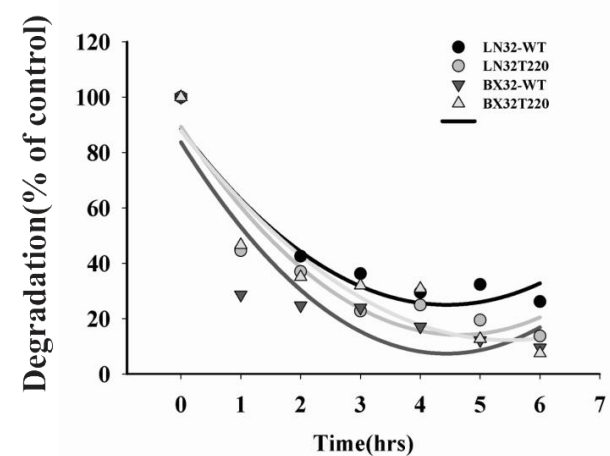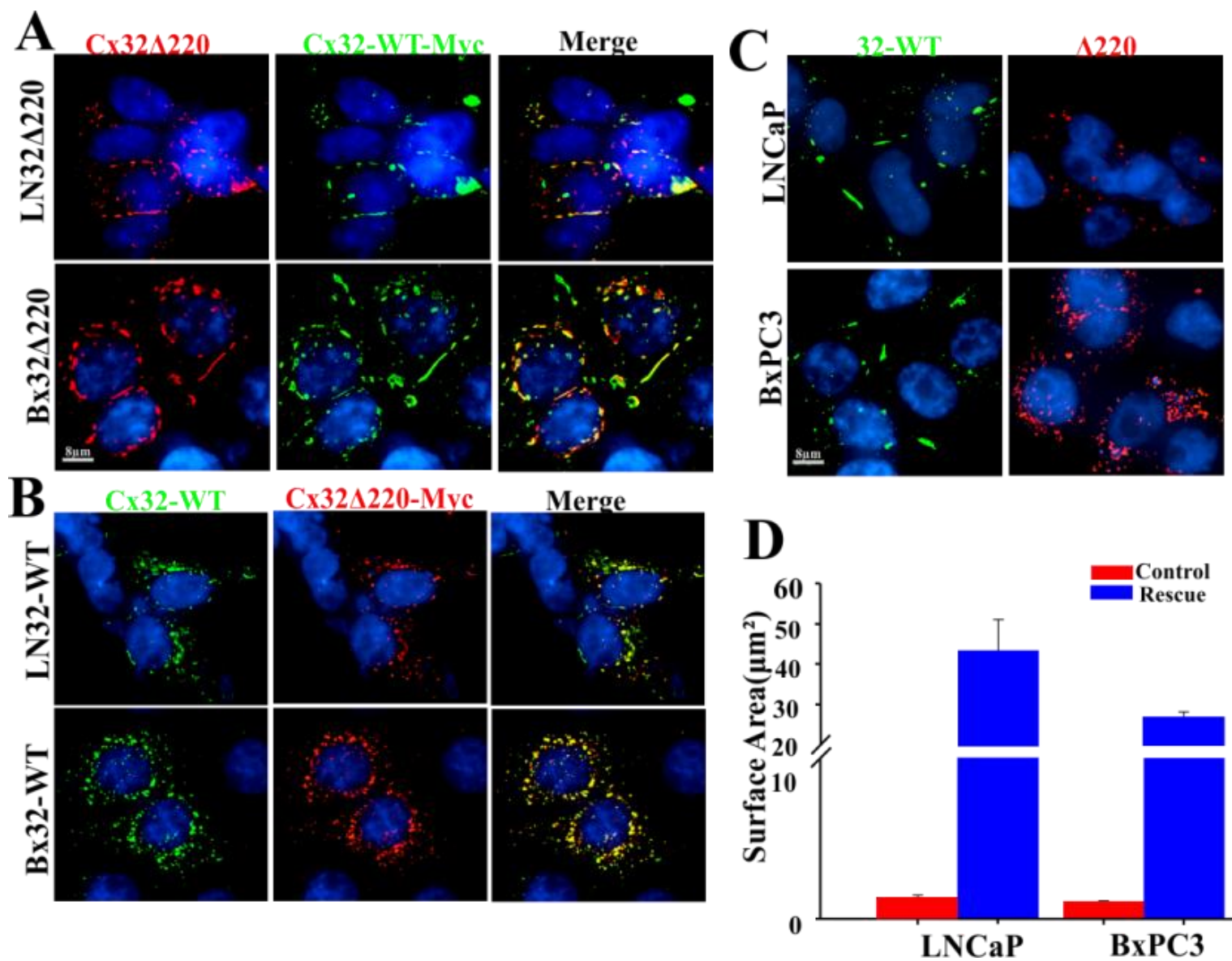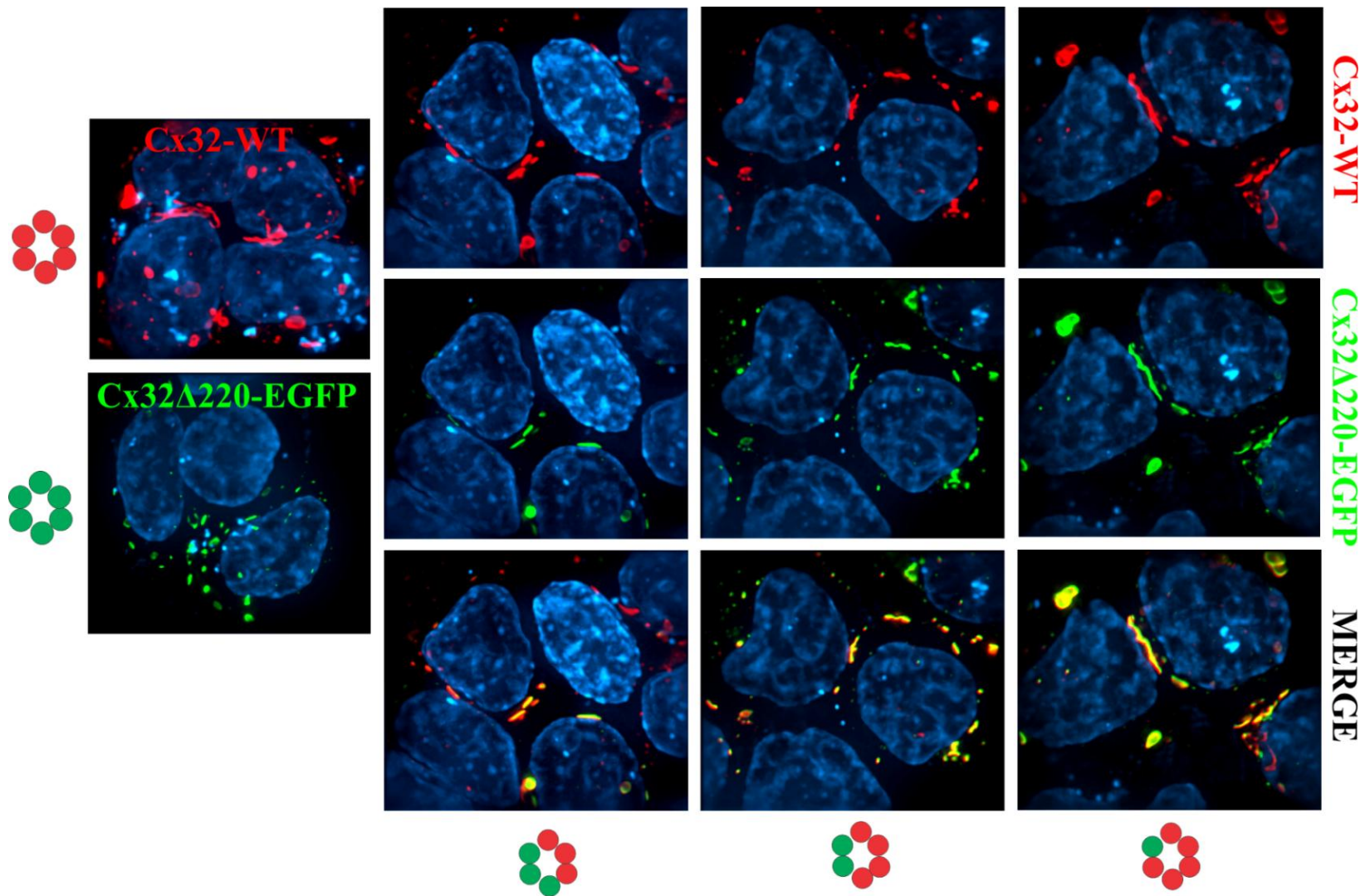
Figure 4

Figure 5

Figure 6

Figure 7

Figure 8

Cx32-WT/E-Cad   Cx32Δ220/E-Cad

−Forskolin

+Forskolin

Figure 9

Bx32-WT-EGFP

Bx32Δ220-EGFP

Figure 10

Figure 11